PERFLUOROALKYL SUBSTANCES IN THE UPPER MISSISSIPPI RIVER BASIN:

OCCURRENCE, SOURCE DISCRIMINATION AND TREATMENT

A DISSERTATION
SUBMITTED TO THE FACULTY OF THE GRADUATE SCHOOL
OF THE UNIVERSITY OF MINNESOTA
BY

Feng Xiao

IN PARTIAL FULFILLMENT OF THE REQUIREMENTS
FOR THE DEGREE OF
DOCTOR OF PHILOSOPHY

Dr. Matt F. Simcik, Advisor
Dr. John S. Gulliver, Co-Advisor

June 2012

Acknowledgements

I would like to express my sincere thanks to my advisors, Dr. Matt Simcik and Dr. John Gulliver. I appreciate for their vision, knowledge, insight and thoroughness in guiding my work in process. I am very grateful for the opportunity to work on this cutting-edge research topic. I also wish to express my gratitude to my thesis committee, Dr. Paul Capel (Department of Civil Engineering & USGS), Dr. John Gulliver (Department of Civil Engineering), Dr. Raymond Hozalski (Department of Civil Engineering), Dr. Lee Penn (Department of Chemistry) and Dr. Matt Simcik (School of Public Health), for their suggestions to my thesis. The kind advice from Ms. Cynthia Davey (Biostatistical Design and Analysis Center) and Prof. Thomas Halbach (Department of Soil, Water and Climate) is appreciated. Special thanks to Dr. Jay Rupp for his prays and for encouraging me to do my best in all matters of life.

I am deeply grateful to all the anonymous reviewers for their constructive comments and suggestions on the publications from this thesis.

I have received great help from my lab mates, Mr. Jeff Lanners and Mr. Patrick McNamara, for using the high-pressure liquid chromatograph–mass spectrometer.

I thank my parents, who have encouraged me to carry on researching. I owed their lovely support and encouragement during the whole study period.

Finally, the acknowledgements would not be complete without a heart-felt thanks to Ka Po Josey Chow, my wife who I met here during my Ph.D. studies. I am fortunate and grateful to have her as my best friend and faithful wife. She has been my biggest support during these years. I deeply thank her for having patiently gone through all the ups and downs of graduate study with me. She has also created so much joy and fun in our life. My life has been made richer because of you, Josey.

March 2012

Feng Xiao

Dedication

This dissertation is dedicated to my wife, Ka Po Josey Chow.

Abstract

Perfluoroalkyl substances (PFASs) are manufactured for use in non-stick cookware, fast-food containers, fire-fighting foams and many other products. These substances, including perfluorooctane sulfonate (PFOS) and perfluorooctane (PFOA), have recently been classified as emerging persistent organic pollutants that are of high concern in the Upper Mississippi River Basin. Several urban lakes in the State of Minnesota (USA) and a 53-km segment of the Upper Mississippi River (Pool 2) have been listed as impaired because of PFOS contamination in fish for human consumption.

This dissertation thus examines: (1) the occurrence of PFASs in the Upper Mississippi River Basin; (2) basin-scale source discrimination of PFASs by exploratory data analysis; (3) PFAS (ad)sorption by clay and polar/non-polar resins; and (4) PFAS removal by coagulation.

PFASs were observed in stormwater runoff from seven separate rain events (2009–2011) at various outfall locations corresponding to different watershed land uses. Elevated levels of PFOS were found on the particulate matter (PM) in runoff collected from both industrial and commercial areas. PFAS adsorption by kaolinite clay was then investigated and modeled, and the solid–water partition coefficient of PFOS was insufficient to explain PFOS associated with runoff PM. PFOS on the PM suggest that it may have originated from industrial/commercial products, entering the waste stream as PFOS containing particulates/substances. Then the current sources of PFASs were studied, confirming that ongoing industrial/commercial activities as a significant determinant of PFAS pollution in the Upper Mississippi River Basin. This was done after

an exploratory data analysis of PFAS concentrations in the influent of 37 wastewater treatment plants (WWTPs) serving more than 40 cities by using a new methodology developed in this dissertation. Both runoff and WWTP discharge can be significant pathways for PFASs into the Mississippi River. Because the drinking water in many cities within this basin comes from the Mississippi River surface water, the mechanisms for removal of PFASs by sorption and coagulation were investigated. PFOS/PFOA removal was minimal under current water treatment operations. The moderately polar XAD-7HP resin, on the other hand, was found to have an excellent potential ability for removing PFASs, including shorter-chained PFASs, from water.

Table of Contents

List of Tables

List of Figures

Chapter 1. INTRODUCTION AND OVERVIEW

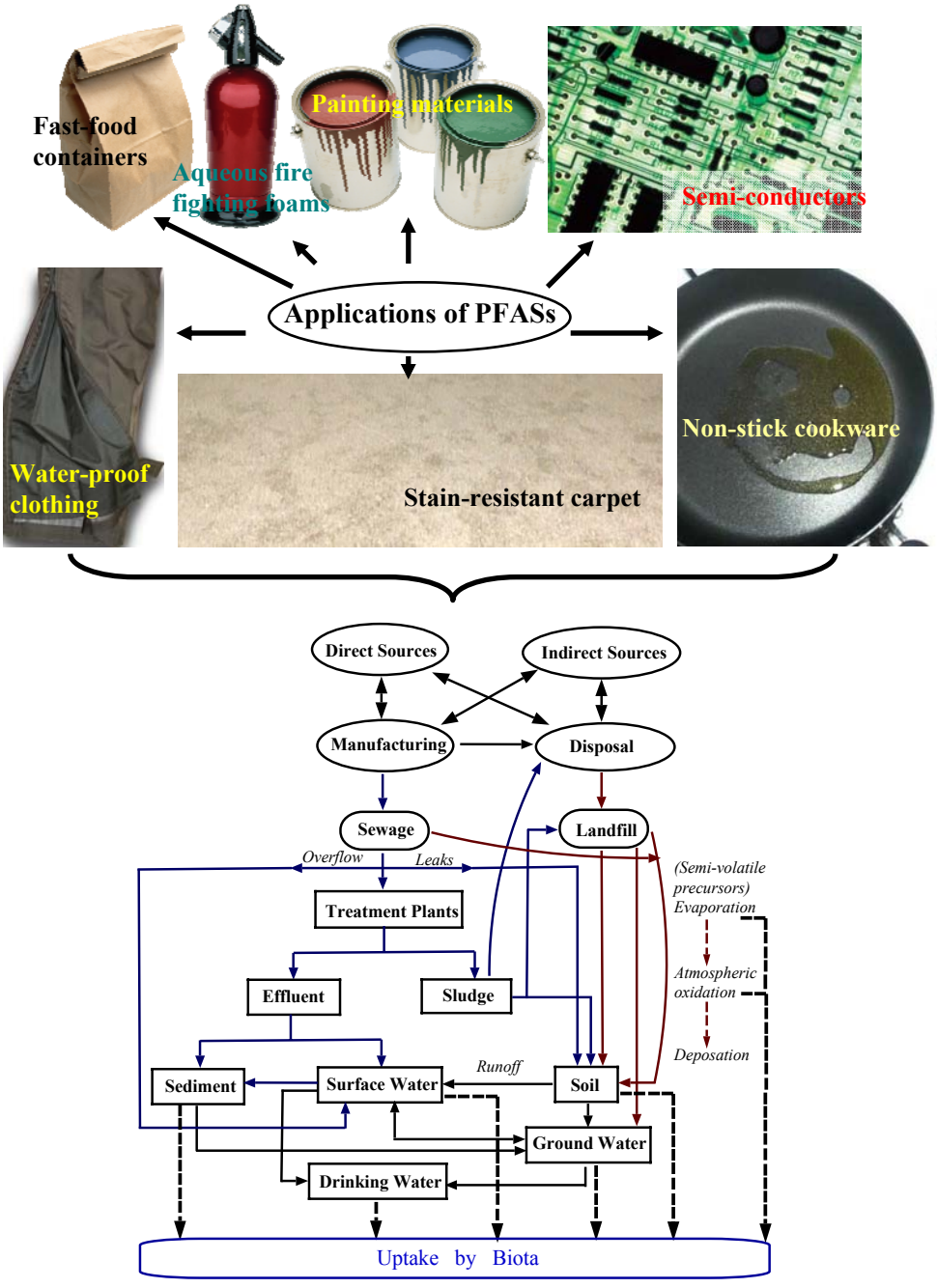

Graphical abstract: Applications of PFASs (the images are from Word 2011 Microsoft™ Cooperation or personal belongings) and proposed pathways for PFASs into the environment.

1.1 PFAS pollution: A worldwide environmental problem

The scientific community and the public have become increasingly concerned about the worldwide contamination of the environment with a group of emerging persistent organic pollutants (POPs), perfluoroalkyl substances (PFASs) (Armitage et al., 2009; Buck et al., 2011a; Giesy and Kannan, 2001; Houde et al., 2011; Lindstrom et al., 2011; Martin et al., 2004a; Paul et al., 2009; Prevedouros et al., 2006; Post et al., 2012; Vestergren and Cousins, 2009). PFASs are industrially produced compounds, primarily used as surface-active agents in food packaging, mist suppressants in the electroplating industry, painting materials, semi-conductors, fire-fighting foams, pesticides, and polymers to repel water and stains on textiles and leather products (Awad et al., 2011; EPA, 2012; Jahnke and Berger, 2009; Lindstrom et al., 2011; Meyer et al., 2011). They contain perfluorinated alkyl moiety of varying chain length and varying functional groups attached to that moiety (see Figure 1.1). Perfluoroalkylsulfonic acids and perfluorocarboxylic acids are two commonly detected classes of PFASs in the environment. Perfluoroalkylsulfonic acids have the general structure $F(CF_2)_nSO_3H$, where typically $n = 4$, 6, 8 or 10 (Stock et al., 2010). Commonly detected perfluoroalkylsulfonic acids in the environment include perfluorooctane sulfonate (PFOS, $n = 8$). The estimated global release of PFOS between 1970 and 2012 to the environment is greater than 45,250 t (Paul et al., 2009). The general structure of perfluorocarboxylic acids is $F(CF_2)_nCOOH$, where typically $n = 5$ to 15 (Stock et al., 2010). A frequently detected perfluorocarboxylic acid in the environment is perfluorooctane (PFOA, $n = 7$). The global historical industry-wide emissions of perfluorocarboxylic acids were estimated to be 3200–7300 t (Prevedouros et al., 2006). The pollution of surface water and drinking water by long-chain PFASs (≥ 7

perfluorocarbons), PFOS and PFOA in particular, is a worldwide problem due to their persistence, ability to bioaccumulate, and toxicity (Bischel et al., 2010; Conder et al., 2007; Emmett et al., 2006; Loi et al., 2011; Martin et al., 2004b; Müller et al., 2011a; Paul et al., 2009; Smithwick et al., 2005; Stock et al., 2010).

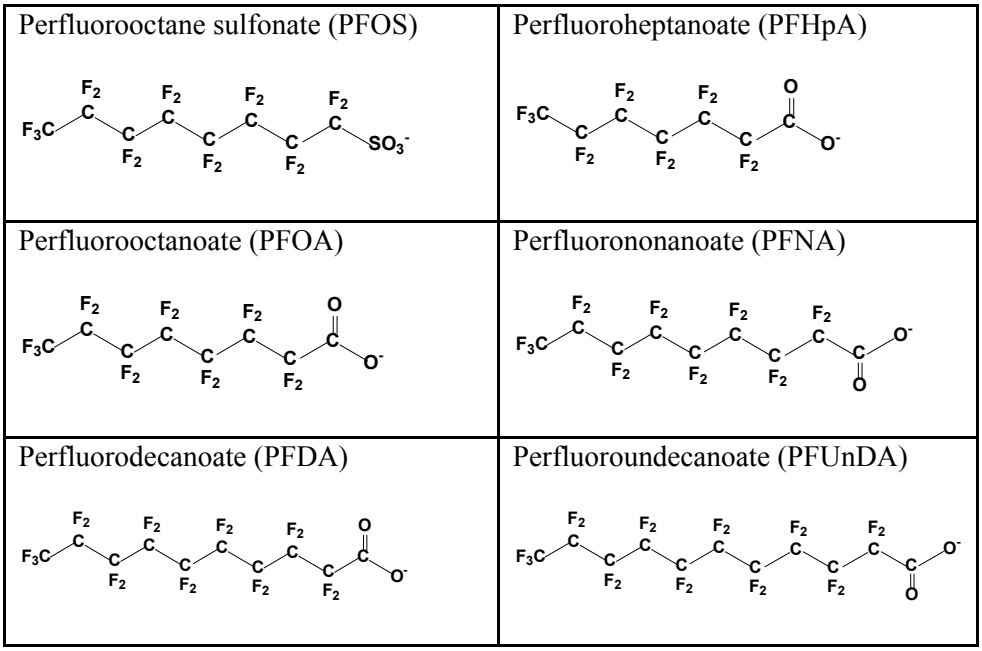

Figure 1.1 Chemical structures of PFASs that are commonly detected in the environment.

Ubiquitous presence: Although PFASs have been produced in large quantities for both industrial and commercial applications since 1950s, their environmental presence was discovered only recently, in the early millennium (Giesy and Kannan, 2001; Müller et al., 2011). Since then, they have been observed in all environmental compartments (Müller et al., 2011). They have been detected in fish, birds and mammals from mid-latitudes to the poles (Giesy and Kannan, 2001; Houde et al., 2006) and in human blood

samples worldwide at typical concentrations of several to tens of μg/L (Haug et al., 2009; Kärrman et al., 2006; Kato et al., 2011; Yeung et al., 2006). As a consequence of their chemical stability, relatively high water solubility, low volatility and extensive historical production, they are common surface and groundwater contaminants detected in numerous sites around the world (Bao et al., 2012; Benskin et al., 2010; Moody et al., 2003; Murakami et al., 2008; Nakayama et al., 2010; Simcik and Dorweiler, 2005; Skutlarek et al., 2006).

PFOS and PFOA have also been frequently detected in drinking water samples at typical concentrations of several to tens ng/L (Ericson et al., 2009; Hoffman et al., 2011b; Jin et al., 2009; Mak et al., 2009; Post et al., 2009; Takagi et al., 2008), and drinking water can be an important source of exposure to these chemicals for the general population (Ericson et al., 2009; Hoffman et al., 2011b; Tanaka et al., 2012; Vestergren and Cousins, 2009).

Environmental fate and transport: PFASs such PFOS and PFOA are chemically and biologically stable in the environment, resistant to direct and indirect photodecomposition, hydrolysis, ozonation, biodegradation, and strong acids or bases (EPA, 2012; Eschauzier et al., 2012; Prevedouros et al., 2006; Schröder and Meesters, 2005; Takagi et al., 2011). In a 2005 study, no measurable degradation of PFOS after 2-h treatment by O_3/UV, O_3, O_3/H_2O_2 and Fenton reagents was found (Schröder and Meesters, 2005).

Table 1.1. Physicochemical properties of PFOS and PFOA (EPA, 2012; OECD, 2002)

Property	PFOS (Potassium salt)	PFOA
CAS Number	2795-39-3	335-67-1
Appearance at normal room temperature and pressure)	White powder	White powder/waxy white solid
Molecular weight (g/mol)	538 (potassium salt); 499 (anionic species)	414; 413 (anionic species)
Water solubility (mg/L at 25°C)	570 (purified), 370 (freshwater)	9500 (purified)
Melting point (°C)	> 400	40 to 50
Boiling point (°C)	Not measurable	188
Vapor pressure at 20°C (mm Hg)	2.48×10^{-6}	0.017
Air–water partition coefficient, K_{aw} (Pa m^3/mol)	$< 2 \times 10^{-6}$	Not available
Octanol–water partition coefficient, K_{ow}	Not measurable	Not measurable
Organic carbon-normalized sorption coefficient, log K_{oc}	2.57	2.06
Half-life	Atmospheric: 114 days; Water: > 41 years (at 25°C)	Atmospheric: 90 days; Water: > 92 years (at 25°C)

PFOS and PFOA have moderate organic carbon–normalized sorption coefficient (K_{oc}), relatively high solubility in water, and low volatility (see Table 1.1). These substances can be released to the environment through their uses in the filed (e.g., fire-fighting foams and pesticides) and through emissions from industrial facilities and wastewater treatment plants (WWTPs) (Xiao et al., 2012b; Xiao et al., 2011a). If water is a receiving medium, they will exclusively remain in this environmental compartment, and volatilization from water appears to be an insignificant fate process. As a result the potential long half-lives in water, they can undergo regional or long-range transport with surface water and end up in remote areas. Longer-chained PFASs such as PFUnDA have

higher K_{oc} ($10^{3.3}$ for PFUnDA, Higgins and Luthy, 2006) and therefore partitioning to sediment is potentially significant, depending on the compartment of release. If released to soil, they can interact with soil organic matter and sorb to soil particles. As a result of their moderate $K_{oc,}$ they can move off-site and reach surface water via runoff and groundwater via leaching. In addition, PFOS and PFOA can be atmospherically oxidized from their (semi-)volatile precursors that can undergo long-range atmospheric transport (Ellis et al., 2003; Martin et al., 2006) and scavenged by precipitation (Armitage et al., 2006; Barton et al., 2007), leading to the occurrences of PFOS and PFOA in remote areas such as the Polar Regions where they have never been used (Giesy and Kannan, 2001; Smithwick et al., 2005; Young et al., 2007).

Bioaccumulation and exposure routes: There is sufficient literature to document that long-chain PFASs (≥7 perfluorocarbons) can biomagnify in both water–breathing and air–breathing animals including the top predator species such as humans (Bischel et al., 2010; Houde et al., 2006; Loi et al., 2011; Müller et al., 2011a; Smithwick et al., 2005). Different from legacy POPs, PFASs do not distribute to fat. Instead, they can bind strongly with proteins, and accumulate primarily in protein-rich compartments such as blood and liver, as documented in animal studies (Cui et al., 2009; Kelly et al., 2009; Yeung et al., 2009). Sources of exposure to PFASs for the general population include PFAS-contaminated drinking water and (sea)food, migration from (fast)food packaging to food, treated fabrics (e.g., carpets and waterproof clothing), house dust, and inhalation of indoor and outdoor air (D'eon and Mabury, 2011; Post et al., 2012).

Drinking water can be an important source of exposure (Ericson et al., 2009; Hoffman et al., 2011b; Post et al., 2012; Tanaka et al., 2012; Vestergren and Cousins, 2009). Several studies have documented that serum PFOA concentrations are elevated in areas with highly PFOA-contaminated drinking water (reviewed by Post et al., 2012). Post et al. (2012) suggested that drinking water PFOA levels of 1 ng/L, 10 ng/L, 40 ng/L, 100 ng/L, and 400 ng/L can contribute approximately 2.4%, 20%, 50%, 71%, and 91% of the total exposure, respectively, in populations with a background serum PFOA concentration of 4 ng/mL from non-drinking water sources. In the State of Minnesota, high concentrations of PFOS (n.d.–3500 ng/L) and PFOA (n.d.–2200 ng/L) were detected in drinking water supplies (MPCA, 2009). In response to the potential threat of PFAS-contaminated drinking water on public health, this thesis examines the removal of PFOS, PFOA, and other PFASs from drinking water by means of sorption and coagulation (see Chapters 5 and 6). PFASs are resistant to oxidation (Eschauzier et al., 2012; Schröder and Meesters, 2005; Takagi et al., 2011), including advanced oxidation processes (Schröder and Meesters, 2005), and physicochemical treatments such as coagulation and sorption may work for these POPs.

Toxicity: PFOS and PFOA exposure at blood levels in the general population may reduce fecundity in women (Fei et al., 2009), and prenatal exposure to PFOS has been associated with a reduced birth weight (Washino et al., 2009). The associations of blood PFOS and PFOA levels with children attention deficit/hyperactivity disorder (Hoffman et al., 2010) and hyperuricemia (Steenland et al., 2010) have also been documented. In addition, PFOS and PFOA have been identified as potent peroxisome proliferators, and

exposure to peroxisome proliferators often results in an accumulation of lipids in the liver (Stock et al., 2010 and the references therein). Long-chain PFASs, including PFOS and PFOA, have also been found to inhibit gap junction intercellular communication in both *in vitro* and *in vivo* studies, which may likely cause liver carcinogenicity (Stock et al., 2010 and the references therein). More adverse effects of PFASs on living organisms can be found in the previous reviews (Beach et al., 2006; Giesy et al., 2010; Post et al., 2012; Stock et al., 2010).

Phase-out: The end of the contamination?: In spite of the phase-out/reduction of the production of PFOS and PFOA by certain major manufacturers, environmental contamination and human exposure from these chemicals are anticipated to continue due to their environmental persistence and continuous PFOS/PFOA emissions from ongoing industrial/commercial activities (Clara et al., 2009; Lin et al., 2009; Müller et al., 2011; Pistocchi and Loos, 2009; Xiao et al., 2012; Xiao et al., 2011a). Recent studies revealed that ongoing industrial/commercial activities as a significant determinant of PFOS/PFOA pollution in the Upper Mississippi River Basin (Xiao et al., 2012b; Xiao et al., 2011a). Furthermore, phasing-out production does not necessarily mean stopping discharges of the compounds into the environment. From 2007 to 2010, elevated concentrations of PFOS (68–9010 ng/L) and PFOA (159–43200 ng/L) have been detected in two discharge points (SD001 and SD002) of 3M's Cottage Grove wastewater treatment facility (MPCA, 2011).

Based on the above, PFASs will continue to be a great environmental and human health concern. The State of Minnesota may be in a unique position in the study of

PFASs: it is home to 3M, which produced and disposed of many of PFASs in its Cottage Grove facility, Oakdale and Woodbury dumping sites, and Washington landfill around the Minneapolis–St. Paul metropolitan area, the sixteenth largest metropolitan area in the U.S.. Several urban lakes (Lake Calhoun, Lake Elmo, Lake Harriet, Lake Johanna, Little Johanna Lake and Lake of the Isles) in Minnesota and the Upper Mississippi River Pool 2 have been PFOS-impaired and currently put on the list of impaired waters by the Minnesota Pollution Control Agency (MPCA) because of the elevated concentrations of PFOS in fish (MPCA, 2012). However, remarkably, these PFOS-impaired lakes, except for Lake Elmo, have no documented connections to 3M's production or disposal. The current sources of PFASs in Minnesota (USA) and in the Upper Mississippi River Basin remain largely unknown, and the relative importance of domestic and industrial influences after the 3M 2000–2002 phase-out of the production of PFOS and PFOA needs to be investigated. In response to this, this dissertation examines the occurrences of PFASs in urban runoff collected from several separate rain events (2009–2011) at various outfall locations corresponding to different watershed land uses (see Chapter 2), and develops a methodology for a source assessment of PFASs in the influent and effluent from 37 WWTPs serving more than 40 cities across Minnesota (USA) (see Chapter 3). Once the geographical distribution of sources is identified and confirmed, reducing the inputs of PFASs to the Upper Mississippi River Basin can be addressed.

1.2 Physicochemical properties of PFASs

Several documents are available for a review of PFAS physiochemical properties (Beach

et al., 2006; Martin et al., 2004a; Rayne and Forest, 2009; Stock et al., 2010). Some important points are summarized here.

1.2.1 pK_a of PFASs

The pK_a of PFOA was estimated to be 3.8 (Burns et al., 2008). However, Goss and Arp (2009) argued that the pK_a of PFOA should be –0.5 based on molecular modeling techniques and software programs. The pK_a of PFOA estimated using the SPARC software program (September 2009 release w4.5.1529-s4.5.1529; http://ibmlc2.chem.uga.edu/sparc/) is −0.21 (0.14 for PFOS). SPARC predicts pK_a values with a mean absolute deviation of 0.65 (Liao and Nicklaus, 2009). Therefore it appears that pK_a of PFOA is not near 4. Nevertheless, the pK_a values of PFASs, including PFOA, have never been experimentally determined in pure water.

Since the dissociated species of PFOS and PFOA will predominate in the environment, almost all of the reported concentrations of PFOS and PFOA in water bodies are actually the concentrations of the anionic forms. Unless otherwise specified, the terms PFAS, PFOS, and PFOA used in this thesis refer to the dissociated species to maintain consistency with the literature.

1.2.2 Air–water partitioning

Not much is known about the air−water partition coefficient (K_{aw}) of PFOS and PFOA. PFOA, for example, is often incorrectly described as its conjugate acid (McMurdo et al., 2008). The SPARC software program estimated K_{aw} values of the protonated species of PFOS and PFOA are $10^{-1.69}$ and $10^{-1.06}$, respectively (Arp et al., 2006). The experimental

K_{aw} value of the protonated species of PFOA is $10^{-2.99}$ (Li et al., 2007). However, these values are all for the protonated/neutral/non-dissociated species of PFOS and PFOA. One may get an erroneously large air−water exchange flux of PFOA if the K_{aw} of the neutral species of PFOA is used. Based on the vapor pressure (0.003 Pa, Barton et al., 2009) and solubility (3.4 g/L) of PFOA (OECD, 2002), its K_{aw} should be ~$10^{-6.8}$, which is close to a value ($10^{-6.5}$) used in a previous study (Kim and Kannan, 2007). PFOS has an estimated K_{aw} of $10^{-7.0}$ (vapor pressure = 0.00033 Pa; solubility = 680 mg/L (OECD, 2002)). Therefore, PFOS and PFOA are essentially nonvolatile from water.

1.3 Knowledge gaps

The occurrence of PFASs in the Upper Mississippi River Basin: Possible PFAS loading pathways in the Upper Mississippi River Basin include atmospheric wet deposition, urban stormwater runoff and municipal/industrial wastewater. Compared to point source pollution, fewer references are available for the environmental contamination of PFASs from nonpoint sources. In Japan, a river received a higher load of PFASs from stormwater runoff than from wastewater treatment plants (WWTPs) (Zushi et al., 2008). Furthermore, different PFAS profiles between WWTPs effluents and street runoff were found (Murakami et al., 2009). Street runoff was found to contain more long-chain (>8 perfluorocarbons) and even-chain perfluorocarboxylates than WWTP effluents (Murakami et al., 2008). Aside from these studies in Japan, however, only one published report has been available about PFASs in surface runoff (Kim and Kannan, 2007). Therefore, a major question regarding the global distribution is whether urban runoff

should be viewed as a potential source of PFASs to urban waters. Concentrations and relative abundances of contaminants in stormwater runoff are closely related to various types of land use (Ha and Stenstrom, 2003). However, little is known about the influences of land uses on the levels of PFASs in urban runoff.

Adsorption of PFASs: A fundamental characteristic of surfactants is their tendency to adsorb at solid–water interfaces in an oriented fashion (Rosen, 2004). PFAS adsorption by natural adsorbents (soils, suspended solids, sediments, and aquifer materials) is an important determinant of their transport and fate in the environment. Previous studies have shown that the adsorption of PFAS is controlled by both hydrophobic and electrostatic effects (Higgins and Luthy, 2006; Johnson et al., 2007; Tang et al., 2010; Wang and Shih, 2011; You et al., 2010). Greater organic carbon content of the adsorbent, higher aqueous Ca^{2+} or H^{+} concentration, or longer perfluorocarbon chains can increase the adsorption of PFASs (Higgins and Luthy, 2006; Johnson et al., 2007; Tang et al., 2010; Wang and Shih, 2011; You et al., 2010). Nevertheless, the published reports do not provide a complete and consistent picture of PFAS adsorption. First, the effect of Na^{+} and the role of electrostatic interactions need to be better understood. NaCl has been used as a road-deicing agent for decades in many northern regions, where snowmelt during the spring carrying a significant load of NaCl runs into storm sewers, ditches and small streams and then empties into wetlands, lakes and rivers. In seawater, the concentration of Na^{+} can reach 0.5 M (Snoeyink and Jenkins, 1980). Knowledge of the effect of Na^{+} on PFAS adsorption may provide key insights into the environmental fate of PFASs and the associated ecosystem risks (Jeon et al., 2010). A recent study (Tang et al., 2010)

described the effect of sodium on the electrostatic interaction between PFAS molecules adsorbed on mineral surfaces. However, there is a lack of quantitative estimations about this interaction. In this dissertation, the effects of sodium on the electrokinetic potential (ζ) of kaolinite suspensions with and without the presence of PFASs are investigated and modeled to provide both the qualitative and quantitative descriptions of the electrostatic interaction. Second, it is not clear whether PFAS molecules compete for suitable sites during adsorption. No competition was found during the sorption of PFASs to sediment (Higgins and Luthy, 2006). However, the hydrophobic effect increases with the hydrophobic length of the PFAS (Higgins and Luthy, 2006), and thus, a longer-chained PFAS may outcompete a shorter-chained PFAS during adsorption. One study observed the competitive adsorption of PFASs to aerobic active sludge (Zhou et al., 2010).

In addition, polymeric resins have attracted increasing attention as an alternative to activated carbon for concentrating and removing organic compounds, primarily because of their favorable physicochemical stability, large sorption capacity, relatively low cost, good selectivity, structural diversity and easy generation (Dominguez et al., 2011; Freitas et al., 2008; Vergili et al., 2010; Wania et al., 2003). In particular, Amberlite XAD-7HP (the only moderately polar XAD resin now available) and XAD-2 (nonpolar) resins have been used widely to isolate and concentrate organic compounds from environmental samples (Scott et al., 2006; Senevirathna et al., 2010a; Tittlemier et al., 2007; Wania et al., 2003). However, surprisingly, a systematic study about the sorption of PFAS by these resins is lacking in the literature. Many studies (i.e., Villagrasa et al., 2006) have been conducted for PFASs being concentrated or cleaned up using Oasis HLB and WAX

resins. Much less attention has been paid to XAD-7HP, a nonionic aliphatic acrylic polymer combining a polar component that can promote hydrophilic interactions with PFASs.

Removal of PFASs by coagulation: As have been discussed in Chapter 1, drinking water can be an important source of exposure to PFOS and PFOA for the general population (Ericson et al., 2009; Hoffman et al., 2011b; Tanaka et al., 2012; Vestergren and Cousins, 2009). Post et al. (2012) suggested that drinking water PFOA levels of 1 ng/L, 10 ng/L, 40 ng/L, 100 ng/L, and 400 ng/L can contribute approximately 2.4%, 20%, 50%, 71%, and 91% of the total exposure, respectively, in populations with a background serum PFOA concentration of 4 ng/mL from non-drinking water sources. In the State of Minnesota, high concentrations of PFOS (n.d.–3500 ng/L) and PFOA (n.d.–2200 ng/L) were detected in drinking water supplies (MPCA, 2009). Therefore, a study examining the effectiveness of drinking-water treatment processes is warranted to increase our understanding of the fate of PFASs during water treatment and to seek the best available technology for removing these POPs from drinking water. However, a study of this kind is rarely available in the literature.

A study (Deng et al., 2010) investigated the removal of PFOA by coagulation using a pre-hydrolyzed aluminum salt, polyaluminum chloride (Al_2O_3 = 29%). Apart from this one, the author of this thesis is not aware of any other studies looking in detail at the mechanisms for removal of PFASs from drinking water by (conventional) coagulation and enhanced coagulation. Deng et al. (2010) suggested that the removal of PFOA (up to 90%) during coagulation was because of the sorption of PFOA to suspended solids.

However, this removal mechanism is debatable given the low adsorptivity of PFOA to solid particles including kaolinite clay and sediments (Higgins and Luthy, 2006; Tang et al., 2010; Xiao et al., 2011b). In addition, alum and ferric chloride are still the most widely used coagulants because of their availability, low cost, ease of use, and ease of storage (Water Environment Federation, 2006). It is thus of interest to examine the fate of PFASs during alum/ferric chloride coagulation. One further objective of this thesis is to examine various solution-specific and coagulant-specific parameters potentially affecting the removal of PFOS and PFOA by conventional and enhanced coagulation, with an overall goal of better control of the occurrence of these chemicals in tap water. This objective is achieved by determining PFOS/PFOA removal under different coagulation conditions and by delineating the proposed removal mechanism on a coagulation diagram.

1.4 Main goals and objectives

The main goals of this thesis are to investigate the major sources of PFASs in the Upper Mississippi River Basin and to evaluate the performance of different processes for removing PFASs from the aqueous phase. The specific objectives of the research are to:

(1) Investigate the levels and fate of PFASs in urban stormwater runoff (see Chapter 2).

(2) Identify input sources of PFASs detected in 37 WWTPs across more than 40 cities in the Upper Mississippi River Basin (see Chapter 3).

(3) Examine and model important chemical and mineralogical factors affecting PFAS adsorption by kaolinite clay (see Chapter 4).

(4) Study the sorption of PFASs by both non-polar and polar resins, with respect to

sorption kinetics, sorption isotherms and the influences of solution pH (see Chapter 5).

(5) Evaluate PFAS removal efficiencies by coagulation under different conditions and delineate the mechanisms on a coagulation diagram (see Chapter 6).

The author of this thesis was the primary author of all publications/manuscripts from these chapters, with review and advice from the co-authors of the manuscripts.

Chapter 2: PERFLUOROALKYL SUBSTANCES IN URBAN STORMWATER RUNOFF: INFLUENCE OF LAND USE

Feng Xiao, Matt F. Simcik, John S. Gulliver, 2012. Perfluoroalkyl acids in urban stormwater runoff: Influence of land use. ***Water Research*** (in press) DOI: 10.1016/j.watres.2011.11.029.

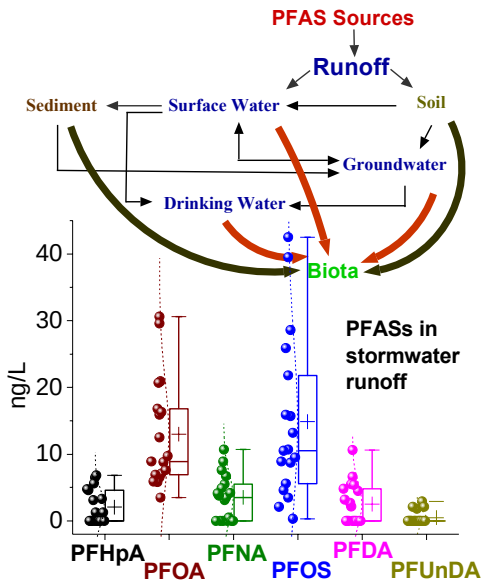

Graphical abstract

2.1 Introduction

Urban stormwater runoff carries various pollutants from the urban watershed, such as nutrients from lawns and landscaped areas, heavy metals from roofs, brake wear and tire wear, and organic pollutants (Baun et al., 2006; Chocat et al., 2007; Davis et al., 2001; Deletic et al., 1997; Eriksson et al., 2007). While stormwater management practices (SMPs) can remove many contaminants (Weiss et al., 2007), conventional SMPs may not efficiently remove PFASs from stormwater. PFASs are industrially produced compounds that contain a perfluorinated alkyl moiety of varying chain length and varying functional groups attached to that moiety. They have been produced for both industrial and residential applications including fire-fighting foams, insecticides and as polymers to repel water and stains on paper and textiles including fabric and carpeting (Emmett et al., 2006; Giesy and Kannan, 2001; Prevedouros et al., 2006). They have recently become the target of investigation by environmental chemists due to their persistence and toxicity and their ubiquitous presence in the environment (Emmett et al., 2006; Giesy and Kannan, 2001; Prevedouros et al., 2006). Because of the strong carbon–fluorine bonds, PFASs are not easily degraded by physical or chemical mechanisms once in the environment. PFASs such as PFOS and PFOA have been found in fish, birds and mammals from mid-latitudes to the poles (Giesy and Kannan, 2001; Houde et al., 2006) and in human blood samples worldwide at typical concentrations of several to tens of μg/L (Haug et al., 2009; Kärrman et al., 2006; Kato et al., 2011; Yeung et al., 2006). High blood PFOS levels in humans have been associated with a low birth weight (Washino et al., 2009). The associations of blood PFAS levels with children attention deficit/hyperactivity disorder

(Hoffman et al., 2010) and hyperuricemia (Steenland et al., 2010) have also been observed.

A previous study (Simcik and Dorweiler, 2005) documented that PFASs in urban water bodies mainly come from non-atmospheric sources, including WWTPs (point source pollution) and surface runoff (nonpoint source pollution). In 2007, several metropolitan lakes in Twin Cities of Minneapolis and St. Paul, Minnesota (USA) were labeled impaired for contamination with a suite of PFASs, primarily PFOS in fish (MPCA, 2009). While Minnesota is home to the 3M corporation that produced and disposed of many of these chemicals, many of the lakes listed as impaired have no connection to 3M's production or disposal (MPCA, 2009). In addition, none of these lakes receives direct wastewater discharge. A significant source of PFASs to surface waters could be urban runoff, which receives PFASs from transportation, industrial and residential sources within its watershed.

Compared to point source pollution, fewer references are available for the environmental contamination of PFASs from nonpoint sources. In Japan, a river received a higher load of PFASs from stormwater runoff than from WWTPs (Zushi et al., 2008). Furthermore, different PFAS profiles between WWTPs effluents and street runoff were found in Japan (Murakami et al., 2009). Street runoff was found to contain more long-chain (>8 perfluorocarbons) and even-chain perfluorocarboxylates than WWTP effluents (Murakami et al., 2009; Murakami and Takada, 2008). Aside from these studies in Japan, however, only one published report has been available about PFASs in surface runoff (Kim and Kannan 2007). Therefore, a major question regarding the global distribution is

whether urban runoff should be viewed as a potential source of PFASs to urban waters. Once significant sources of contaminants are identified and confirmed, reducing these inputs to receiving waters can be addressed (Davis et al., 2001). Concentrations and relative abundances of contaminants in stormwater runoff are closely related to various types of land use (Ha and Stenstrom, 2003). However, little is known about the influences of land uses on the levels of PFASs in urban runoff.

The objective of this chapter is to monitor stormwater runoff and evaluate the concentrations of PFASs present in urban runoff. It will present results from an urban runoff study, in which runoff was collected and analyzed from different storm events at various outfall locations corresponding to different land uses (industrial, residential, and commercial areas).

2.2 Materials and methods

2.2.1 Chemicals

PFHpA (99 percent), PFOA (~95 percent), PFNA (97 percent), PFOS (≥98 percent), PFDA (98 percent), and PFUnDA (95 percent) were purchased from Sigma(–Aldrich) (Milwaukee, WI, USA & Steinheim, Switzerland) (Table A-1, Appendix A). Isotopically labeled surrogate standards, $^{13}C_4$-PFOA, $^{13}C_5$-PFNA, $^{13}C_4$-PFOS, and $^{13}C_2$-PFDA, were acquired from Cambridge Isotope Laboratories (MA, USA). The labeled PFASs were dissolved into methanol (Optima grade, Fisher Scientific, Hanover Park, IL) to 600 ng/mL of each PFAS as internal standards. Methanol and reverse osmosis (R.O.) or HPLC water (HPLC grade, Fisher Scientific, Hanover Park, IL) were used to clean the

containers and equipment. PFASs were not found in the methanol or the water when this was checked by using a Hewlett Packard model 1090 high-performance liquid chromatograph (HPLC) coupled to a Hewlett Packard 1100 MSD mass spectrometer with an electrospray ionization source (ESI-MS).

2.2.2 Site selection and sample collection

The samples of stormwater runoff were taken from three residential sites, labeled CSCC (44°59'17"N, 93°12'54"W), CTC (44°58'46"N, 93°11'00"W) and Mayo (44°58'20"N, 93°13'56"W) (Figure A-1, Appendix A), one commercial and heavily trafficked area (Dinkytown, 44°58'52"N, 93°14'13"W) (Figure A-1, Appendix A), and multiple sites near an industrial area of suspected PFAS contamination (Figure A-2, Appendix A). Land use of these sites is characterized with percent urban land use ranging from 45.8 to 62.9% and with a 1.3–3.1% increase in households from 2000 to 2010 (Metropolitan Council, 2011). Dinkytown is within the same county as CSCC and Mayo; however, it is a busy commercial center with a mix of bars, retail and entertainment uses. Figure A-3 (Appendix A) shows the land use information of Dinkytown.

Runoff was collected for seven separate rain events with a precipitation rate larger than 8 mm/h from 2009 to 2011 (event 1: Sep 25 2009; event 2: Aug 20 2010; event 3: Sep 01 2010; event 4: Sep 15 2010; event 5: Sep 23 2010; event 6: Oct 26 2010; event 7: May 12 2011). At each site, about four liters of runoff samples were collected by lowering a high-density polyethylene container into the stormwater flow from street level storm sewers. Samples were taken after the initial surface runoff (first flush), in spite of

the fact that the concentrations of short- to medium-chain-length PFASs (PFOA, PFNA and PFOS) were not changed significantly in runoff in a fixed-point hourly monitoring experiment (Zushi and Masunaga, 2009). Rainfall was collected at three heavy rain events (event2, even 4, and event 6) from roof downpipe. All the containers and equipment were pre-cleaned by rinsing with Optima grade methanol (five times) followed by R.O. water (ten times) and then rinsed with runoff water (three times) at each site before collecting samples. The collected samples were transported to the lab and refrigerated at 4°C for further treatment.

2.2.3 Sample pretreatment

Before separating particles from water, samples were taken from refrigeration and allowed to reach room temperature (22°C). Samples were filtered through a 0.5- and then a 0.2-μm pre-weighed polycarbonate membrane (Millipore) into a pre-cleaned polyethylene vacuum flask. Filter membranes were determined to be PFAS-free and did not retain dissolved target analytes. Several filters were required per water sample as the particles in the samples clogged the filters and the head pressure increased (or flow decreased). The membranes with the retained particles were completely dried at 50°C, cooled, weighed, and stored in a desiccator with anhydrous Na_2SO_4. R.O. water was used to rinse the containers to recover possible adsorbed PFASs. The rinsate was filtered and combined with the filtrate and the volume of the final solution was measured and recorded. Then the water samples were spiked with 60 ng of each isotopically labeled PFAS (100 μL of internal standard solution) and extracted by a solid-phase extraction

(SPE) method. Briefly, water samples were pumped through a XAD-7 cartridge at flow rate of 2 mL/min. The XAD-7 resin was pre-clean by Optima grade methanol and then by in R.O. water, and stored in R.O. water. The flow rate was optimized by checking the recovery rates of PFAS-spiked HPLC water. The cartridges were then washed with R.O. water and air-dried. PFASs retained on the resin were eluted with 40 mL methanol three times into a 50-mL polystyrene tube. These extracts were concentrated to approximately 0.5 mL under a gentle stream of pre-purified nitrogen, filtered using a 0.2-μm nylon filter into a 300 μL insert (Chrom Tech, Minneapolis, MN) in a Wheaton vial, and was crimp-sealed with a natural rubber septum (Chrom Tech, Minneapolis, MN).

The particles in runoff retained on the membrane filters were put into a pre-cleaned 50-mL polystyrene tube containing 100 μL of isotopically labeled PFAS stock solution. The samples were extracted by 10–15mL Optima grade methanol, centrifuged, and the supernatant was collected. The particles were re-suspended in methanol, centrifuged again, and the supernatant was combined with the first one. The procedure was repeated one more time to yield ~40 mL extract which was then concentrated to approximately 0.5 mL for HPLC–MS analysis.

2.2.4 Sample quantification

Samples were quantified using internal standards (Lanners, 2010). The mass of PFAS in each sample was calculated the relative response factor method (*RRF*). The *RRF* was calculated by putting a known amount of internal standard into a standard with unlabeled

PFASs and then dividing the mass to area rations of both labeled and unlabeled compounds:

$$RRF = \frac{\text{Peak Area of Analyte} \,/\, \text{Mass of Analyte}}{\text{Peak Area of Internal Standard} \,/\, \text{Mass of Internal Standard}} \qquad (2.1)$$

The *RRF* calculated from Eq 2.1 was applied to compute PFAS concentrations in samples:

$$\text{Mass of Analyte} = \frac{\text{Peak Area of Analyte} \,/\, RRF}{\text{Peak Area of Internal Standard} \,/\, \text{Mass of Internal Standard}} \qquad (2.2)$$

The optimized parameters for operating the HPLC–MS can be found in previous studies (Dorweiler, 2004; Johnson et al., 2007). The instrumental limit of detection (LOD) was determined based on a peak signal-to-noise (S/N) ratio of 3:1, and the limit of quantification (LOQ) was calculated based on a peak S/N ratio of 10:1. The LODs were determined to be: PFHpA 20 ng/ml, PFOA 8 ng/ml, PFNA 8 ng/ml, PFOS 5 ng/ml, PFDA 5 ng/ml and PFUnDA 5 ng/ml. The LOQs were determined as: PFHpA 50 ng/ml, PFOA 20 ng/ml, PFNA 20 ng/ml, PFOS 12 ng/ml, PFDA 15 ng/ml, and PFUnDA 12 ng/ml. Actual LOD and LOQ were calculated based on the volume of a sample being analyzed.

2.2.5 Recovery and procedural blanks

The method developed by Nakayama et al. (2010) was modified and used to determine PFAS recoveries. Stormwater runoff was spiked with known amounts of PFASs and internal standards and then extracted using SPE as described above. The eluate was concentrated, filtered, and analyzed by HPLC–MS. The same volume of unspiked

stormwater runoff was extracted using another SPE cartridge, and the eluate was concentrated, filtered, spiked by the same amount of PFASs and internal standards, and analyzed by HPLC–MS. Recoveries were calculated by dividing the peak area ratio of the first sample (pre-addition to cartridge) by that of the second eluate (post-addition). Average recoveries (n = 7) from matrix spikes were 78.7 ± 22.6% (mean ± SD) for PFHpA, 93.6 ± 12.6% for PFOA, 103.4 ± 14.3% for PFNA, 102.7 ± 19.1% for PFOS, 82.5 ± 17.4% for PFDA, and 92.1 ± 22.5% for PFUnDA.

Procedural/SPE blanks were prepared by adding 4 liters of R.O. or HPLC-grade water to pre-cleaned high-density polyethylene containers and processed as a sample. The only PFAS detected in four procedural blanks was PFOS (during Sep 2010 and May 2011 for runoff and rain sampling) and the concentrations were below LOQ. Therefore, pre-cleaned containers, SPE cartridges and the water were basically free of PFASs.

2.2.6 Statistical analysis

To compare means between three or more groups, ANOVA and the following post-hoc test (Tamhane's T2 test for unequal variance) were applied to data that were normally distributed (Pagano and Gauvreau, 2000). The normality was checked by the Shapiro–Wilk test. For data that were not normally distributed, a non-parametric test, Mann–Whitney–Wilcoxon (MWW) test, was used to compare the medians between groups. The widely adopted significance level, 0.05, was adjusted during multiple comparisons to avoid increasing the risk of rejecting a true null hypothesis (Pagano and Gauvreau, 2000). For four groups, six comparisons were needed ($= {}^{4!}\!/\!_{(4-2)!2!}$) and the significance level

was adjusted to 0.0083. For the comparison between six groups, the significance level was adjusted to 0.0033. For comparing the proportions between groups, a non-parametric test (Chi-square test) was used and the significance level was set at 0.05.

All of the tests were performed using SPSS 17.0 (now known as PASW, for Window, SPSS Inc. IL, USA). The statistical analysis results are provided in the Appendix A.

2.3 Results and discussion

2.3.1 Concentrations of PFASs in stormwater runoff in urban residential and commercial areas

As shown in Figure 2.1, the concentrations of PFASs in stormwater runoff differ from event to event. The total concentration of PFASs ranged from 14.3 ng/L for event 4 at CTC to 96.0 ng/L for event 5 at Dinkytown. The most abundant PFASs in stormwater runoff were PFOS and PFOA. The concentrations ranged up to 42.5 ng/L for PFOS and 30.6 ng/L for PFOA. For the three residential areas (CSCC, CTC and Mayo), the total concentrations of PFASs in runoff were smaller than 30 ng/L and no PFAS concentration was larger than 20 ng/L. On the other hand, relatively high concentrations of PFOS and PFOA were found in runoff collected from Dinkytown, the commercial area. One-way ANOVA and the following post-hoc test were used to determine the significance of the differences among the four sites (CSCC, CTC, Mayo and Dinkytown) in terms of PFAS concentrations in the stormwater runoff. The values of skewness of the PFAS concentrations in the four areas lie mostly between 0 to 1 (except PFUnDA), indicating

that the data of PFAS concentrations can be treated as normally distributed and can be tested by the robust one-way ANOVA and post-hoc tests. The Tamhane's T2 post-hoc test was chosen for unequal variance (the ratios of the largest standard deviation to the smallest standard deviation are larger than two for all PFASs cases) (Pagano and Gauvreau, 2000).

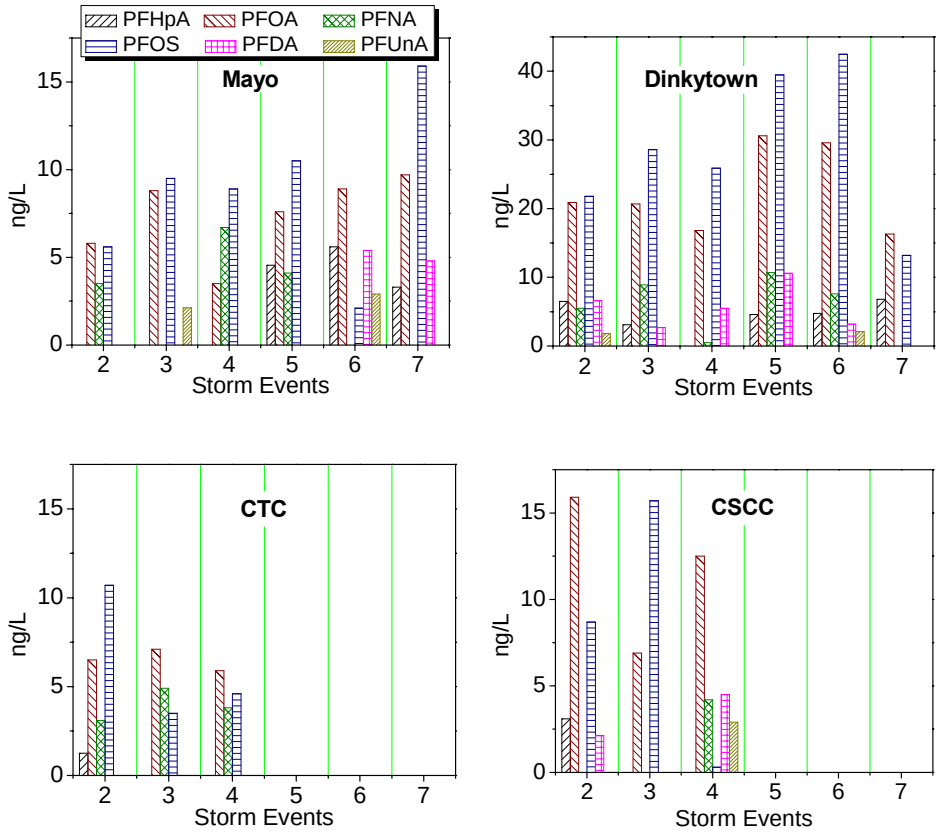

Figure 2.1 PFAS concentrations in street runoff in different locations during six storm events. Non-detect values were measured at CTC and CSCC for events 5, 6, and 7. The results of event 1 were tabulated in Table 2.2.

The one-way ANOVA and Tamhane's T2 post-hoc test results are shown in the Appendix A. At a significance level of 0.0083, no significant differences among CSCC, CTC, Mayo and Dinkytown were found with respect to the mean concentrations of PFHpA, PFNA and PFDA in stormwater runoff. However, the mean concentrations of PFOS and PFOA in stormwater runoff at Dinkytown were significantly higher than the mean concentrations in stormwater runoff at CTC (two-sided p value = 0.008 for PFOA and p = 0.001 for PFOS) and at Mayo (two-sided p value = 0.007 for PFOA and p = 0.004 for PFOS). Compared to CTC and Mayo, Dinkytown is a busy district containing several city blocks occupied by various small businesses, restaurants, food courts and bars. Murakami and Takada (2008) found that the PFAS content was significantly higher in heavily trafficked street dust than in residential street dust. High concentrations of PFOA were found in runoff collected at a site influenced by heavy traffic (Kim and Kannan, 2007). The traffic flow (the number of vehicles passing a reference point per unit of time) around the sampling site at Dinkytown is about 1416 vehicles per hour (15 min counts started at 4:30 p.m.), which is much higher than the residential areas (CSCC, 456; CTC, 216; Mayo, 84 vehicles per hour). Therefore, the vehicular traffic around Dinkytown possibly acts as an important source of PFASs in runoff. Several studies have found PFASs in dust from cars (Bjorklund et al., 2009; Goosey and Harrad, 2011). In addition, given that PFASs have been used in various materials (including commercial food packaging), these materials used in the (fast food) restaurants of Dinkytown could be another source of PFASs in runoff collected from this area.

2.3.2 Profile of PFASs in urban runoff

The PFAS concentrations are presented in a box plot (Figure 2.2). Although Dinkytown is a commercial area, the concentrations of PFASs in runoff collected from Dinkytown were included in Figure 2.2 to better represent the multiple land uses of urban areas.

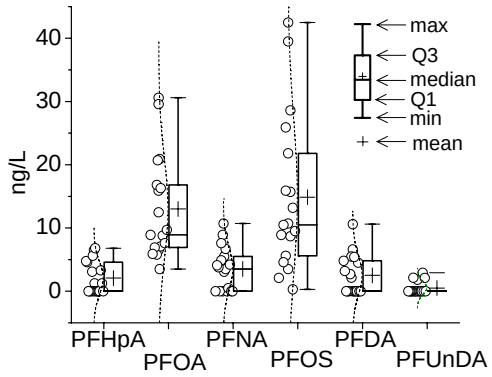

Figure 2.2 PFAS concentrations in stormwater runoff collected from Dinkytown, CTC, CSSS, and Mayo. The concentrations of PFASs less than LOQ were assigned as half of the LOQ value, and the concentrations of PFASs that were below LOD were assigned as zero.

The data shown in Figure 2.2 are positively skewed (except PFNA); the skewness is caused by the outliers that are large values relative to the mean. For skewed data, the median is a better measure of the center than the mean (Pagano and Gauvreau, 2000). To determine the relative abundance of PFAS in urban stormwater runoff, the MWW test of population medians was applied to the data. For multiple comparisons of the sampling distribution of the sample median among six groups, the significance level was adjusted to 0.0033 to avoid increasing the risk of rejecting a true null hypothesis (Pagano and Gauvreau, 2000). The MWW test results reveal that the median concentration of PFOA

(9.3 ng/L) is not significantly different from the median concentration of PFOS (10.6 ng/L). However, their median concentrations are significantly higher than other PFASs. The results also show that the median concentrations of PFHpA (0.63 ng/L), PFNA (3.65 ng/L), and PFDA (1.07 ng/L) are not significantly different from each other. The overall median PFAS concentration is 25.8 ng/L.

The frequencies of detection for PFASs in urban stormwater runoff are presented in Figure A-4 (Appendix A) As shown, PFOS and PFOA were detected in all samples from residential areas. A Chi-square test was used to examine whether the differences in the proportion of detection were significant. The test results show that the frequencies of detection of PFOS and PFOA are much higher than the other four PFASs at a significance level of 0.05. Overall, PFOS, PFOA, and PFNA are the major species, accounting for 38.3 ± 3.7% (mean ± SEM), 37.0 ± 2.3%, and 11.2 ± 2.6%, respectively, of the total PFASs in the monitored residential stormwater runoff.

2.3.3 Comparison between stormwater runoff and rainfall

PFASs were analyzed in rainfall from six rain events, three of which were at the same dates when surface runoff samples were taken (Figure A-5, Appendix A). The median concentrations were 1.3, 8.4, 1.3, 6.7, 2.6, and <LOD ng/L for PFHpA, PFOA, PFNA, PFOS, PFDA, and PFUnDA, respectively, or a total median PFAS concentration in rain of approximately 24.8 ng/L. These levels were compared to the median concentrations in stormwater runoff collected in three residential areas, one commercial area and one industrial area by the MWW test. The significance level was set at 0.01 (5 comparisons).

At this alpha level, no significant differences were found between stormwater runoff and rainfall, with regard to the median concentrations of PFHpA, PFNA, PFDA, and PFUnDA according to the MWW test results (see Appendix A), suggesting that these four PFASs in runoff mainly come from rainfall. On the other hand, the median concentrations of PFOS and PFOA in stormwater runoff at Dinkytown were significantly higher than the median concentrations of PFOS and PFOA in rainfall (two-tailed p = 0.004 for PFOS and two-tailed p = 0.01 for PFOA), indicating that non-atmospheric sources here are important. Furthermore, the PFAS profiles in rainfall were similar to the profiles in runoff from three residential areas (CSCC, CTC, and Mayo) but distinctively different from the profiles in runoff from the commercial area (Dinkytown) (Figure 2.3). Both statistical analysis and Figure 2.3 indicate that non-atmospheric sources existed in the Dinkytown that contribute PFOS and PFOA to stormwater runoff.

Table 2.1 summarizes previously reported concentrations of PFASs in runoff. The profiles of PFASs in U.S. stormwater runoff are different from those in Japan and Singapore (Murakami et al., 2009; Nguyen et al., 2011; Zushi and Masunaga, 2009), where PFNA is a primary PFAS in the environment (Table 2.1). One possible reason for the difference is that the ammonium salt of PFNA is primarily manufactured in Japan while the ammonium salt of PFOA is largely manufactured in the U.S. (Murakami et al., 2009).

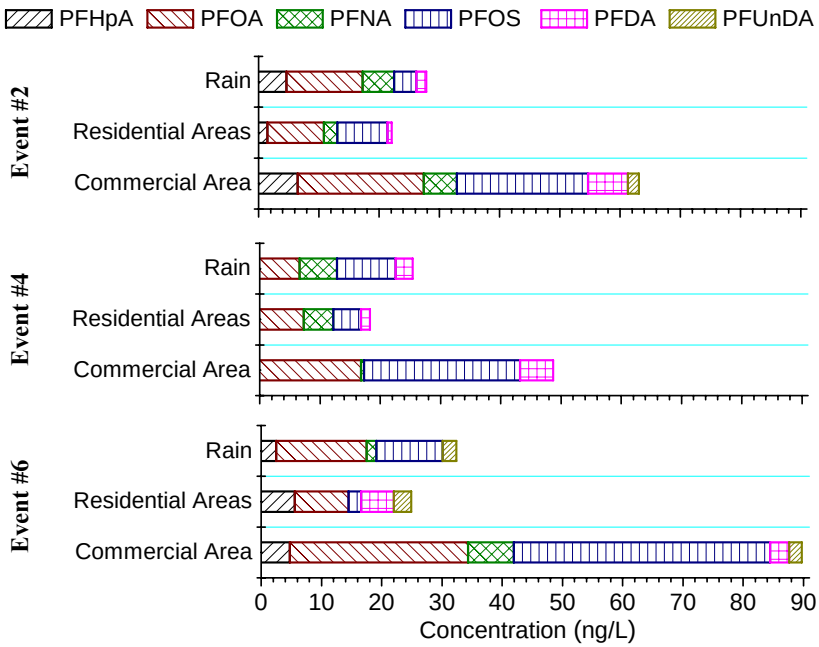

Figure 2.3 PFAS profiles in stormwater runoff at the residential and commercial areas and in rainfall collected from roof downpipe at three heavy rain events (Event 2: August 20 2010; Event 4: Sep 15 2010; Event 6: Oct 26 2010). For the Residential Areas, the results represent the median of combined data from two residential areas.

2.3.4 Industrial area

Monitoring similar to the residential and commercial areas was conducted near a suspected industrial source (Table 2.2). Relatively high concentrations of PFOS (median concentration = 55.4 ng/L) were measured in the runoff, without any other PFASs detected. The MWW test results indicate that the median PFOS concentration in stormwater runoff around the industrial area is significantly higher than the median concentration either in the stormwater runoff at the residential/commercial areas or in rainfall (see Appendix A for the statistical analysis). The industrial area and the subsequent loadings to stormwater were expected to be responsible for PFOS

contamination of nearby Lake Calhoun in Minneapolis (MN, USA) (MPRB, 2008). Many years after the phase-out of the production of PFOS by a major manufacturer, the relatively high-level PFOS in runoff around the industrial source was traced to an industry nearby that used PFOS coated materials in their process (MPRB, 2008). As a result of their relatively high solubility, PFASs could be washed out from the products within the industrial source by rain and enter into surface runoff.

Table 2.1. Concentrations of PFASs in stormwater runoff (ng/L) in previous studies and in the present study.

	PFHpA	PFOA	PFNA	PFOS	PFDA	PFUnDA
Japan [a]	—	17–174	4.7–70	2.8–50	1.8–77	n.a.–45
Japan [b]	5.7–6.4	22.5–28.4	84.9–92.8	38.7–44.1	1.5–5.0	3.3–6.7
Singapore [c]	<0.7–10.5	7.2–38.2	0.9–78.3	4.5–139.0	0.7–28.2	0.2–3.1
U.S. [d]	<LOQ–6.4	0.51–29.3	<LOQ–5.9	<LOQ–14.6	n.d.–8.4	n.d.–2.0
U.S. [e]	n.d.–6.8	3.5–30.6	n.d.–10.7	<LOQ–155.8	n.d.–10.6	n.d.–2.9

[a]: Murakami et al., 2009b; [b]: Zushi and Masunaga, 2009a; [c]: Nguyen et al., 2011; [d]: Kim and Kannan, 2007; [e]: the current study (including PFOS concentrations in runoff collected from the industrial area); n.a.: not available; n.d.: not detected.

Table 2.2. PFOS in stormwater runoff around an industrial source and on particles in stormwater runoff (other five PFASs were either not detected or below the detection limits).

PFOS in stormwater runoff (ng/L) collected at an industrial area (Sep 25 2009)	
36th and Brunswick	50.0
36th and Alabama	8.7
36th and Yosemite	55.4
36th and Kenwood	156.0
351/2	59.6
Extractable PFOS on particles in stormwater runoff, ng/gTPM	
36th and Brunswick [a]	280.4
36th and Kenwood [a]	120.5
351/2 [a]	590.0
Dinkytown [b]	19.8
Dinkytown [c]	45.9
[a]: Sep 25 2009; [b]: Sep 01 2010; [c]: Sep 15 2010; LOD: detection limit; TPM: total particulate matter.	

2.3.5 Extractable PFASs on particles in stormwater runoff

Urban runoff transports a wide gradation of anthropogenic aqueous complexes and particulate matter (PM) (Kim and Sansalone, 2008). No previous studies have yet been performed to determine the level of PFASs on PM in stormwater runoff. When one considers the aqueous concentrations of PFASs in the runoff (a few tens of ng/L), the total particulate matter (TPM) of stormwater runoff (e.g., 100 mg/L), and the low solid–water partitioning coefficient (K_d) (several L/kg) (Higgins and Luthy, 2006), no PFASs are expected to be detected on the solid particles in the runoff. However, high levels of PFOS were detected on the solid particles in stormwater runoff collected from the industrial area and the commercial area (Table 2.2). The TPM of the stormwater runoff at the two areas ranged from 22 to 137 mg/L. Therefore, solid–water partitioning cannot be the mechanism responsible for the high PFOS levels on PM. Otherwise the K_d value of

PFOS will reach $10^{4.0}$ L/kg, which would be orders of magnitude higher than ever before reported in the literature (Higgins and Luthy, 2006; Xiao et al., 2011b). The PFOS should be inherent in the particles/debris, possibly including the debris of textiles and carpet, and several industrial polymers containing PFOS. The debris from these products and solids could have been carried by stormwater into surface runoff. For the Dinkytown area, which also had substantial particulate PFOS concentrations, fine PM from vehicular traffic (Murakami and Takada, 2008) and the debris of commercial food packaging (such as microwave popcorn bags, fast food and candy wrappers, and pizza box liners (Weise, 2005)) are suspected to contribute PFOS on the particles in stormwater runoff.

2.3.6 Mass loads of PFASs from stormwater runoff

The equation used in a previous study (Murakami et al., 2009) was modified for estimating the loads (L) of background PFASs from surface runoff in the Minneapolis–St. Paul metropolitan area where the measurements were taken:

$$L = SR_{PFAA} \times SV = SR_{PFAA} \times P \times k \times A_I \qquad (2.3)$$

where SR_{PFAS} is the PFAS concentration in the surface runoff; SV is the surface runoff volume; k is a runoff coefficient that converts rainfall to runoff; P is the average annual precipitation (747 mm); and A_I is the impervious area of the region (679.9 km^2, see Table A-2, Appendix A). The value of the runoff coefficient, k, used for the calculation is 0.6 after taking account of the connectivity of impervious area (see Table A-3, Appendix A). The results are as follows: PFHpA, 0.19 ± 0.79; PFOS, 3.23 ± 3.74; PFOA, 2.83 ± 2.48; PFNA, 1.11 ± 1.04; PFDA, 0.32 ± 0.95; PFUnDA, 0 ± 0.30 kg/year. The relatively large

standard deviation reflects that the data of PFAS concentrations at different sampling sites are skewed. The total load of PFASs was estimated as 7.86 ± 9.30 kg/year. These values do not include the load of PFASs from industrial areas because they have not been well quantified, and should not be seen as urban background concentrations. These values are smaller but close to the PFAS loads from street runoff in Japan (Murakami et al., 2009). The mass load of PFOS in urban runoff is one fourth of the total PFOS load at the confluence (Minnesota) to the Upper Mississippi river (Nakayama et al., 2010), indicating urban runoff is an important source of PFOS to urban waters. As more evidence accumulates that urban areas can contribute PFAS pollution to surface water through surface runoff and storm sewers, the ability of SMPs to remove PFASs requires investigation in the future. Many stormwater SMPs are being implemented in metropolitan areas to remove suspended solids and particle-associated pollutants from stormwater runoff (Weiss et al., 2007). However, to date, no information is available on the removal of PFASs by SMPs.

The loads of PFASs from rainfall were computed by multiplying the concentrations determined for rainfall, the average annual rainfall per year and the metropolitan area in the Minneapolis–St. Paul region. The results are 1.89 ± 0.43 (PFOA), 1.48 ± 0.30 (PFOS), 0.29 ± 0.65 (PFNA), 0.28 ± 0.34 (PFHpA), 0.25 ± 0.10 (PFDA), 0 ± 0.08 (PFUnDA) kg/year. The total load of PFASs was estimated as 4.17 ± 1.92 kg/year. When multiplied by the runoff coefficient, k = 0.6, rainfall can account for a PFAS load of 2.52 ± 1.15 kg/year, which is about one third of PFAS load computed from runoff concentrations applied to Eq 2.3 of 7.86 ± 9.30 kg/year.

Chapter 3: CHARACTERIZATION OF PERFLUOROALKYL SUBSTANCES IN WASTEWATER TREATMENT PLANTS

Feng Xiao, Thomas R. Halbach, Matt F. Simcik, John S. Gulliver, 2012. Input characterization of perfluoroalkyl substances in wastewater treatment plants: Source discrimination by exploratory data analysis. ***Water Research*** 46, 3101–3109.

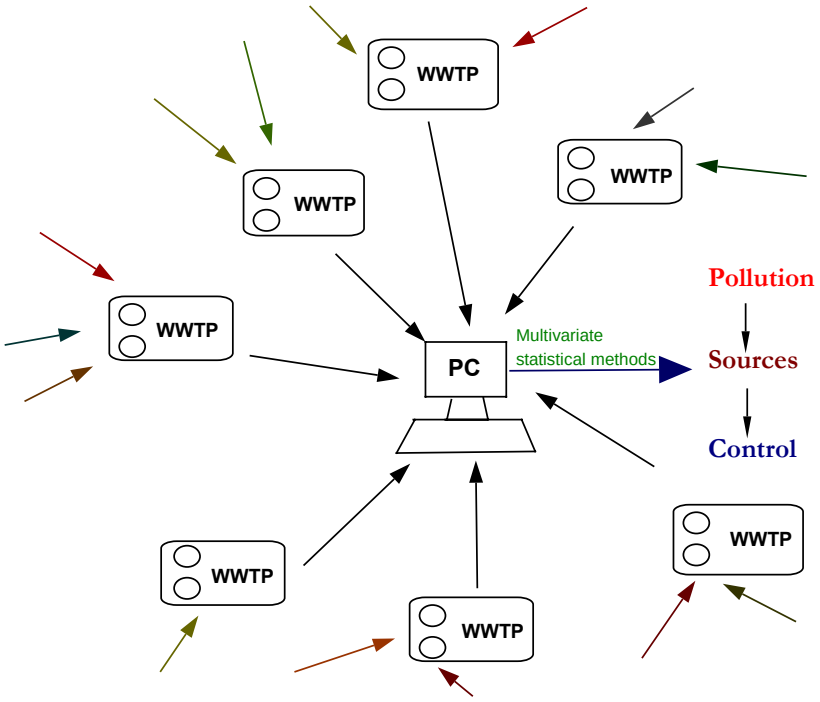

Graphical abstract

3.1 Introduction

The pollution of long-chain PFASs is a worldwide problem due to persistency, toxicity and tendency to bioaccumulate (Jahnke and Berger, 2009). They have been detected in many components of the biosphere, including human blood samples worldwide at typical concentrations of several to tens of μg/L (Haug et al., 2009; Kärrman et al., 2006; Kato et al., 2011; Yeung et al., 2006). The presence of PFAS in human blood has been associated with attention deficit/hyperactivity disorders in children (Hoffman et al., 2010) and hyperuricemia (Steenland et al., 2010).

PFASs in WWTPs are of great concern because wastewater treatment processes show no significant removal of PFASs (Loganathan et al., 2007; Schröder and Meesters, 2005; Schultz et al., 2006a; Yu et al., 2009a). WWTP effluent has been confirmed to be an important route of discharging PFASs into the receiving water bodies (Ahrens et al., 2011a; Boulanger et al., 2005; Clara et al., 2009; Clara et al., 2008; Guo et al., 2010; Huset et al., 2008; Murakami et al., 2008; Schultz et al., 2006a; Schultz et al., 2006b; Sinclair and Kannan, 2006; Yu et al., 2009a), which can bioaccumulate in aquatic food webs and ultimately end up being consumed by humans. Clara et al. (2009) found that more than 50% of the PFAS mass flows in Danube River can be attributed to wastewater discharges. Probable sources of PFASs in WWTPs include domestic and industrial wastewater inputs, due to the use of fluorochemicals in household cleaners and industrial/commercial products (Huset et al., 2008).

The State of Minnesota may be in a unique position in the study of PFASs: it is home to 3M, which produced and disposed of many of PFASs in its Cottage Grove

facility, Oakdale and Woodbury dumping sites, and Washington landfill around the Minneapolis–St. Paul metropolitan area, the sixteenth largest metropolitan area in the U.S.. Minnesota is also the place where the Mississippi River, the largest river system in North America, has its origin. The effluent of many Minnesota WWTPs is discharged into the Mississippi River or its tributaries, including the Minnesota River.

Previous studies have documented that PFASs are widely present in the Minnesota environment (Delinsky et al., 2010; Nakayama et al., 2010; Xiao et al., 2011a). However, the sources of PFASs remain largely unknown, especially the relative importance of domestic and industrial influences after the 2000–2002 phase-out of the production of perfluorooctane sulfonate (PFOS) and perfluorooctanoate (PFOA) by 3M. Once the geographical distribution of sources is identified and confirmed, reducing the inputs of PFASs to the Upper Mississippi River Basin can be addressed. This study develops a methodology for a source assessment of PFASs in the influent and effluent from 37 WWTPs serving more than 40 cities across Minnesota (USA). The methodology is built upon a comprehensive and exploratory multivariate data analysis including the hierarchical clustering method and the scatter matrix. The use of this methodology makes it possible to (a) obtain more information about the structure of the data; and (b) separate and track down the sources of PFASs. Despite 3M's phase-out, there is a substantial reservoir of PFAS-containing substances/products still in use in metal plating, carpets, paper and packaging, leather/apparel, textiles and household cleaning products (Paul et al., 2011). This analysis indicates that ongoing emissions from industrial sources continue discharging significant mass flows of certain PFASs into the aquatic environment.

3.2 Methods

3.2.1 A database of PFASs in Minnesota WWTPs

A database of PFASs in Minnesota WWPTs (MPCA, 2009) was used to develop this methodology. The WWTPs in a statewide survey (MPCA, 2009) were selected to represent a wide geographic distribution in Minnesota (USA), receipt of a variety of wastewater (domestic, commercial and industrial) and a variety of treatment processes (see Figure 3.1 for the geographic distribution of WWTPs surveyed). The State of Minnesota (44–47°N; 91–97°W) has a total area of 2×10^5 km^2 and a population of more than five million. A total of 13 PFASs were analyzed in influent, effluent and sludge from 37 WWTPs serving more than 40 cities in Minnesota with perfluorohexanoic acid (PFHxA), PFHpA, PFOA, PFNA and PFOS being the most frequently detected medium- to long-chain PFASs. Minnesota also conducted a similar but smaller-scale statewide survey in 2007, and the samples were analyzed by Axys Analytical Services, British Columbia, Canada (Kelly and Solem, 2008). PFAS concentrations were analyzed by Axys Method MLA-060 by liquid chromatography–tandem mass spectrometry (LC–MS/MS), following solid-phase extraction and selective elution procedures. Target compounds were quantified using the internal standard method, comparing the area of the quantification ion to that of the labeled standard and correcting for response factor. Samples were collected by pre-cleaned and proofed polypropylene bottles, and PFAS-free blue ice was used for shipping. PFAS-containing materials were avoided during sampling and analysis. QA/QC considerations also include using nitrile gloves, wearing

old clothing (laundered at least six times), avoiding pre-wrapped food and snacks, and avoiding wearing water resistant clothing and insect repellant/sunscreen (Erickson, 2008). The reporting limits can be found in the literature (MPCA, 2009).

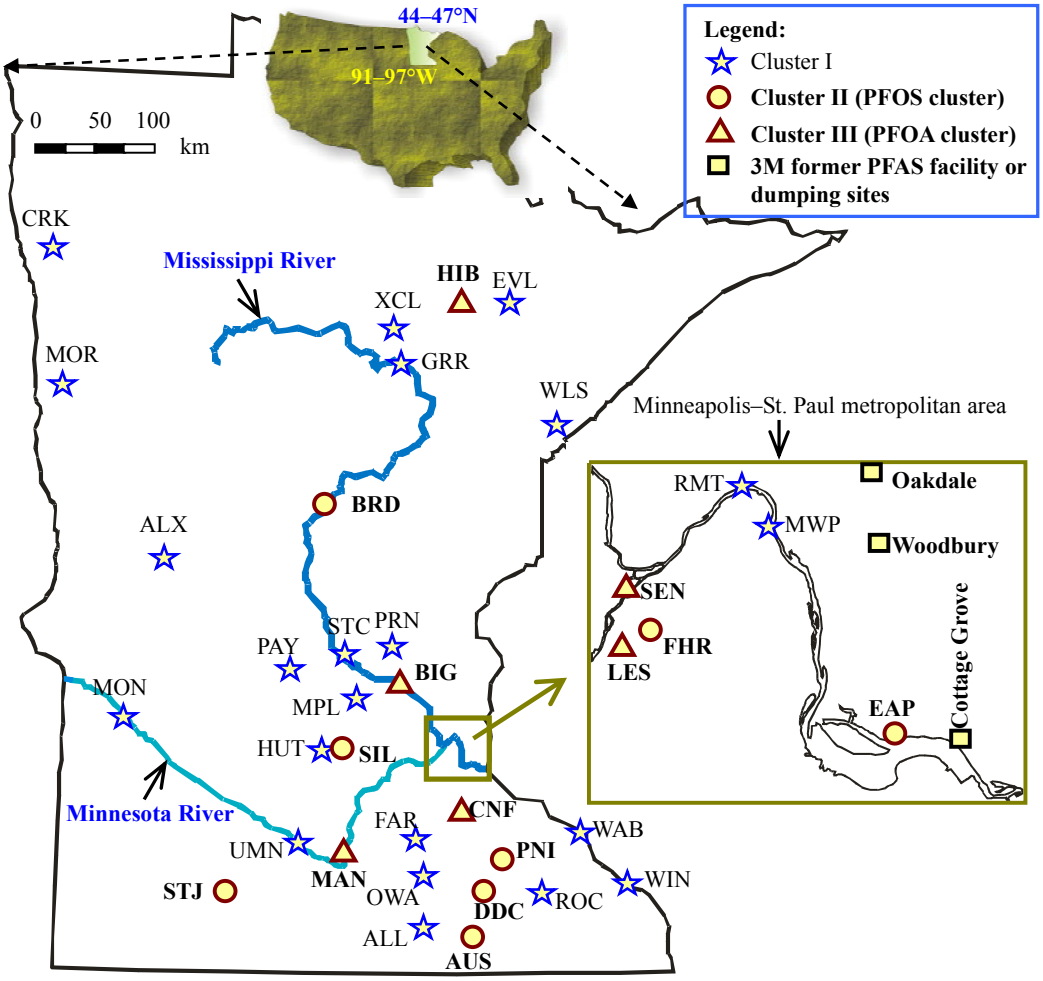

Figure 3.1 Wastewater treatment plants included in a statewide survey. Included were the WWTPs of the Minneapolis–St. Paul metropolitan area (MWP), Flint Hills Resources (FHR), Xcel Energy (XCL), and the Cities of Albert Lea (ALL), Alexandria (ALX), Austin (AUS), Big Lake (BIG), Brainerd (BRD), Cannon Falls (CNF), Crookston (CRK), Dodge Center (DDC), Eveleth (EVL), Faribault (FAR),), Grad Rapids (GRR), Hibbing (HIB), Hutchinson (HUT), Le

Sueur and Henderson (LES), Mankato (MAN), Maple Lake (MPL), Cottage Grove (EAP), Rosemount (RMT), Eagan (SEN), Montevideo (MON), Moorhead (MOR), New Ulm (NUM), Owatonna (OWA), Paynesville (PAY), Pine Island (PNI), Princeton (PRN), Rochester (ROC), Silver Lake (SIL), St. Cloud (STC), St. James (STJ), Wabasha (WAB), Winona (WIN), and Duluth, Cloquet, Hermantown, Proctor, Carlton, Scanlon, Thomson, and Wrenshall (WLS).

3.2.2 Statistical analysis

Large-scale surveys and water-quality monitoring programs provide a knowledge base for understanding the status of PFAS pollution. However, they produce large sets of data that are often difficult to interpret. The problem of data reduction and the interpretation of the occurrence of PFASs can be approached through the application of exploratory and multivariate statistical methods.

Cluster analysis is a multivariate data analysis tool for sorting monitoring points into clusters/groups, so that the degree of association is weak between members of different clusters and strong between members of the same cluster, and has been largely used in source apportionment of organic pollutants (Haack et al., 2003; Ikonomou et al., 2002; Kavouras et al., 2001; Lohmann et al., 1999). In the present work, cluster analysis serves to aggregate the PFAS patterns of WWTP influent samples so that the patterns in any one cluster are as similar to each other as possible, and as different from other clusters as possible. During cluster analysis, the closest pair of PFAS samples was linked into a cluster according to a similarity measure. The similarity measure generally used here is the squared Euclidean distance (Johnson and Wichern, 1998), which is given as

$$d_{ij} = \sum_{k=1}^{m} \left(X_{ik} - X_{jk} \right)^2 , \qquad (3.1)$$

where d_{ij} is the distance between the i^{th} and j^{th} observations, and X_{ik} is the value of i^{th} observation for the k^{th} variable of m variables.

For the cluster analysis, the raw data—the measured concentrations of five PFASs—needs to be suitably transformed. Values below specified limits were assigned a value of one-half of the limits. The concentration of each of the five PFASs was normalized by the total concentration of PFASs in every setting in order to avoid misclassifications arising from the different order of magnitude of PFAS concentrations. As the method of classification used makes no *priori* assumptions about the underlying statistical distribution of the data (non-parametric), no evaluation of normal distribution of the data is necessary. There are several methods for linking clusters. The Ward's method results were considered the most reasonable based on comparison of the results from different classification methods with the background information (Johnson and Wichern, 1998). In all clustering algorithms discussed herein, Ward's method was used as an agglomeration technique while the squared Euclidean distance was used to measure similarity among monitoring points. The clustering is carried out by minimizing the sum of squared Euclidean distance, *SS*, which is given as

$$SS = \sum_{k=1}^{M} \sum_{j=1}^{N} \sum_{i=1}^{P_k} \left(X_{ijk} - \overline{X_{jk}} \right)^2 , \qquad (3.2)$$

where M is the number of clusters, X_{ijk} is the value of the j^{th} variable for the i^{th} observation in the k^{th} cluster, N is the total number of variables (37 WWTPs), P_k is the number of observations in the k^{th} cluster, and $\overline{X_{jk}}$ is the k^{th} cluster sample mean of the j^{th} variable. The value of M was determined based on the stability of the results of different cluster analyses and background information (Johnson and Wichern, 1998).

The cluster and correlation analysis, ANOVA test and scatter matrix were performed using SPSS 17.0 (now known as PASW, for Windows, SPSS Inc. IL, USA). The box plot was created by Origin 8 (for Windows, OriginLab, MA, USA).

3.2.3 Fugacity analysis

Fugacity (*f*, Pa) is a surrogate for chemical concentrations for chemical fate modeling (Wania et al., 2003). A mass balance model based on fugacity analysis (STP, Trent University) was used to evaluate the fate of a precursor of PFOA, 8:2 fluorotelomer alcohol (8:2 FTOH), in a WWTP. The input parameters for the model were given in Table B-1, Appendix B.

3.3 Results and discussion

A data analysis was carried out, covering the entire geographical area of the Upper Mississippi River Basin in Minnesota and considering the following individual molecular markers: PFHxA, PFHpA, PFOA, PFNA, and PFOS. The dendrogram of sampling points obtained by the cluster analysis is shown in Figure 3.2 (or see Figure B-1 of the Appendix B showing the raw dendrogram with lower resolution). Six sub-clusters were identified, and three well-differentiated clusters were observed: (I) a cluster containing WWTPs with low concentrations of PFOS and PFOA in the influent (MPL through CRK); (II) a cluster characterized by high concentrations of PFOS (STJ through PNI); and (III) a cluster formed by two subclusters characterized by high concentrations of PFOA (HIB through LES).

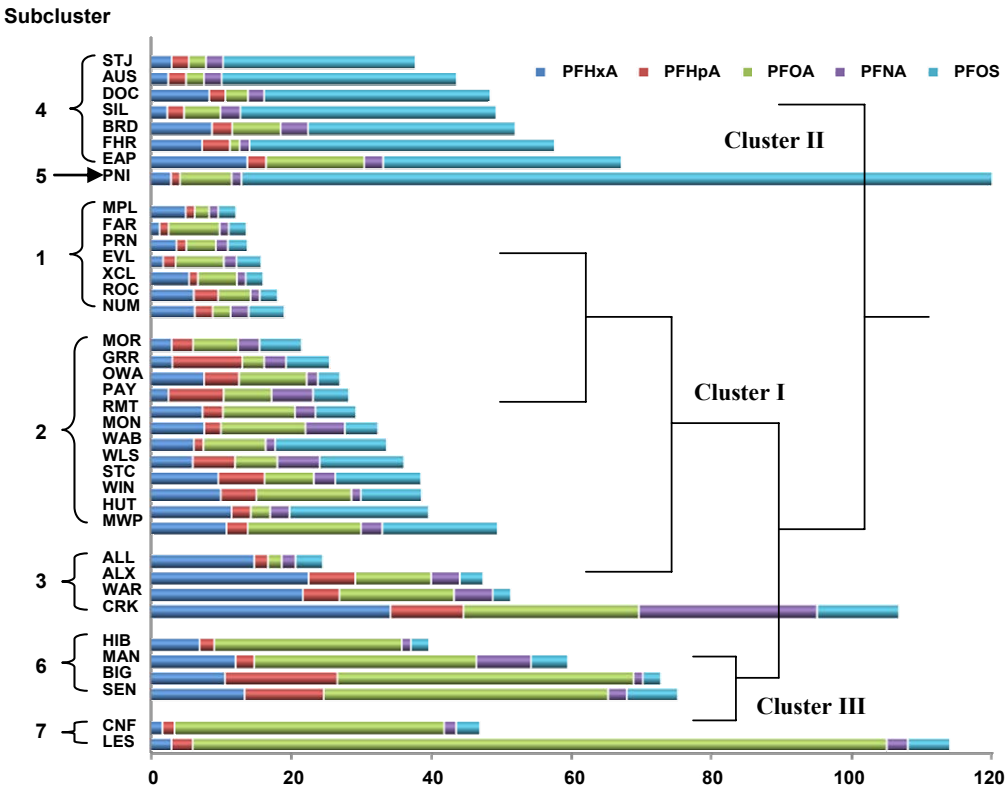

Figure 3.2 Cluster analysis of MPCA (2009) influent PFAS concentrations (ng/L) in WWTPs (*n* = 37).

3.3.1. Domestic inputs (Subclusters 1 and 2)

Cluster I is the largest, formed by three subclusters (1–3) (see Table B-2 or Figure B-1 in the Appendix B). WWTPs in Subclusters 1 and 2 have low influent concentrations of all PFASs. Low specific per capita discharges have been identified as an indicator for domestic inputs, while high specific per capita discharges have been identified as an indicator for potential industrial inputs (Clara et al., 2009; Huset et al., 2008). Based on the treatment capacities provided by WWTP operators, the calculated per capita

discharges were: PFHxA, 0.67–5.1; PFHpA, 0.17–1.4; PFOA, 0.30–7.6; PFNA, 0.17–1.4; PFOS, 0.35–7.8 μg/capita/d. These values are significantly smaller than those determined for WWTPs strongly influenced by industrial sources (Clara et al., 2009). Clara et al. (2009) found that the per capita discharges of PFHxA, PFHpA, PFOA, PFNA and PFOS were 40 (45), 12 (8), 73 (14), 8 (1) and 66 (10) μg/capita/d for two WWTPs receiving industrial wastewater, respectively. In addition, a significant correlation (two-sided p = 0.017; R^2 = 0.52) between population and PFAS concentrations in the influent was observed (see Figure 3.3). These results indicate that PFASs in WWTPs of Subclusters 1 and 2 were mainly derived from domestic sources.

The skewness of the PFAS concentrations in the influent of Subclusters 1 and 2 WWTPs lies mostly between 0 to 1, indicating that the data can be treated as normally distributed and the means can be tested by the robust one-way ANOVA and post-hoc tests. The Tamhane's T2 post-hoc test was chosen for unequal variance and the significance level, 0.05, was adjusted during multiple comparisons to avoid increasing the risk of rejecting a true null hypothesis (Pagano and Gauvreau, 2000). The results have been presented in Table B-3, Appendix B. At a significance level of 0.01 (=5!/(5–2)!/2!, five comparisons), the mean concentrations of PFHxA (6.0 ng/L), PFOA (7.1 ng/L), and PFOS (7.2 ng/L) are not significantly different from each other (see Table B-3). However, their mean concentrations are significantly higher than PFHpA and PFNA (see Table B-3). The overall mean concentration of five PFASs is 5.3 ng/L, which can be seen as a background/control PFAS concentration in WWTP influent. The box-whisker plots in

Figure B-2 (Appendix B) illustrate the five-number summaries, e.g., the lower and upper quartiles.

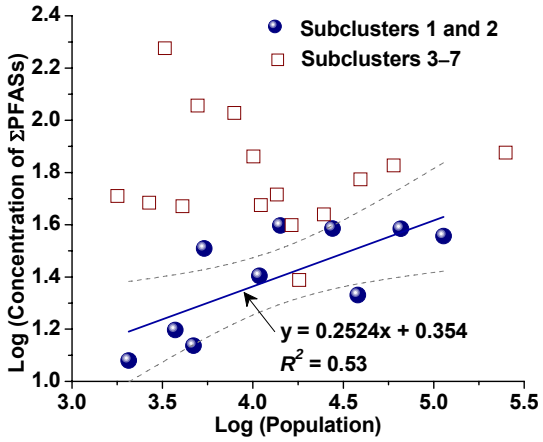

Figure 3.3 Correlation between population and (MPCA, 2009) influent PFAS concentrations (ng/L) in WWTPs.

Correlation analysis was conducted to further understand the sources of PFASs in WWTPs. As evident in the scatter matrix (Figure B-3, Appendix B), PFOS concentrations displayed a significant linear correlation with PFHxA concentrations (two-sided $p = 0.002$; $r = 0.658$), suggesting a relationship between the sources of these two compounds. Furthermore, PFHxA and PFOA concentrations were correlated ($r = 0.418$); the relationship is insignificant at an alpha level of 0.05 but significant at an alpha level of 0.1 (Figure B-3, Appendix B), indicating a relationship between their sources.

3.3.2 Plausible non-domestic sources

3.3.2.1 PFHxA cluster

The Subcluster 3 in Cluster I contains four WWTPs serving four cities, which is characterized by elevated levels of PFHxA in WWTP influent compared to the other 33 WWTPs. The per capita discharges of PFHxA calculated from the populations served by Subcluster 3 WWTPs (e.g., 36.2 and 38.6 μg/capita/d for ALX and ALL respectively) are higher than those in Subclusters 1 and 2 but are close to the levels for WWTPs with known industrial sources (Clara et al., 2009). The results indicate that industrial sources of PFHxA are probably present in Subcluster 3 WWTPs' catchment areas, contributing PFHxA in WWTPs. Like PFOA, PFHxA has also been used in food/pharmaceutical packaging and water/oil repellent paper coating. The restriction on the production of PFOA may force manufacturers to find other replacements. Currently there are no restrictions on the production/use of PFHxA in the U.S., with 3M and DuPont being the major manufactures in the U.S. (Environmental Working Group, 2012).

3.3.2.2 PFOS cluster

Cluster II is the second largest cluster with two subclusters (4 and 5), characterized by significantly high-level PFOS in WWTP influent. The concentration of PFOS at PNI is the highest among all 37 WWTPs. The PNI WWTP receives wastewater from an electroplating industry that uses a PFOS-containing mist suppressant to control hexavalent chromium emissions. The BRD WWTP in this cluster receives industrial wastewater from another chrome plating industry (Kelly and Solem, 2008). From the viewpoint of worker safety, PFOS-containing mist suppressants have been exempted from the recent (2007) USEPA Significant New Use Rule regarding PFASs (Kelly and

Solem, 2008). The USEPA estimates that up to 8000 kilograms of PFOS-containing mist suppressants are used per year in the U.S. (Kelly and Solem, 2008). Considering the suppressants contain 1–10% PFOS by weight, 80–800 kilograms of PFOS are directly discharged into the environment annually through the use of mist suppressants in the United States. The high PFOS concentration in the EAP WWTP could be due to fact that EAP receives wastewater from the City of Cottage Grove, which contains a former PFOS disposal site.

The cluster analysis provides an estimate of source profiles of poorly characterized sampling sites. If a poorly characterized site merges with a group of sampling sites of known source type or types, the poorly characterized site is likely to have similar source types (Wongphatarakul et al., 1998). The clustering methods show that AUS, STJ, DDC, FHR and SIL merged with PNI, BRD and EAP into one cluster. The linkage distances between them were small on the dendrogram, indicating high composition similarity. PNI, BRD and EAP have known local non-domestic PFOS sources. Therefore, although no definitive explanation can be given at this stage, it is probable that non-domestic sources also exist in other sampling sites within the PFOS cluster.

3.3.2.3 PFOA cluster

The Cluster III WWTPs have high concentrations of PFOA (see Figure 3.2). The dendrogram reveals that the data points can be classified into two subclusters (6 and 7) (see Figure 3.2 or Figure B-1 of Appendix B). The data points which had divergent patterns (high-level PFOA and moderate-level PFHxA and/or PFHpA) were merged into

Subcluster 6, while those with high-level PFOA concentrations only were grouped in Subcluster 7. The per capita discharges of PFOA for Cluster III WWTPs ranged from 20.8 μg/capita/d for SEN to 30.3 μg/capita/d for LES, much higher than the average value in 10 WWTPs across the U.S. (11 μg/capita/d) (Huset et al., 2008). This is taken as a sign of non-domestic sources. The exact sources of PFOA in Cluster III are not clear; however, SEN is near the 3M facility or dumping sites (see Figure 3.1) and could be influenced by the past industrial activities. In addition, LES WWTP receives food-processing wastewater from a cheese and food ingredient manufacturers in LES. PFOA has been widely used in food-packaging and paper grease-proofing treatments (European Food Safety Authority, 2008), which could be the source for PFOA in LES WWTP. The insignificant and weak relationship between influent PFAS concentrations and the populations in the Cluster III WWTPs' catchment areas (see Figure 3.3) also indicate that domestic human activities are not the major source. The results agree with a Pan-European survey (Pistocchi and Loos, 2009), which concludes that PFOA discharges are strongly influenced by emissions from industrial facilities.

3.3.3 PFASs in WWTP effluent

PFASs in WWTP effluent could be degraded from corresponding precursors (Dinglasan et al., 2004; Rhoads et al., 2008). For example, 8:2 FTOH could be biodegraded, producing PFOA, and 6:2 FTOH could form PFHxA (Dinglasan et al., 2004). As illustrated in Figure 3.4, concentrations of PFHxA and/or PFOA were significantly higher in the effluent than in the influent of WWTPs (two-sided $p < 0.05$) in 22 out of 37

WWTPs (59%). The results indicate that these WWTPs received wastewater containing large amounts of precursors of PFHxA and PFOA. Several WWTPs (e.g., OWA, PRN, RMT, ROC and STC) were observed to have a significant concentration increase of both PFHxA and PFOA in the effluent. By contrast, only two WWTPs (EAP and MWP) with the 3M's Cottage Grove facility and Oakdale and Woodbury dumping sites around received wastewater containing considerably high concentration of PFOS' precursors. Although it is unsure whether FTOHs have been used as the replacements to PFOS or PFOA by some industries under USEPA pressure, FTOHs are used in the manufacture of a wide range of products, such as metals, paints, electronics and adhesives, and have similar applications as PFOS-based products (Dinglasan et al., 2004). The fate of PFASs in WWTPs has been studied (Guo et al., 2010; Yu et al., 2009); however, little is known about their precursors. The fate of one precursor (8:2 FTOH) was modeled based on fugacity analysis (see Table B-1, Appendix B). The results show that 9.0% of 8:2 FTOH can be biodegraded to PFOA or other similar compounds in the activated sludge tank (see Figure 3.5), consistent with the range (1–10%) estimated by Wang et al. (2005). It is interesting to note that more than 25% of 8:2 FTOH can be emitted to air in the aeration tank, mainly because of its high vapor pressure (see Table B-1, Appendix B). This agrees with the observations that WWTPs are an important source of FTOHs to the atmosphere (Dinglasan et al., 2004; Weinberg et al., 2011). Because only less than 10% of 8:2 FTOH can be eventually converted to PFOA, the significant increase of PFAS mass flows observed in the effluent of some WWTPs (e.g., ROC, PRN and OWA) implies that these

WWTPs received high loads of 82 FTOH and/or other precursors, such as polyfluoroalkyl phosphates (Lee et al., 2010), could also be present in the influent.

In addition, PFASs did not exhibit significant removal across all 37 WWTPs. Advanced and/or tertiary treatment (e.g., UV sterilization in EAP and chlorination in MWP) did not appear to decompose PFASs. The results are consistent with previous studies indicating that PFASs are not readily removed by physicochemical and biological treatment processes (Loganathan et al., 2007; Schröder and Meesters, 2005; Schultz et al., 2006a; Yu et al., 2009a). The limitations proposed by MPCA (Minnesota Pollution Control Agency) are 10 ng/L monthly average and 17 ng/L daily maximum of PFOS in the effluent from WWTPs. The effluent PFOS concentrations in ten (27%) of the WWTPs surveyed would not be able to meet the daily maximum being proposed by MPCA, which calls for significant and expensive modification to the current plant treatment processes to attempt to remove PFOS.

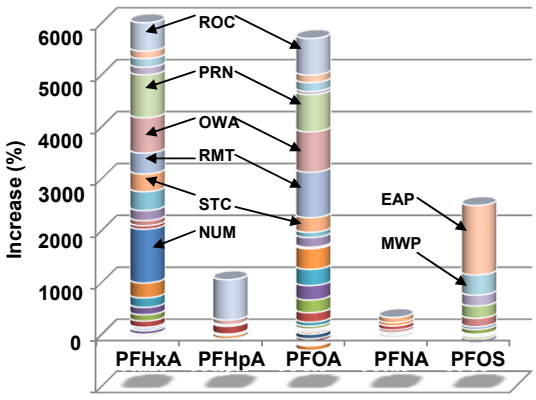

Figure 3.4 Percent increase in MPCA (2009) PFAS concentrations from WWTP influent to effluent.

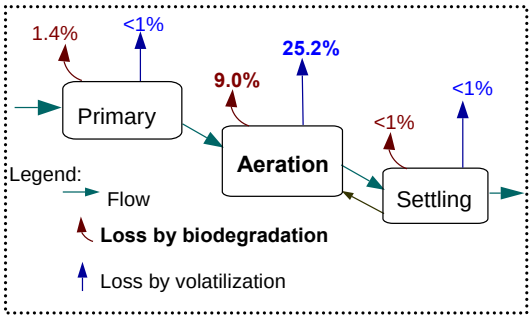

Figure 3.5 Mass losses of 8:2 FTOH during the primary treatment and secondary treatment consisting of aeration and secondary settling.

3.3.4 Limitations

One important limitation of cluster analysis is that it can provide a solution even when it is applied to random data. Therefore, it is important for researchers to assess the quality of the cluster solution and to determine whether the clusters are conceptually meaningful (Bengtson et al., 2005).

Chapter 4: EFFECTS OF MONOVALENT CATIONS ON COMPETITIVE ADSORPTION OF PERFLUOROALKYL SUBSTANCES BY KAOLINITE: EXPERIMENTAL STUDIES AND MODELING

Feng Xiao, Xiangru Zhang, Lee Penn, John S. Gulliver, Matt F. Simcik, 2011. Effects of monovalent cations on the competitive adsorption of perfluoroalkyl substances by kaolinite: Experimental studies and modeling. ***Environmental Science & Technology*** 45(23), 10028–10035.

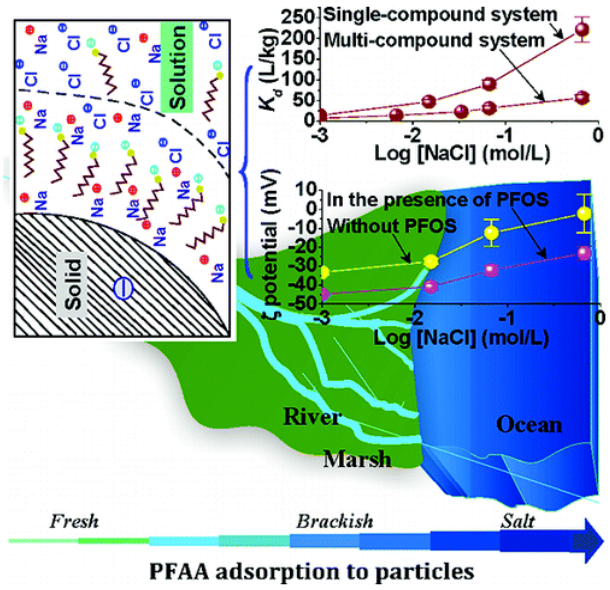

Graphical abstract

4.1 Introduction

Concern has grown over the contamination of worldwide freshwater and marine sites by PFASs. PFASs are synthetic organic compounds in which all the C−H bonds are replaced by C−F bonds. PFASs and their precursors have been produced and used widely for decades in cookware, fast food containers, fire-fighting foams and painting materials (Giesy and Kannan, 2001, Jeon et al., 2010). Long-chain PFASs (≥7 perfluorocarbons) are persistent organic pollutants that cannot be hydrolyzed, directly photolyzed, or biodegraded under environmental conditions (OECD, 2002, Prevedouros et al., 2006). In surface water, the levels of PFASs range from tens to hundreds of ng/L. In some contaminated groundwater, the concentrations can be thousands of ng/L. The presence of PFAS in human blood has been associated with attention deficit/hyperactivity disorders in children (Hoffman et al., 2010) and hyperuricemia (Steenland et al., 2010).

A fundamental characteristic of surfactants is their tendency to adsorb at solid–water interfaces in an oriented fashion (Rosen, 2004). PFAS adsorption by natural adsorbents (soils, suspended solids, sediments, and aquifer materials) is an important determinant of their transport and fate in the environment. Previous studies have shown that the adsorption of PFASs at solid–water interfaces is controlled by both hydrophobic and electrostatic effects (Higgins and Luthy, 2006; Johnson et al., 2007; Tang et al., 2010; Wang and Shih, 2011; You et al., 2010). Greater organic carbon content of the adsorbent, higher aqueous Ca^{2+} or H^{+} concentration, or longer perfluorocarbon chains can increase the adsorption of PFASs (Higgins and Luthy, 2006; Johnson et al., 2007; Tang et al., 2010; Wang and Shih, 2011; You et al., 2010).

Nevertheless, the published reports do not provide a complete and consistent picture of PFAS adsorption. First, the effect of Na^+ and the role of electrostatic interactions need to be better understood. NaCl has been used as a road de-icing agent for decades in many northern regions, where snowmelt during the spring carrying a significant load of NaCl runs into storm sewers, ditches and small streams and then empties into wetlands, lakes and rivers. In seawater the concentration of Na^+ can reach 0.5 M (Snoeyink and Jenkins, 1980). Knowledge of the effect of Na^+ on PFAS adsorption may provide key insights into the environmental fate of PFASs and the associated ecosystem risks (Jeon et al., 2010). A recent study (Tang et al., 2010) described the effect of sodium on the electrostatic interaction between PFAS molecules adsorbed on mineral surfaces. However, there is a lack of quantitative estimations about this interaction. In the present study, the effects of sodium on the electrokinetic potential (ζ) of kaolinite suspensions with and without the presence of PFASs are investigated and modeled to provide both the qualitative the quantitative descriptions of the electrostatic interaction. Second, it is not clear whether PFAS molecules compete for suitable sites during adsorption. No competition was found during the sorption of PFASs to sediment (Higgins and Luthy, 2006). However, the hydrophobic effect increases with the hydrophobic length of the PFAS (Higgins and Luthy, 2006) and thus a longer-chained PFAS may outcompete a shorter-chained PFAS during adsorption. One study has observed the competitive adsorption of PFASs to aerobic active sludge (Zhou et al., 2010).

The purpose of this chapter is to experimentally examine and model important chemical and mineralogical factors affecting PFAS adsorption. With this goal, PFAS

adsorption by kaolinite clay is investigated with respect to the influences of sodium concentration and PFAS perfluorocarbon chain length. The effect of PFAS adsorption on kaolinite surface charges is also studied. Kaolinite was selected as the adsorbent because it is a major type of clay mineral in the soils and sediments in warm climates. Understanding the interactions between kaolinite and PFASs can provide mechanistic insights into the adsorption behavior of PFASs and can facilitate the assessment of the relative contribution from mineral components to PFAS adsorption by soils and sediments.

4.2 Materials and methods

4.2.1 Chemicals

PFHpA, PFOA, PFNA, PFOS, PFDA, and PFUnDA were purchased from Sigma(–Aldrich) (Milwaukee, WI, USA & Steinheim, Switzerland) (see Table C-1, Appendix C). Methanol (Optima grade from Fisher Scientific) and water (HPLC grade from Fisher Scientific) were used to clean the containers and tubes used in the experiments. No PFASs were found in the methanol or water when this was checked using an HPLC coupled to a Hewlett Packard 1100 MSD mass spectrometer with an electrospray ionization source (ESI-MS). Two kinds of stock solutions were prepared. The individual PFAS stock solutions were prepared by dissolving a single PFAS in methanol (1 mM). A multiple PFAS stock solution was made by dissolving all the PFASs except for PFHpA in methanol (1 mM for each PFAS). Each stock solution was split into three aliquots. One

was used in the experiment, and the other two were used to periodically check for any changes in the concentration. All the stock solutions were stored at –20 °C.

4.2.2 Adsorption experiments

The batch adsorption experiments were carried out in triplicate in 50-mL polystyrene tubes containing 40 mL of test suspension, which were continuously shaken by a wrist action shaker (Burrell) for 48 h at 22.2 ± 0.5 °C. Preliminary tests had shown that the time required to reach adsorption equilibrium was 48 h. Unless otherwise specified, the test suspension was composed of 1.0 mM $NaHCO_3$ (alkalinity), 1.0 mM NaCl, and 20 mg kaolinite clay (Fluka) that had been ultrasonically dispersed in the water. The size distribution of the kaolinite suspension was measured by a Coulter laser diffraction particle size analyzer (LS 320, Coulter Electronics, USA). The kaolinite had a mean diameter of 1.1 μm with a narrow size distribution (Figure C-1, Appendix C). The surface area of the kaolinite particles was 10 m^2/g and the cation exchange capacity of kaolinite was 3.3 meq/100 g measured by a summation method (Research Analytical Laboratory, University of Minnesota). Before being used, the kaolinite was stored in a desiccator. Except for the isotherm tests, the initial concentration of PFAS in the tests was 1.0 μM (413 μg/L for PFOA, 463 μg/L for PFNA, 499 μg/L for PFOS, 513 μg/L for PFDA, and 563 μg/L for PFUnDA; these concentrations were in the linear adsorption range as determined by isotherm tests). This was ensured by spiking 40 μL of PFAS stock solution into 40 mL of the test suspension. The tiny amount of methanol (40 μL) from the stock solution did not have a detectable effect on the adsorption results (Figure C-2, Appendix

C). The adsorption of PFASs by kaolinite was conducted at different aqueous Na^+ concentrations to study the effect of Na^+ concentration. The solution pH was adjusted to 7.5 with 0.1 M HCl or NaOH. Because the effect of H^+ on the adsorption of PFASs is well-known (Higgins and Luthy, 2006, Johnson et al., 2007, Tang et al., 2010, Wang and Shih, 2011, You et al., 2010), there is no need to study the pH effect further.

Adsorption isotherms were obtained to assess the PFAS distribution between the solid and aqueous phases as a function of the aqueous PFAS concentration at equilibrium (C_w). Both single-compound and multi-compound adsorption experiments were studied. In the single-compound system, only one PFAS was used as the adsorbate, while all the PFASs were dosed in the multi-compound system.

4.2.3 Determination of solid–water distribution coefficient (K_d)

After 48 h of equilibration, the samples were pretreated using an approach similar to that reported previously (Johnson et al., 2007). The detailed steps for determining the values of K_d can be found in Appendix C.

4.2.4 Quantification of PFASs

Each sample for HPLC–ESI-MS analysis was placed in a 300 μL insert (Chrom Tech) in a Wheaton vial and was crimp-sealed with a natural rubber septum (Chrom Tech). The analytical column was a Luna C_{18} column (50 × 1.0 mm, 5 micron) (Phenomenex). The guard column was a KJO-4282 one (Phenomenex). The parameters for operating the HPLC/ESI-MS system were set according to the methods reported in previous studies

(Johnson et al., 2007). The detailed information about the HPLC/ESI-MS analysis of samples, instrumental detection/quantification limits, quality assurance and quality control results (blanks and recovery rates), and typical HPLC/ESI-MS chromatograms for the calibration standard and blank (Figure C-3, Appendix C) can be found in Appendix C.

4.2.5 ζ-potential measurement

Kaolinite is a 1:1 layered clay composed of repeating tetrahedral sheets of "SiO_4^{4-}" and octahedral sheets of "$Al(OH)_6^{3-}$". It is negatively charged in water in the circumneutral pH range as a result of the deprotonation of the hydroxyl groups on the octahedral sheets and the permanent charge deficiency on the tetrahedral layers (Schwarzenbach et al., 1993). Cationic counterions (e.g., Na^+) are attracted to the negatively charged kaolinite surface resulting in the so-called electric double layer (EDL). A measure of ζ-potential of kaolinite suspension in the presence of PFASs can provide useful information about the interactions of kaolinite particles and PFAS molecules. The ζ-potential was measured by means of a zeta potential analyzer (ZetaPlus, Brookhaven) in PFOS/kaolinite suspensions at different Na^+ concentrations and in PFAS/kaolinite suspensions at a single Na^+ concentration. The ζ-potential analyzer was calibrated at 22 °C. The measurements were repeated to provide 10 ζ-potential data points for each sample.

4.3 Results and discussion

4.3.1 Linear adsorption isotherms and the effect of PFAS structure

The observed adsorption isotherms were linear over the concentration range examined in this study (Figure C-4, Appendix C). The linearity indicates the value of K_d was insensitive to the concentration within the examined range. The results also indicate that the K_d values calculated from a single compound concentration could be used for comparing PFAS adsorption. This finding about the linear adsorption isotherms is consistent with previous studies (Ahrens et al., 2011b; Liu and Lee, 2005).

The single-point K_d values are presented in Table 5.1. The data show that each CF_2 moiety increased the distribution coefficient by 0.46 log units in the single-compound system. The difference in log K_d per CF_2 moiety can vary when the adsorbent is different, for example, mineral surfaces as compared to organic matter in sediments. A greater contribution from each CF_2 to log K_d during the sorption of PFASs to sediments has been reported (Higgins and Luthy, 2006). Furthermore, a comparison of the partitioning characteristics of PFOS and PFNA reveals that the sulfonate moiety contributed 0.42 log units to the distribution coefficient (Table 4.1). The slightly larger size of the sulfonate moiety as compared to the carboxylate moiety (leading to slightly more hydrophobicity) (Higgins and Luthy, 2006; Schwarzenbach et al., 1993) is not sufficient to explain the observed difference in adsorption potentials between PFOS and PFNA. The difference is more likely due to specific electrostatic interactions. According to Pearson's concept of hard and soft acids and bases, the carboxylate group is a soft base while the sulfonate group is a relatively hard one (Snoeyink and Jenkins, 1980). A hard base is more readily adsorbed on oxide surfaces, which are hard acids (Duda et al., 2005, Snoeyink and

Jenkins, 1980). In short, the results indicate that both the hydrophobic chain length (*m*) of a PFAS and the functionality of the head group affect its adsorption to kaolinite.

Amphiphilic compounds have the potential to adsorb onto minerals in hemi-micelles when the organic ions are present at 0.001 to 0.01 of the critical micelle concentration (Schwarzenbach et al., 1993). Hemi-micelle adsorption is usually characterized by a normal adsorption isotherm at low concentrations and then a sharp increase in adsorption at hemi-micelle concentrations (Johnson et al., 2007). In the current study, the adsorption isotherms indicate that hemi-micelles were unlikely to have formed.

Table 4.1. The solid–water distribution coefficients in logarithmic form (log K_d, L/kg)

	single-compound system	**multi-compound system**	**Δ (%)**
PFHpA	ND	NA	–
PFOA	0.36 ± 0.08	ND	–
PFNA	0.74 ± 0.06	0.30 ± 0.11	***63.6*** †
PFOS	1.16 ± 0.05	0.88 ± 0.03	***48.6*** †
PFDA	1.30 ± 0.04	1.05 ± 0.04	***43.4*** †
PFUnDA	1.70 ± 0.05	1.72 ± 0.04	*5.7*

Measured at pH 7.5 with 1 mM NaCl and $NaHCO_3$. ND: not detected. NA: not applicable (PFHpA was not involved in the multi-compound system). † Bold values are significant at the alpha level of 0.05 (see Table C-0, Appendix C).

4.3.2 Effects of monovalent cations: Modeling

A model including both hydrophobic and electrostatic components has been developed to predict the organic carbon-normalized distribution coefficients of PFASs (Higgins and

Luthy, 2007). While their work offers a knowledgeable discussion of an important topic, their model should be more applicable to PFAS sorption by sediments or sorbents rich in organic matter. This is because their model was built on the basis that sediment sorption of PFAS and the electrostatic potential of the sediment organic matter were both insensitive to aqueous [Na^+] (Higgins and Luthy, 2007). In the present study, a change of kaolinite surface charge with the addition of Na^+ and the effect of Na^+ addition on kaolinite adsorption of PFASs (Figures 4.1–4.4) were observed. Therefore, a new model of the adsorption of PFASs on mineral surfaces needs to be established. In addition, it has been suggested that the electrostatic repulsion between adsorbed PFAS molecules (Tang et al., 2010). This effect was considered in our model.

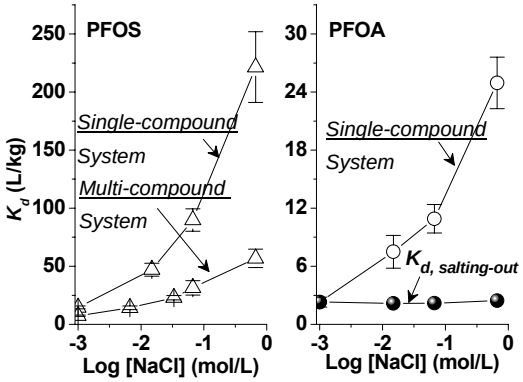

Figure 4.1 Effects of sodium concentration on the adsorption of PFOS and PFOA by kaolinite in a single-compound system and in a multi-compound system (pH: 7.5; initial PFAS concentration: 1×10^{-6} mol/L). $K_{d,salting\text{-}out}$ is the calculated distribution coefficient considering the salting-out effect only.

The model developed here was mainly based on previous work (Schwarzenbach et al., 1993; Tang et al., 2010). It has been documented that PFAS adsorption to a mineral surface is controlled by several effects or forces: (1) the hydrophobic effect that is the tendency of a PFAS molecule to exclude water molecules and to adsorb on an interface. It also includes the interaction between the perfluorocarbon chain of the PFAS and a hydrophobic moiety on the adsorbent surface; (2) the electrostatic interactions between the negatively charged groups of PFASs and the adsorbent surface; and (3) the electrostatic repulsion between adsorbed PFAS molecules (Tang et al., 2010). Correspondingly, the change in total free energy $\Delta G_{adsorption}$ associated with PFAS adsorption can be broken into hydrophobic and electrostatic parts:

$$\Delta G_{adsorption} = \Delta G_{hydrophobic} + \Delta G_{electrostatic,adsorbate–adsorbent} + \Delta G_{electrostatic,adsorbate–adsorbate} \quad (4.2)$$

The three terms on the right-hand side of Eq 4.2 correspond to the hydrophobic effect, the PFAS–surface electrostatic interaction, and the electrostatic repulsion between the adsorbed PFAS molecules, respectively. The contribution of the CF2 moiety to $\Delta G_{hydrophobic}$ can be expressed as (Schwarzenbach et al., 1993):

$$\Delta G_{hydrophobic} = m \times \Delta G_{CF2} \quad (4.3)$$

where ΔG_{CF2} is the hydrophobic contribution made by each CF_2 moiety driving these sorbates into the diffuse double layer–vicinal water layer, and m is the number of perfluorocarbons of PFAS. This approach has also been applied to the adsorption of other surfactants (Schwarzenbach et al., 1993; Wang et al., 1999). When the adsorption reaches equilibrium, we have the following relationship:

$$\Delta G_{adsorption} = RT \ln K_d = \Delta G_{hydrophobic} + \Delta G_{electrostatic,adsorbate–adsorbent} + \Delta G_{electrostatic,adsorbate–adsorbate} = m \times \Delta G_{CF2} + b \quad (4.4)$$

where $b = \Delta G_{electrostatic,adsorbate–adsorbent} + \Delta G_{electrostatic,adsorbate–adsorbate} = \Delta G_{electrostatic}$. The slope of $\Delta G_{adsorption}$ versus m is the value of ΔG_{CF2}.

4.3.3 Effects of monovalent cations: Experimental results

The adsorption of PFASs on kaolinite increased with increasing Na^+ concentration Figures 4.1 and 4.2). This result is consistent with the previous finding that increasing Na^+ concentration enhanced the adsorption of sodium dodecylsulfate (a C_{12} anionic surfactant) onto negatively charged clay (Pavan et al., 1999).

To gain more insight into PFAS adsorption, the K_d values of PFAS obtained at different Na^+ concentrations were fitted to Eq 4.4. The results are presented in Figure 4.2. As the figure shows, each CF_2 moiety contributed 2.5−2.7 kJ/mol to $\Delta G_{hydrophobic}$. The values of $\Delta G_{hydrophobic}$ and ΔG_{CF2} varied little at different Na^+ concentrations, whereas $\Delta G_{electrostatic}$ was overwhelmingly affected by sodium. As illustrated in Figure 4.2, increasing Na^+ concentration shifted $\Delta G_{electrostatic}$ to a less positive value and thus reduced the minimum m required for spontaneous adsorption ($\Delta G_{adsorption} \leq 0$). For example, the value of m_c declined from 7 to 5 with the increasing Na^+ concentration from $10^{-3.0}$ to $10^{-1.2}$ (see Figure 4.2) (the term m_c refers to the value of m corresponding to $\Delta G_{adsorption} = 0$). As a result, the adsorption of PFHpA (m = 6) by kaolinite became possible at the higher Na^+ concentration (Figure 4.2).

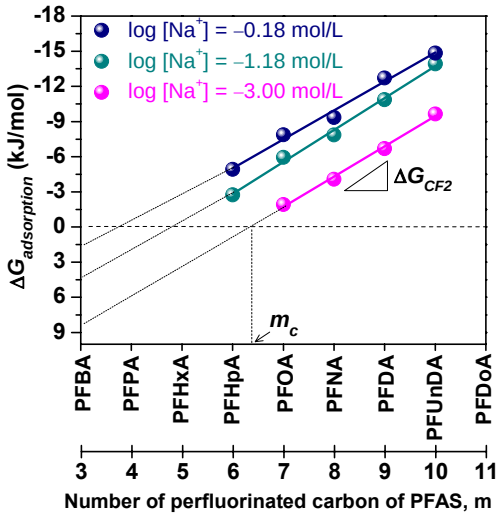

Figure 4.2 The adsorption free energy ($\Delta G_{adsorption}$) as a function of m at different sodium concentrations (pH 7.5; Initial PFAS concentration: 1×10^{-6} mol/L; $\Delta G_{adsorption} = \Delta G_{hydrophobic} + \Delta G_{electrostatic} = m \times \Delta G_{CF2} + b$). $\Delta G_{adsorption} = -2.58\ m + 16.33$ at $[Na^+]$ of $10^{-3.00}$ mol/L; $\Delta G_{adsorption} = -2.69\ m + 13.27$ at $[Na^+]$ of $10^{-1.18}$ mol/L; and $\Delta G_{adsorption} = -2.47\ m + 9.83$ at $[Na^+] = 10^{-0.18}$ mol/L. R^2>0.97 for the linearity of all the fitted lines. m_c is m corresponding to spontaneous adsorption ($\Delta G_{adsorption} = 0$). PFHxA: perfluorohexanoic acid; PFPA: perfluoropentanoic acid; PFBA: perfluorobutanoic acid; PFDoA: perfluorodecanoic acid.

The variation of $\Delta G_{electrostatic}$ with solution sodium concentration should be related with changes in the kaolinite's surface charge. The pH of the zero point of charge of the kaolinite used in this study was 5.1; therefore, there is essentially no positive charge on the kaolinite surface at pH 7.5. Because the kaolinite surface charge is of the same sign as the functional groups of PFASs, there will be electrostatic repulsion between them (Schwarzenbach et al., 1993). As apparent in Figure 4.3, the kaolinite surface became less negatively charged at a high Na^+ concentration because the EDL around the kaolinite

surface was compressed by sodium ions. Consequently, the PFAS–surface electrostatic repulsion was reduced and the PFAS adsorption was enhanced.

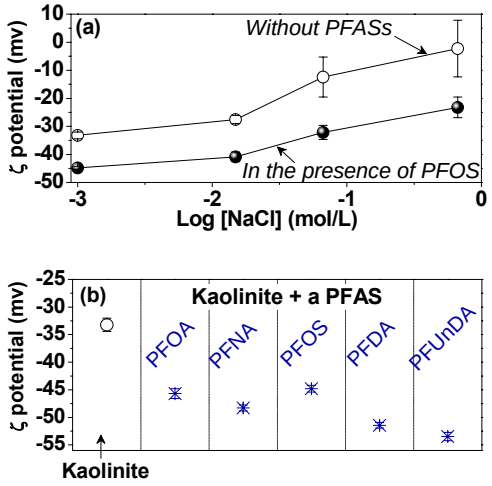

Figure 4.3 (a) Effects of sodium on the surface charge of kaolinite at different ionic strengths with and without the presence of PFOS (pH: 7.5; initial PFAS concentration: 1×10^{-6} mol/L); (b) Changes in the surface charge of kaolinite because of the adsorption of a PFAS ([NaCl]: 1×10^{-3} mol/L; pH: 7.5; Initial PFAS concentration: 1×10^{-6} mol/L).

Figure 4.4 presents the values of m_c as functions of Na^+ concentration and ionic strength I. A strong linear relationship ($R^2 = 0.99$) was found between m_c and $\log[Na^+]$. The t-test of the slope (see Appendix C) shows that the linear relationship between m_c and $\log[Na^+]$ is significant ($p = 0.037$) at a significance level of 0.05. The relationships imply that the adsorption of PFASs with m smaller than six is not thermodynamically favorable in freshwater with a typical $-\log I = 2.5$ (Snoeyink and Jenkins, 1980). This is consistent with reports in the literature that PFHxA, perfluoropentanoic acid (PFPA), and

perfluorobutanoic acid (PFBA) are rarely found to be adsorbed on particles in freshwater. According to Figure 4.4, for these shorter-chained PFASs, higher Na^+ concentrations are required to induce spontaneous adsorption. Their adsorption of the shorter-chained PFASs on particles can be thermodynamically possible in seawater, where the Na^+ concentration can reach 0.5 M (corresponding to m_c = 3.5) (Snoeyink and Jenkins, 1980), or under other high-ionic-strength environmental conditions.

Previous studies have documented that solution pH has a remarkable influence on the adsorption of PFASs onto charged solid surfaces (Higgins and Luthy, 2006, Johnson et al., 2007, Tang et al., 2010, Wang and Shih, 2011). It is illustrative to revisit one previous study (Higgins and Luthy, 2006). A strong linear relationship ($R^2 > 0.97$) could be obtained between $\Delta G_{adsorption}$ and m by processing their PFAS-sediment interaction data at different pH values using Eq 4.4 (see Figure C-5, Appendix C). As $[H^+]$ increased, the sediment surface charge became less negative (Higgins and Luthy, 2007), and thus $\Delta G_{electrostatic}$ shifted to a less negative value, which in turn increased PFAS sorption to sediments. Similar to Figure 4.4, a moderately strong linear relationship ($R^2 = 0.60$) could be obtained between pH/$[H^+]$ and m_c from Figure C-5 (see Figure C-6, Appendix C); the spontaneous sorption of a shorter-chained PFAS to sediments is more thermodynamically favorable at a higher hydrogen ion concentration or lower pH. For example, the spontaneous adsorption of PFHpA on sediment in 0.50 mM $CaCl_2$ occurred only at pHs less than 5.6 (see Figure C-6).

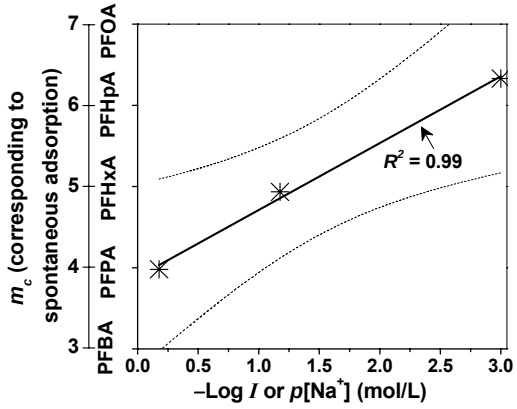

Figure 4.4 The change in m_c as a function of ionic strength (I) or sodium concentration (pH 7.5; initial PFAS concentration: 1×10^{-6} mol/L.). $p[Na^+] = -\log [Na^+]$. $m_c = -0.82 \log[Na^+] + 3.89$ or $m_c = 0.82\ p[Na^+] + 3.89$. m_c is the number of perfluorocarbons of PFAS corresponding to $\Delta G_{adsorption} = 0$. The dashed lines are the 95% confidence bands.

In addition to the electrostatic effect, a salting-out effect has been suggested as the cause of the positive effects of cations on PFAS adsorption. The salting-out effect during PFAS adsorption can be estimated using

$$K_{d,salting-out} = K_d \times 10^{a \cdot K^s \cdot [NaCl]} \qquad (4.5)$$

where K^s is the salting-out (Setschenow) constant, which is usually about 0.1–0.4 (Ni and Yalkowsky, 2003). It can be calculated using an empirical relationship based on 101 organic compounds including halogenated acetic acids (Ni and Yalkowsky, 2003) as 0.23, 0.27, 0.30, and 0.34 for PFOA, PFNA, PFDA, and PFUnDA, respectively. The value of a was 0.35, which was obtained by the linear free energy relationship between log K_d and log C_w^{sat} (C_w^{sat} is the solubility of PFASs; see Figure D-7 and Table D-4 of Appendix C). As evident in Figure 5.1, the increase in PFOA's K_d modeled by the empirical relationship for the salting-out effect (Eq 4.5) was negligible compared to the observed

increase in K_d, implying that the salting-out effect was unimportant, at least for the range of Na^+ concentrations examined in this work. In addition, the K_d values of PFOS and PFOA increased linearly instead of the exponential increment as predicated by Eq 4.5, hinting that the effect of sodium on the sorption was not caused by the salting-out effect. These findings agree with the recent observations that the salting-out effect was not evident for PFAS adsorption on clay (Jeon et al., 2011).

4.3.4 Electrostatic repulsion between adsorbed PFAS molecules

The value of $\Delta G_{electrostatic,adsorbate–adsorbent}$ was evaluated by Eq 4.6 (Schwarzenbach et al., 1993):

$$\Delta G_{electrostatic,adsorbate–adsorbent} = zF\Psi_d = -F\Psi_d \approx -F\zeta \qquad (4.6)$$

where z is the valence of PFAS (−1), F is the Faraday constant (96485 C/mol), and Ψ_d is the diffuse layer potential (V). Ψ_d can be approximated by the ζ-potential because the shear plane is often located close to the inner boundary of the diffuse layer (Carnali and Shah, 2008, Kretzschmar et al., 1997). Therefore, on the basis of Eqs 4.2–4.6, $\Delta G_{electrostatic,adsorbate–adsorbate}$ can be calculated by:

$$\Delta G_{electrostatic,adsorbate–adsorbate} = \Delta G_{adsorption} - (\Delta G_{hydrophobic} + \Delta G_{electrostatic,adsorbate–adsorbent})$$

$$= \Delta G_{adsorption} - m \times \Delta G_{CF2} - F\Psi_d \qquad (4.7)$$

The values of $\Delta G_{adsorption}$, $\Delta G_{hydrophobic}$, $\Delta G_{electrostatic,adsorbate–adsorbent}$, and $\Delta G_{electrostatic,adsorbate–adsorbate}$ are tabulated in Table C-2, Appendix C. As shown, the value of $\Delta G_{electrostatic,adsorbate–adsorbate}$ differed insignificantly among PFASs and was ~11.5 kJ/mol, which was about double of the $\Delta G_{electrostatic,adsorbate–adsorbent}$. The result indicates

that the electrostatic repulsion between adsorbed PFAS molecules is an important thermodynamic inhibitor for PFAS adsorption. The results agree with the finding that increasing the Na^+ concentration increased the adsorption of PFOS on a weakly positively charged surface, because of the reduced electrostatic repulsions between adsorbed PFOS molecules (Tang et al., 2010).

Remarkably, the electrostatic intermolecular repulsion between adsorbed PFAS molecules is a particular characteristic of these chemicals. The negative charge of PFASs in water comes not only from their functional groups but also from their special molecular structures (Johnson et al., 2007). Figure C-8 (Appendix C) shows the partial atomic charges in PFOS and its non-fluorinated counterpart, octanesulfonate. The electrostatic partial maps of PFOS and octanesulfonate were then built using MarvinSketch software (ChemAxon, Hungary) on the basis of calculation results presented in Figure C-9 (Appendix C). As shown, PFOS and octanesulfonate have distinctively different charge characteristics (Figure C-9). In PFOS the partially negatively charged fluorine, oxygen and sulfur form an electron shell around the partially positively charged carbon framework; the carbon atoms are screened by fluorine, oxygen, and sulfur. A PFOS molecule is negatively charged to the surrounding water because of both its ionized functional group and its partially negatively charged hydrophobic chain.

4.3.5 Competitive adsorption

Previous studies have observed competitive adsorption between ionizable surfactants (Parida et al., 2006). For PFASs there is limited information available on the possibility

of competitive adsorption. In the present study, the competition among PFASs during their adsorption on the kaolinite surface was observed. The K_d values of PFASs obtained from the single-compound system and the multi-compound system were tabulated in Table 4.1. The adsorption of the shorter-chained PFASs (PFOA, PFNA and PFOS) was significantly influenced by the presence of other PFASs. The K_d values of PFNA and PFOS in the multi-compound system were around half of the values in the single-compound system (Table 4.1). Table C-0 (Appendix C) includes the 95% confidence intervals for the difference in the K_d values obtained from the two systems. The 95% confidence intervals do not contain zero for PFNA, PFOS, and PFDA; therefore, the differences in the K_d values obtained between the two systems for these relatively shorter-chained PFASs are significant at the alpha level of 0.05. On the other hand, the 95% confidence interval contains zero for PFUnDA, the longest-chained PFAS in this study, indicating that it's K_d values in the two systems differ insignificantly at the alpha level of 0.05 (Table 4.1). The statistical analysis results show that the adsorption of PFUnDA was not significantly influenced by the presence of shorter-chained PFASs but that the adsorption of shorter-chained PFASs was greatly influenced by the presence of other PFASs.

The competitive adsorption among PFASs is also evident after comparing the effects of Na^+ in the two adsorption systems (Figure 4.1). In the single-compound system, the addition of the counterion significantly increased the adsorption of PFASs (Figure 4.1), as has been discussed. In the multi-compound system, adding Na^+ also increased the adsorption of PFOS, but the degree of increase was much smaller than that in the single-

compound system. For PFOA, the Na^+ effect on its adsorption by kaolinite was so weak in the multi-compound system that the mass of adsorbed PFOA was below the instrumental quantification limit, in contrast with the substantially positive effect of Na^+ on PFOA adsorption in the single-compound system (Figure 4.1).

The competitive adsorption should be caused by site competition and electrostatic effects. As a result of the stronger hydrophobic effect, a longer-chained PFAS can outcompete a shorter-chained PFAS. Furthermore, as mentioned earlier, PFASs have a unique negatively charged shell (Figure D-9). Within the electrical field of a PFAS molecule, other molecules may not be allowed to adsorb.

4.3.6 Kaolinite's ζ-potential in the presence of PFAS(s) and possible orientation of PFAS molecules on the kaolinite surface

Figure 4.3 shows the ζ-potentials of the kaolinite suspensions in the presence of PFOS at different Na^+ concentrations and in the presence of different PFASs at a single Na^+ concentration. After adsorbing PFASs, the kaolinite surface's ζ-potential was shifted to a more negative value (Figure 4.3). Previous studies have observed that the surface ζ-potential can be shifted to a more negative value because of the adsorption of an anionic surfactant (Pavan et al., 1999; Wang et al., 1999). As evident in Figure D-10 (Appendix C) which links the kaolinite surface's ζ-potentials in the presence of PFASs and the K_d values of PFASs, a PFAS with a higher K_d value can change the kaolinite surface's ζ-potential to a larger degree. The results (illustrated in Figure 4.3) indicate that the adsorbed PFAS molecules were within the EDL of the kaolinite surface and contributed

to the potential at the slipping plane (ζ-potential). Furthermore, the ζ-potential of PFOS-adsorbed kaolinite was much less negative than that of PFNA-adsorbed kaolinite, and it was close to that of PFOA-adsorbed kaolinite (Figure 4.3b). This was observed despite the fact that PFOS had a higher K_d than PFOA and PFNA. The observation indicates that different functional groups of PFASs have different effects in changing the ζ-potential of the kaolinite surface. This is consistent with the above discussion of the possible specific interactions between the sulfonate group and the oxide surface; the sulfonate group of PFOS was further away from the shear plane or closer to the mineral surface, which resulted in greater EDL screening than PFNA.

An interesting question that has yet to be answered is the orientation and packing of PFAS molecules at the kaolinite–water interface. The thickness of the EDL or the Debye length can be estimated as $0.28 \times I^{-0.5}$ (nm) (Schwarzenbach et al., 1993). For the ionic compositions of the test suspensions in this study, this means that the adsorbed PFAS molecules were packed into a layer of water 0.3–6.3 nm thick. This leads to a basic question as to how the head or tail of each PFAS was aligned on the kaolinite surface in this thin water layer. In a low ionic strength environment, the hydrophilic head of an adsorbed PFAS molecule should be oriented predominately toward the aqueous phase (Figure C-11, Appendix C) so as to minimize both the contact between the charged head and the charged kaolinite surface and the contact between the hydrophobic tail and the water molecules. Interestingly, at high ionic strength (e.g., $\log[Na^+] = -0.18$) when the EDL is only ~0.3 nm thick, PFAS molecules cannot be aligned as they are at low ionic strength as a result of their relatively long perfluorocarbon chains (~1 nm, see Appendix

C). The adsorbed PFAS molecules were thus proposed to be aligned as illustrated in Figure C-11 when the repulsion between the mineral surface and the PFAS is low in high ionic strength conditions.

Chapter 5: BATCH AND COLUMN STUDY: SORPTION OF PERFLUOROALKYL SUBSTANCES FROM WATER AND COSOLVENT SYSTEMS BY AMBERLITE XAD RESINS

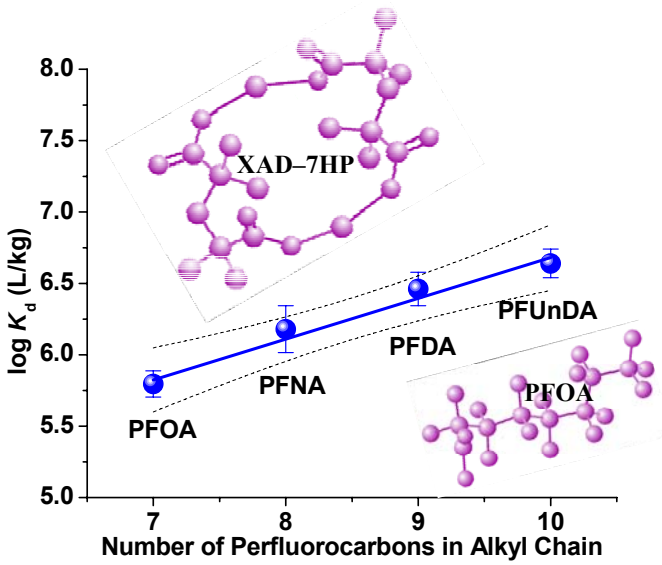

Graphical abstract (logK_d versus the number of perfluorocarbons in PFCs (sorbent: XAD-7HP).

5.1 Introduction

PFASs, PFOS and PFOA in particular, have recently become targets of investigation within the scientific community due to their persistence and toxicity and their ubiquitous presence in the environment (Awad et al., 2011; Jahnke and Berger, 2009; Lindstrom et al., 2011; Meyer et al., 2011). PFASs are a group of man-made surfactants that contains a perfluorinated alkyl moiety of varying chain length and varying functional groups attached to that moiety. The structure of these compounds makes them very stable, hydrophobic (water-repelling), and oleophobic (oil-repelling). These particular properties have led to extensive use of PFASs and their precursors in cookware, fast food containers, fire-fighting foams, and painting materials (Armitage et al., 2009, Emmett et al., 2006). Long-chain PFASs (≥7 perfluorocarbons) are persistent organic pollutants that cannot be hydrolyzed, directly photolyzed, or biodegraded under environmental conditions (Nakayama et al., 2010). PFASs have been found in fish, birds and mammals from mid-latitudes to the poles (Giesy and Kannan, 2001). PFASs have relatively high solubility in water (i.e., 9.5 g/L for PFOA and 0.26 g/L for PFDA) and low volatility and sorption potentials (Bhhatarai and Gramatica, 2011). PFASs that pass the drinking-water treatment processes will end up in the tap water (Hoffman et al., 2011a). Each 1-µg/L increase in PFOA levels in drinking water was associated with a 141.5-µg/L increase in human blood PFOA concentrations (Hoffman et al., 2011a). PFASs have been found in tap water samples collected from China, Japan, India, Spain, and the United States (Ericson et al., 2009; Post et al., 2009), with typical concentrations ranging up to several tens of ng/L. Therefore, accurately quantifying the trace levels of PFASs in environmental/tap water

samples is important for understanding the global distribution of these chemicals and for identifying sources and routes of human exposure to PFASs. However, this relies on a powerful sorbent for concentrating these compounds at trace levels in water.

Polymeric resins have attracted increasing attention as an alternative to activated carbon for concentrating and removing organic compounds, primarily because of their favorable physicochemical stability, large sorption capacity, relatively low cost, good selectivity, structural diversity, and easy generation (Dominguez et al., 2011; Freitas et al., 2008; Vergili et al., 2010; Wania et al., 2003). In particular, Amberlite XAD-7HP (the only moderately polar XAD resin commercially available) and XAD-2 (nonpolar) resins have been used widely to isolate and concentrate organic compounds from environmental samples (Scott et al., 2006; Senevirathna et al., 2010a; Tittlemier et al., 2007; Wania et al., 2003). However, surprisingly, a systematic study about the sorption of PFAS by these resins is lacking in the literature. Numerous studies have been conducted for PFASs being concentrated using Oasis HLB and WAX resins (Villagrasa et al., 2006). Much less attention has been paid to XAD-7HP, a nonionic aliphatic acrylic polymer combining a polar component that can promote hydrophilic interactions with PFASs. In this chapter, sorption of five PFASs by XAD-7HP and XAD-2 was examined in batch experiments with respect to sorption kinetics, sorption isotherms, and the influences of solution pH and methanol. Column tests were also run to investigate the number of times XAD resins can be regenerated without loss of performance.

5.2 Materials and methods

5.2.1 Chemicals and materials

The most common and environmentally relevant PFASs, PFOA (~95 percent), PFNA (97 percent), PFOS (≥98 percent), PFDA (98 percent) and PFUnDA (95 percent), were purchased from Sigma(–Aldrich) (Milwaukee, WI, USA & Steinheim, Switzerland). Methanol (Optima grade from Fisher Scientific) and reverse osmosis (RO) or HPLC water (HPLC grade from Fisher Scientific) were used to clean the containers and equipment. PFASs were not found in the methanol or the water using a 1100 MSD mass spectrometer (MS) equipped with an ESI source and interfaced to a HPLC. Amberlite XAD-2 (particle size of 20–60 mesh; mean pore diameter of nine nm; mean surface area of 300 m^2/g) and Amberlite XAD-7HP (particle size of 20–60 mesh; pore diameter of 45–50 nm; surface area of ≥380 m^2/g) were purchased from Sigma–Aldrich (St. Lowis, US). The detailed properties of the resins can be found Table D-1, Appendix D.

Before serving as sorbents, the resins were pre-cleaned thoroughly with RO water, followed by methanol, and a final rinse with RO water, and then stored under RO water.

5.2.2 Batch sorption experiments

The sorption of PFASs on pre-cleaned Amberlite XAD was carried out in triplicate in 50-mL polystyrene tubes containing 40 mL of test solution, which were continuously shaken by a wrist action shaker (Burrell) for 60 h at temperature, T = 22.2 ± 0.5 °C. Sorption kinetic results show that the 60-h sorption accounted for ~96% of the estimated ultimate uptake. Unless otherwise specified, the test solution was composed of 1.0 mM $NaHCO_3$ (alkalinity and pH buffer) and 1.0 mM NaCl (ionic strength). The pH of the test solution

was adjusted to 7.8. Except for the isotherm tests, the initial concentration of PFASs in the tests was 1.0 μM (in the linear sorption range as determined by isotherm tests). This was ensured by spiking 40 μL of PFAS stock solution (in methanol) into 40 mL of the test suspension. The solution pH was adjusted with 0.1 M HCl or NaOH.

After 60 h of shaking, the tube was centrifuged with an Eppendorf centrifuge, and an aqueous aliquot was transferred a 300-μL insert (Chrom Tech, Minneapolis, MN) in a Wheaton vial, which was then crimp-sealed with a natural rubber septum (Chrom Tech, Minneapolis, MN). The concentrations of PFASs were determined by HPLC–ESI-MS with a selected ion-monitoring mode. The parameters for running the HPLC–ESI-MS system were set according to the methods reported in Johnson et al. (2007). The parameters for running the HPLC–ESI-MS system and instrumental quantification limits can be found in Appendix D.

5.2.3 Column tests

A fixed bed column study was conducted using a column of 20 mm diameter and 850 mm length. The column was packed with XAD-7HP (particle size of 20–60 mesh) and the depth was 25 mm. XAD-7HP was pre-cleaned by Optima methanol and then by RO water, and stored in RO water. Column tests were performed to study the long-term performance of XAD-7HP for sorbing PFASs from both Mississippi River and tap water (Minneapolis, MN). River water samples were taken from the Upper Mississippi River (44°58'12.74"N, 93°14'11.62"W) by pre-cleaned high-density polyethylene containers and filtered through a 0.5-μm- and then a 0.2-μm pre-weighed polycarbonate membrane

(Millipore) into a pre-cleaned polyethylene vacuum flask. The river water filtrate or tap water was spiked with a known mass of PFOS or PFOA (up to 10 nmol/L of PFOS or PFOA) and pumped through the XAD-7HP column at a volumetric flow rate of 2 mL/min. The flow rate was optimized to result in the maximum recovery rates of PFAS-spiked HPLC water. After extraction, the cartridges were washed with RO water and air-dried. PFASs retained on the resin were eluted with a total of 40 mL methanol three times into a 50-mL polystyrene tube. These extracts were concentrated to 0.5 mL under a gentle stream of pre-purified nitrogen, filtered (0.2-μm nylon filter) into a 300-μL insert (Chrom Tech, Minneapolis, MN) in a Wheaton vial, and crimp-sealed with a natural rubber septum (Chrom Tech, Minneapolis, MN) for HPLC–ESI-MS analysis.

The method of Nakayama et al. (2010) was modified and used to determine PFAS recoveries (see Appendix D). River water filtrate or tap water was spiked with a known amount of PFAS and then extracted following the steps as described above. The eluate was concentrated, filtered, and analyzed by HPLC–ESI-MS. The same volume of unspiked river water filtrate or tap water was extracted using another XAD-7HP column, and the eluate was concentrated, filtered, spiked by the same amount of PFAS, and analyzed by HPLC–ESI-MS. Recoveries were calculated by dividing the peak area ratio of the first sample (pre-addition to cartridge) by that of the second eluate (post-addition).

The XAD-7HP was regenerated by washing the resin with 2 bed volumes of 0.01 M NaOH solution for eluting weakly acidic compounds present in Mississippi River water, followed by 10 bed volumes of RO water, followed by 15 bed volumes of methanol, and a final rinse with 20 bed volumes of RO water.

The use of Teflon was avoided during the experiment because of possible contamination from additives in this perfluorinated polymer. Blank polystyrene tubes and columns without PFAS but with pre-cleaned XAD-7HP/XAD-2 were used to check the possible contamination of the resins and the tubes/columns by PFASs.

5.3 Results and discussion

5.3.1 Sorption kinetics

The equilibrium time and sorption mechanisms are determined by a time response in the batch experiments. As apparent in Figure 5.1, the rate of PFOS sorption by XAD-7HP was rapid initially. It was noticed that the aqueous PFOS concentration dropped by 60% during the initial two hours. PFOS continued to be sorbed to the resin for at least four additional hours, although uptake rates gradually decreased. Since sorption kinetics experiments can display an early period of extensive uptake [fast uptake rate (k_{fast})] followed by a prolonged time of slowly proceeding mass transfer [slow uptake rate (k_{slow}-)], sorption processes have been characterized with a biexponential/two-box model (Wu and Gschwend, 1986). The batch results (see Figure 5.1) were fitted with the biexponential decay function (Eq 5.1) of Prism 5 for Mac OS X (GraphPad Software Inc., California, USA):

$$C(t) = C_{ultimate} + (C_0 - C_{ultimate}) \times F \times 0.01 \times \exp(-k_{fast} \times t) + (C_0 - C_{ultimate}) \times (100 - F) \times 0.01 \times \exp(-k_{slow} \times t), \quad (5.1)$$

where t is sorption time (min), $C_{ultimate}$ is the PFOS aqueous concentration ($C(t)$) when t approaches $+\infty$, $C_0 - C_{ultimate}$ is the estimated ultimate uptake, and F is a fraction reflecting the change in C due to the sorption, as percent.

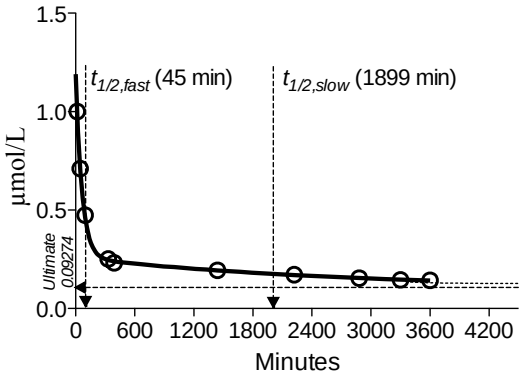

Figure 5.1 Batch sorption kinetics of PFOS on XAD-7HP (T = 22.2 ± 0.5 °C; pH 7.8). Symbols: experimental data. Solid line: best-fit line by a two-box model (Wu and Gschwend, 1986)**. Goodness of fit: R^2 = 0.9997. Kinetic parameters: k_{fast} = 0.0155 min^{-1} (95% confidence interval: 0.0142 to 0.0168 min^{-1}), k_{slow} = 0.000343 min^{-1} (95% confidence interval: 0.0 to 0.000086 min^{-1}).**

As illustrated in Figure 5.1, the data were described well by the biexponential model. The kinetic profile (Figure 5.1) implies a rapid initial PFOS transfer into the near-surface boundary layer of XAD-7HP, which should be triggered by the high concentration difference between bulk solution and solid phase (film diffusion control) (Adak et al., 2005). This was followed by a prolonged diffusional transport into the resin micropores.

5.3.2 Sorption isotherms

Sorption isotherms were obtained to assess the PFAS distribution between the solid phase and the aqueous phase as a function of PFAS aqueous concentration at equilibrium (C_w). The sorption isotherms can be described by the Freundlich model (Eq 5.2) or by a simple linear model (Eq 5.2) when the concentration of the sorbate is relatively low.

$$C_s = K \times C_w^{\,n}, \qquad (5.2)$$

where C_s is the equilibrium sorption amount (μg/g), K is the sorption coefficient (K_d, L/g or more commonly L/kg) for a linear sorption isotherm or the Freundlich affinity constant (K_f, (μg/g)(μg/L)$^{-n}$) for a Freundlich sorption isotherm, and n is the Freundlich exponent, an indicator of nonlinearity, which equals to 1 for a linear sorption isotherm. The Freundlich exponent n provides a measure of the sorption site heterogeneity.

The experimental data of C_s as a function of C_w were presented in Figure 5.2 and fitted by both the linear model and the Freundlich model. The coefficient of determination of the least-squares regression line was larger than 0.90 in all cases (see Figure 5.2), indicating that both models can describe the sorption isotherms on XAD-7HP. Based on the results of Freundlich fitting, the values of n are close to 1 for all PFASs (0.96 for PFOA, 0.96 for PFOS, 0.95 for PFDA, and 0.90 for PFUnDA), except for PFNA (0.83). The smaller value of n in the case of PFNA could be caused by experimental errors because the sorption site heterogeneity should be the same for all PFASs. The value of K_f [(μg/g)(μg/L)$^{-n}$] or the sorption affinity of PFASs to XAD-7HP increased in the following order: PFOA (K_f = 1831) < PFNA (K_f = 2213) < PFOS (K_f = 3095) ≈ PFDA (K_f = 3320) < PFUnDA (K_f = 8110). XAD-7HP performance was compared with other kinds of resins (including two anion exchange resins and three

nonpolar resins) (see Table 5.1). XAD-7HP is the only aliphatic polymer; other resins are aromatic polymers based on a styrene-divinylbenzene coplymeric structure. As presented in Table 5.1, the performance of anion exchange resins (Amberlite IRA 400) was changed greatly with the sorbate equilibrium concentration. Sorption of PFOS to IRA 400 at high equilibrium concentrations was about two orders of magnitude above that at low equilibrium concentrations (see the K_f values in Table 5.1). One possible reason is that the sorption is driven by the concentration gradient at the solid–water interface compared to the bulk solution (film diffusion control). Comparing nonionic resins to anion exchange resins, a study finds that the sorption capacity of the former was higher than the latter at a low equilibrium PFOS concentration (100 ng/L) (Senevirathna et al., 2010b). From Table 5.1, XAD-7HP has a higher affinity for PFASs than nonpolar resins.

Table 5.1. Sorption of PFOS and PFOA by various commercially available resins.

Sorbent	Matrix	Functional group[a]	PV[a]	SA[a]	Sorbate	C_w (μg/L)	K_f	n
					PFOS	20000–150000	12972[b]	0.17[b]
Amb IRA 400	Styrene-DVB, gel	$-N^+R_3(Cl^-)$	–	–	PFOA	16000–170000	309671[b]	0.13[b]
					PFOS	0.2–6.0	108.9	2.08[c]
DowMarathonA	Styrene-DVB, gel	$-N^+R_3(Cl^-)$	–	–	PFOS	0.2–6.0	95.90	1.68[c]
DowL493	Styrene-DVB, macroporous	Nonionic, nonpolar	1.16	>1100	PFOS	0.2–200	54.60	0.84[c]
DowV493		Nonionic, nonpolar	1.16	>1100	PFOS	0.2–200	81.30	0.94[c]
Amb XAD 4	Styrene-DVB, macroporous	Nonionic, nonpolar	~0.68	725	PFOS	0.15–8.0	79.10	1.61[c]
Amb XAD 2		Nonionic, nonpolar	~0.65	300	PFOS	100–800	440	0.60[c]
Amb XAD 7HP	Nonionic aliphatic acrylic polymer, macroporous	Nonionic, moderately polar	~0.42	>380	PFOS	80–1800	3095	0.96[c]
					PFOA	160–3100	1831	0.96[c]

PV: pore volume (mL/g). SA: surface area (m^2/g). C_w: sorbate equilibrium concentration. K_f: Freundlich affinity constant (μg/g)(μg/L)$^{-n}$. n: Freundlich exponent. DVB: divinylbenzene. [a]: provided by the suppliers. [b]: re-calculated values from mmol$^{(1-1/n)}$L$^{1/n}$g^{-1} in Yu et al (2009b). [c]: from Senevirathna et al (2010b). [d]: results obtained by the current work.

The good linear fitting results indicate that monolayer sorption occurred (see Fig. 5.2). As the Freundlich model is a purely empirical formula while the linear model is a special case of the Langmuir model derived from the assumption of monolayer coverage. The following discussion will mainly focus on K_d, the linear sorption coefficient. The

isotherm-determined K_d was obtained from the slope of the least-squares regression line of C_s on C_w. The values of log K_d ranged from 5.80 to 6.64 depending on the length of perfluorocarbon chain (PFOA, 5.80; PFNA, 6.18; PFDA, 6.46; PFUnDA, 6.64). The values are greater than K_{oc} (organic carbon normalized partitioning coefficient) of PFASs for sediments (Higgins and Luthy, 2006), and about five times of magnitude greater than K_d values of PFASs for kaolinite clay (Johnson et al., 2007). The results indicate that PFASs have a substantially high affinity for XAD-7HP.

The K_d values of PFASs as a function of the length of perfluorocarbon chain were plotted and presented in Figure D-1 (Appendix D). As shown, a strong linear relationship (R^2 = 0.97) was observed between log K_d and the length of the perfluorocarbon chain, indicating that the hydrophobic effect is one of the driving forces for sorption. Each CF_2 moiety increased the partitioning coefficient by about 0.28 ± 0.03 log units for perfluorocarboxylates.

The critical micelle concentration is ~6.3 mM for PFOS and 0.8 mM for PFDA (Johnson et al., 2007). Amphiphilic compounds have the potential to adsorb onto minerals in hemi-micelles when the organic ions are present at 0.001–0.01 of the critical micelle concentration (Schwarzenbach et al., 1993). Hemi-micelle sorption is normally characterized by a normal sorption isotherm at low concentrations and then a sharp increase in sorption at hemi-micelle concentrations (Johnson et al., 2007). In the current study, both the concentrations of PFASs and the sorption isotherms indicate that the formation of hemi-micelles in solution were unlikely. However, it is possible that hemi-micelles or even micelles were formed within the pores of resins where PFASs were

concentrated (Yu et al., 2009b). The ~0.28 log unit difference in log K_d per CF_2 moiety is equivalent to a difference in free energy of –3.12 kJ/mol, which is very close to the free energy of transfer (per CF_2 moiety) from solution to a micellar environment (3.18 kJ/mol) as reported by Lamesa and Sesta (1987).

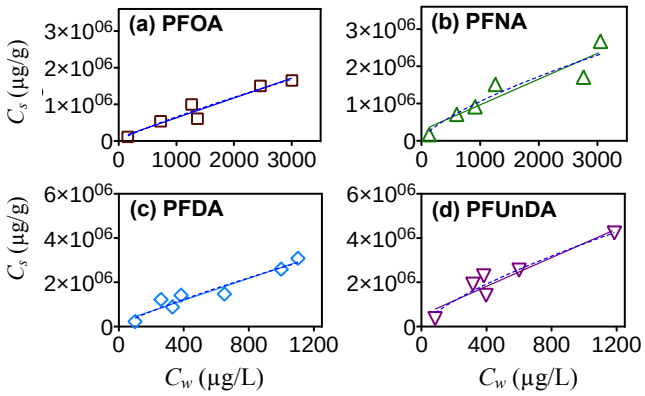

Figure 5.2 Sorption isotherms of PFASs on resins (T = 22.2 ± 0.5 °C; pH 7.8). Solid lines: modeled by a linear sorption isotherm (The values of goodness of fit R^2 are 0.93, 0.92, 0.93 and 0.95 for PFOA, PFNA, PFDA and PFUnDA, respectively). Dashed lines: modeled by Freundlich equation (The values of R^2 are 0.94, 0.95, 0.93 and 0.96 for PFOA, PFNA, PFDA and PFUnDA, respectively).

Furthermore, PFBS, a shorter-chained C4 PFAS, has been used to replace PFOS (Betts, 2007). PFBS and other C4 PFASs have been detected in rivers and food samples (MPCA, 2009). With a shorter chain and thus a weaker hydrophobic effect, these C4 PFASs may not readily be sorbed by XAD-7HP. The ability of XAD-7HP for concentrating shorter-chained PFASs can be examined by:

$$\Delta G_{sorption} = RT \ln K_d = m \times \Delta G_{CF2} + b \,, \qquad (5.3)$$

where m is the number of perfluorocarbon in PFASs and b is the change of free energy associated with the electrostatic effect. The detailed information of the modeling approach is provided in the Appendix D. The experimental data were fitted to Eq 5.3 and the critical m value corresponding to a positive $\Delta G_{sorption}$ (endergonic or nonspontaneous sorption) can be obtained. As shown in Figure 5.3, a strong linear relationship ($R^2 = 0.98$) was found between $\Delta G_{sorption}$ and m ranging from 7 to 10. The t test of the slope shows that the linear relationship is significant (two-sided $p = 0.026$) at a significance level of 0.05. Therefore, the value of $\Delta G_{sorption}$ at m of 3 can be approximated by the linear interpolation, and the value is negative (see Figure 5.3). Although the sorption of C4 PFASs on XAD-7HP was not conducted, Figure 5.3 implies that XAD-7HP can sorb these shorter-chained PFASs.

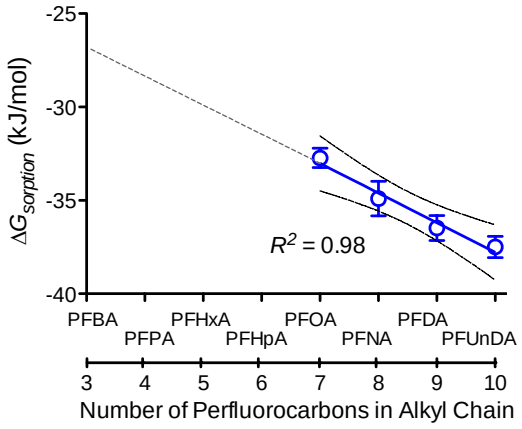

Figure 5.3 The change in sorption free energy as a function of the perfluorocarbon chain length of PFASs (T = 22.2 ± 0.5 °C; pH 7.8; sorbent: XAD-7HP; PFBA: perfluorobutanoic acid; PFPA: perfluoropentanoic acid; PFHxA: perfluorohexanoic acid; PFHpA: perfluoroheptanoic acid).

5.3.3 Effect of water-miscible solvent

Methanol is commonly used to elute target compounds from XAD resins. However, the effects of methanol on the sorption of PFASs on XAD-7HP have not been examined. The presence of methanol can greatly reduce the sorption of PFASs on XAD-7HP (Figure 5.4). The K_d value of PFOS, for example, decreased by 88% when f_c reached 0.12 (f_c is the organic solvent volume fraction). This may be due to the increased solubilities of PFASs in the water−methanol cosolvent system. The findings differ somewhat to previous results that methanol could not extract sorbed PFOS from anion exchange resins (Deng et al., 2010).

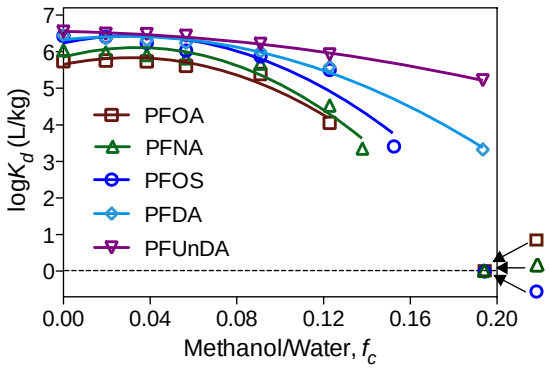

Figure 5.4 Sorption of PFASs by XAD-7HP in the water–methanol cosolvent system (T = 22.2 ± 0.5 °C; PFASs were allowed to sorb in each experimental setting for 60 h).

A linear relationship between log K_d and f_c, is given by (Rao et al., 1985):

$$\log K_{d,mix} = \log K_{d,w(\mathrm{model})} + c \times f_c , \qquad (5.4)$$

where c reflects cosolvent−water−sorbent interactions and $K_{d,w(model)}$ is the solid−water partition coefficient modeled by Eq 5.4. By plotting log $K_{d,mix}$ as a function of f_c, the values of c and log $K_{d,w(model)}$ can be obtained. However, the experimental data cannot be modeled by Eq 5.4, as reflected by poor linear regression coefficients of determination (see Figure 5.4).

As evident in Figure 5.4, the longer the chain of a PFAS, the greater the volume of methanol needed to extract PFAS from XAD-7HP. The K_d value of PFUnDA, for example, decreased by 76% when f_c was 0.09, in comparison with the 98% decrease in the K_d value of PFOA. A longer-chained PFAS has a stronger tendency to exclude water and methanol molecules, which requires more methanol molecules to promote charge–polar force with PFUnDA and thus to extract it from XAD-7HP.

5.3.4 Effect of solution pH

In addition to the hydrophobic effect, other interactions are expected to influence PFAS sorption on XAD-7HP. Figure 5.5 and 5.6 show the effect of solution pH on the sorption of PFOS on XAD-7HP. The sorption increases in the order of pH: 7.8<6.8<5.9<4.8, with a rate of change of ~0.17 log units per unit pH (Figure 5.6). Since the pK_a value of PFOS should be smaller than 1 (Goss, 2008), the observed pH effect should be caused by pH-dependent changes in the sorbent (Dominguez et al., 2011). The pH_{pzc} of Amberlite XAD-7 is 6.2 (Dominguez et al., 2011). Therefore, at pH 7.8, the surface of XAD-7HP is almost completely negatively charged, and thus, the sorption of PFOS on XAD-7HP should be driven mainly by the hydrophobic effects. On the other hand, when pH is 6.8,

5.9 or 4.8, the surface of XAD-7HP is partly or completely positively charged, and there will be the electrostatic attraction between XAD-7HP and the PFOS functional group (negatively charged at circumneutral pH), which can explain the increased PFOS sorption at low pHs. In addition, XAD-7HP is prone to both charge–polar force and H-bonding/bridging, which are more intensive at low pHs (Kyriakopoulos et al., 2005). These effects may also contribute to the increase in PFOS sorption.

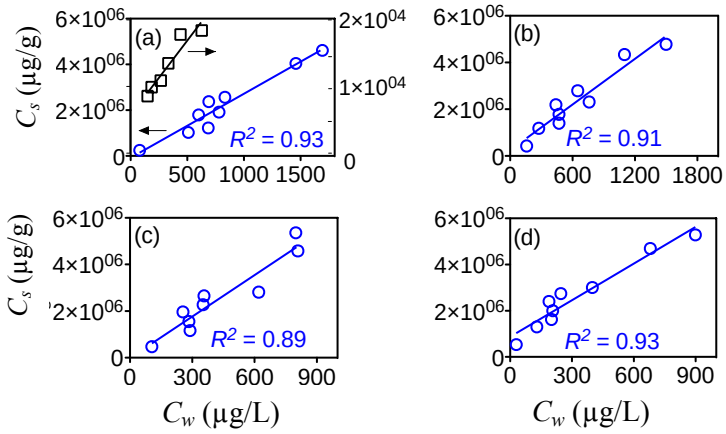

Figure 5.5 Effects of solution pH on the sorption of PFOS by XAD resins (T = 22.2 ± 0.5 °C; symbols: square: XAD-2; circle: XAD-7HP). (a) pH 7.8; (b) pH 6.8; (c) pH 5.9; (d) pH 4.8.

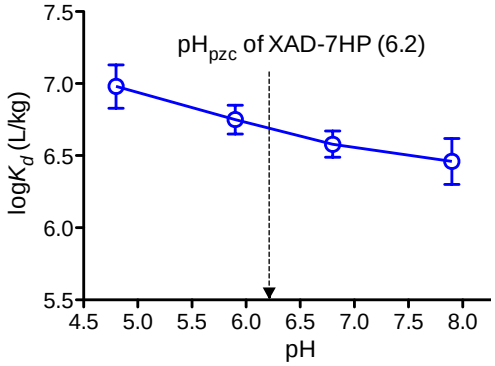

Figure 5.6 Effects of solution pH on PFOS sorption by XAD-7HP (T = 22.2 ± 0.5 °C; K_d: isotherm-determined sorption coefficient modeled by a linear sorption isotherm).

XAD-2 has also been widely used to collect, sorb or concentrate organic compounds, especially for sampling airborne contaminants (Freitas et al., 2008). In water, as shown in Figure 5.5, XAD-2 can sorb PFASs; however, the corresponding partitioning coefficient is two orders of magnitude smaller than the partitioning coefficient for XAD-7HP. The mean pore size of XAD-2 is nine nm, which may be difficult for PFAS, with a size that can reach one nm (see Appendix D) to form micelles within the micropores. Another possible reason is that the nonpolar resin, XAD-2, cannot offer charge–polar force and H-bonding.

5.3.5 Fixed bed column studies

Very few studies are available about the number of times (N) XAD resins can be effectively regenerated without loss of performance. The recoveries of PFOS or PFOA from four liters of PFOS/PFOA-spiked Mississippi River water by repeatedly regenerated XAD-7HP were plotted as a function of N (see Figure 5.7). The slope of the least-squares

regression line of the recoveries on N (up to $N = 8$) did not differ significantly from zero (two-sided p values are 0.79 for PFOA and 0.75 for PFOS, see Appendix D). Therefore, by regeneration, XAD-7HP can be reused at least eight times (~780 bed volumes of Mississippi River water sampled each time) without significant loss of performance. Similarly, XAD-7HP can be regenerated and reused at least nine times (~1970 bed volumes of tap water sampled each time) for concentrating PFOS from tap water without significant loss of performance (see Figure 5.7).

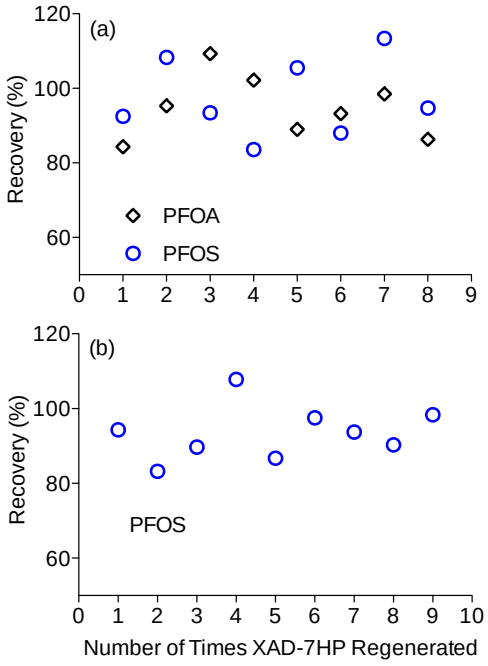

Figure 5.7 PFOS/PFOA recovered from PFOS/PFOA-spiked (10 nmol/L) matrices (a) Mississippi River water and (b) tap water using solid-phase extraction with XAD-7HP.

Chapter 6: MECHANISMS FOR REMOVAL OF PERFLUOROALKYL SUBSTANCES FROM DRINKING WATER BY CONVENTIONAL AND ENHANCED COAGULATION

Feng Xiao, Matt Simcik, John Gulliver, 2012. Mechanisms for removal of perfluorooctane sulfonate and perfluorooctanoate from drinking water by conventional and enhanced coagulation, ***Water Research*** (Accepted).

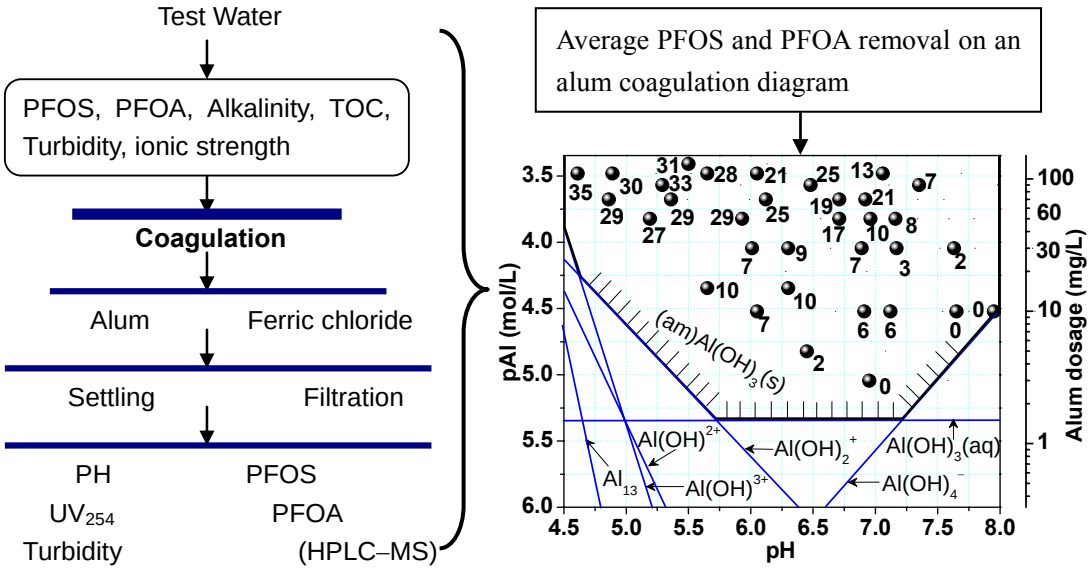

Graphical abstract

6.1 Introduction

The scientific community and the public have become increasingly concerned about the worldwide contamination of surface water and drinking water by two emerging persistent organic pollutants (POPs), perfluorooctane sulfonate (PFOS) and perfluorooctanoate (PFOA) (Armitage et al., 2009; Buck et al., 2011; Giesy and Kannan, 2001; Martin et al., 2004a). PFOS and PFOA are synthetic organic chemicals, primarily used as surface-active agents in food packaging, mist suppressants in the electroplating industry, fire-fighting foams, pesticides and polymers to repel water and stains on textiles and leather products (Awad et al., 2011; Jahnke and Berger, 2009; Lindstrom et al., 2011; Meyer et al., 2011). These chemicals are resistant to degrade by physical or chemical mechanisms once in the environment (Eschauzier et al., 2012; Prevedouros et al., 2006; Schröder and Meesters, 2005; Takagi et al., 2011). As a consequence of their chemical stability, relatively high water solubility, low volatility and extensive historical production, they are common surface and groundwater contaminants detected in numerous sites around the world (Bao et al., 2012; Benskin et al., 2010; Moody et al., 2003; Murakami et al., 2008; Nakayama et al., 2010; Simcik and Dorweiler, 2005; Skutlarek et al., 2006).

PFOS and PFOA have also been frequently detected in drinking water samples (Ericson et al., 2009; Hoffman et al., 2011b; Jin et al., 2009; Mak et al., 2009; Post et al., 2009; Takagi et al., 2008), and drinking water can be an important source of exposure to these chemicals for the general population (Ericson et al., 2009; Hoffman et al., 2011b; Tanaka et al., 2012; Vestergren and Cousins, 2009). Several studies have documented

that serum PFOA concentrations are elevated in areas with highly PFOA-contaminated drinking water (Post et al., 2012 and the references therein). PFOA-contaminated drinking water as an exposure medium for the general population becomes significant at a concentration of 40 ng/L or higher, and dominates exposure at > 500 ng/L (Vestergren and Cousins, 2009). Post et al. (2012) suggested that drinking water PFOA levels of 1 ng/L, 10 ng/L, 40 ng/L, 100 ng/L, and 400 ng/L can contribute approximately 2.4%, 20%, 50%, 71%, and 91% of the total exposure, respectively, in populations with a background serum PFOA concentration of 4 ng/mL from non-drinking water sources. In the State of Minnesota, high concentrations of PFOS (n.d.–3500 ng/L) and PFOA (n.d.–2200 ng/L) were detected in drinking water supplies (MPCA, 2009). Therefore, a study examining the effectiveness of drinking-water treatment processes is warranted to increase our understanding of the fate of PFASs during water treatment and to seek the best available technology for removing these POPs from drinking water. However, a study of this kind is rarely available in the literature. PFOS and PFOA are resistant to oxidation (Eschauzier et al., 2012; Prevedouros et al., 2006; Schröder and Meesters, 2005; Takagi et al., 2011), including advanced oxidation processes (Schröder and Meesters, 2005), but physicochemical treatments such as coagulation and carbon filtration may work for these chemicals.

Coagulation using hydrolyzable metal salts, particularly alum, is commonly employed in drinking-water treatment plants for removing suspended solids and natural organic matter (NOM) (Adachi and Tanaka, 1997; Amirtharajah and Mills, 1982; Dentel, 1988; Edzwald and Tobiason, 1999; Letterman and Vanderbrook, 1983; Singer and Bilyk,

2002; Stumm and O'Melia, 1968). A coagulation process is typically composed of two stages: rapid mixing and subsequently slow mixing. During the rapid mixing, dosed alum is quickly distributed into water to promote the contact between aluminum (Al) hydrolyzed species and contaminants in the raw water. During the slow mixing, or flocculation, Al hydroxide precipitate and particulates/contaminants clump together into flocs. The flocs then sink, float by air bubbles, or directly filtered, consequently retaining particulates/contaminants out of the water. At pH of 6–8 and an alum dosage of 30–110 mg/L, enmeshment dominates as a coagulation mechanism (Xiao et al., 2008a). Enmeshment refers to a process in which amorphous flocs adsorb and/or enmesh contaminants or particles (Xiao et al., 2008a).

There are two common types of coagulation in drinking-water treatment, conventional coagulation that is used for removing mainly turbidity particles and a portion of organic pollutants, and enhanced coagulation, a practice of using a coagulant dosage in excess of what is required for turbidity removal to achieve a greater removal of organic pollutants (Edzwald and Tobiason, 1999; Singer and Bilyk, 2002). Enhanced coagulation has been used to control the formation of disinfection by-products in drinking water (Xiao et al., 2010).

The literature is limited and somewhat contradictory with respect to the fate of PFOS/PFOA during drinking water treatment. Eschauzier et al. (2012) and Takagi et al. (2011) analyzed concentrations of PFOS and PFOA in every units of drinking water treatment plants with advanced treatment processes including ozonation and activated carbon filtration. Both studies find that activated carbon filtration is the only unit that can

remove PFOS and PFOA to a significant degree. However, Deng et al. (2010) found that coagulation can remove up to 90% of PFOA from water by using polyaluminum chloride (Al_2O_3 = 29%), and they suggested that the removal was caused by PFOA sorption to suspended solids. In addition, alum and ferric chloride are still the most widely used coagulants because of their availability, low cost, ease of use, and ease of storage (Water Environment Federation, 2006). The author of this thesis is not aware of any studies looking in detail at the mechanisms for removal of PFASs from drinking water by alum/ferric chloride coagulation. The objective of the present study was to examine various solution-specific and coagulant-specific parameters potentially affecting the removal of PFOS/PFOA by conventional and enhanced coagulation, with an overall goal of better control of the occurrence of these chemicals in tap water. This objective is achieved by determining PFOS/PFOA removal under different coagulation conditions and by delineating the proposed removal mechanism on a coagulation diagram. Only PFOS and PFOA were tested, because they are two frequently detected perfluoroalkyl substances (PFASs) in various environment matrices including drinking water and human blood samples worldwide (Haug et al., 2009; Kärrman et al., 2006; Kato et al., 2011; Yeung et al., 2006). In spite of the phase-out/reduction of the production of PFOS and PFOA by certain major manufacturers, environmental contamination and human exposure from these chemicals are anticipated to continue due to their environmental persistence and continuous PFOS/PFOA emissions from ongoing industrial/commercial activities (Clara et al., 2009; Lin et al., 2009; Müller et al., 2011; Pistocchi and Loos, 2009; Xiao et al., 2012b; Xiao et al., 2011a). Recent studies revealed that ongoing

industrial/commercial activities as a significant determinant of PFOS/PFOA pollution in the Upper Mississippi River Basin (Xiao et al., 2012; Xiao et al., 2011a).

6.2 Materials and methods

6.2.1 Jar tests

Jar tests are commonly used to simulate coagulation and settling processes by drinking-water treatment plants primarily for estimating the optimum coagulant dosage (Xiao et al., 2008b). Coagulation of PFOS&PFOA-spiked synthetic surface water was performed in jar tests at different turbidities, initial pHs (IpHs), and the dosages of alum ($Al_2(SO_4)_3 \cdot 18H_2O$) or ferric chloride ($FeCl_3 \cdot 6H_2O$). Unless otherwise specified, the synthetic surface water was prepared by adding kaolinite clay (10 mg/L, turbidity) and Suwannee River water-soluble NOM (5.72 mg/L) to deionized (D.I.) water spiked with 1.0 mM $NaHCO_3$ as an alkalinity and pH buffer and 1.0 mM NaCl to provide ionic strength. The initial turbidity of the synthetic surface water was ~7 NTU, formed by 10 mg/L kaolinite clay that was ultrasonically dispersed in the water. The amount of Suwannee River NOM was selected so that the dissolved organic carbon (DOC) was 3 mg/L, a typical DOC value for surface water. Suwannee River NOM was purchased from the International Humic Substances Society. The carbon and oxygen compositions of Suwannee River NOM are 52.47% and 42.59%, respectively, and the functional group distributions are: carbonyl, 8%; carboxyl, 20%; aromatic, 23%; aliphatic, 27% (IHSS, 2012). Suwannee River NOM is extracted and purified from the Suwannee River through a series of processes (IHSS, 2012), including reverse osmosis, and has been used in

numerous environmental studies (Comerton et al., 2009; Lee and Elimelech, 2007; Xiao et al., 2010).

Before a jar test, PFOS and PFOA were added to the synthetic surface water to reach 0.2 μM of each (or 0.1 mg/L of PFOS and 0.083 mg/L of PFOA), and the solution was mixed and kept at room temperature (~22^{o}C) for 48 h to reach equilibrium. Then the equilibrated solution underwent coagulation by using alum or ferric chloride. Relatively high PFOS/PFOA concentrations were used in jar tests, compared to the levels in natural water (Jahnke and Berger, 2009 and the references therein), in order to facilitate the analytical procedures and to obtain a better accuracy of the measurements by avoiding the uncertainties associated with the exaction and concentration.

During a typical jar test (see Figure 6.1a), a known volume of the coagulant stock solution was added to the equilibrated solution, and the tester immediately triggered the stirrer to rapidly mix the solution for 1 min at 150 rpm and then slowly mix the solution at 45 rpm for 20 min. After coagulation, the solution was settled for 30 min. Supernatants were taken and the coagulated water pH (or final pH) and residual turbidity were measured. The supernatants were filtered by passing through a 0.45-μm polycarbonate membrane (Millipore). The concentration of PFOS/PFOA in the filtrate (C_w, μg/L) was quantified. Meanwhile, the UV absorbance of the filtrate was measured using a Beckman UV–VIS spectrometer at 254 nm (UV_{254}). UV_{254} represents the aromatic functional groups and has been used to represent the aqueous level of NOM (Chin et al., 1994; Korshin et al., 1997). After the completion of a jar test, methanol (Optima grade from Fisher Scientific) and D.I. water were used to clean the beakers and the jar-test stirrer.

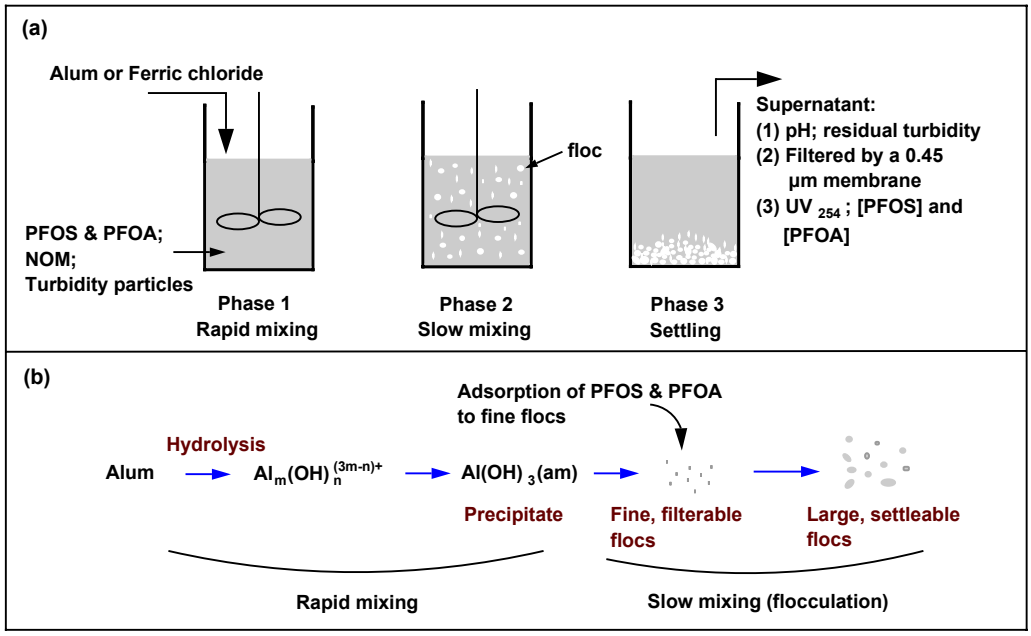

Figure 6.1 (a) A typical jar-test procedure (before a jar test, PFOS & PFOA were equilibrated with NOM and turbidity particles at room temperature (~22°C) for 48 h, see Section 6.2.1); (b) A proposed PFOS/PFOA removal mechanism (the floc formation process was adopted from Xiao et al. (2008a)).

6.2.2 Quantification of PFOS/PFOA concentration, QA and QC

The aqueous PFOS/PFOA concentrations were quantified by using a Hewlett Packard model 1090 high-performance liquid chromatograph (HPLC) coupled to a Hewlett Packard 1100 MSD mass spectrometer with an electrospray ionization source (ESI-MS). The steps and information for operating the HPLC–ESI-MS system can be found in our previous study (Xiao et al., 2011b). Briefly, the flow rate of the HPLC mobile phase was set at 0.20 mL/min. The mobile phase consisted of eluent A (2.0 mM NH_4Ac in a mixture of water and methanol (7:3, v/v)) and eluent B (2.0 mM NH_4Ac in methanol). The A/B

ratio changed linearly in the first 13 min from 100/0 to 43.9/57.1, which was held for 5 min then changed linearly over the next 15 min to 0/100, which was held for 3 min then changed linearly over the next 1 min to 100/0, which was held for 8 min. Although the latest eluting peak (PFOS) was observed at 21 min, sufficient run time (45 min) was used to condition the column for subsequent injections. The analytical column was a Luna C_{18} one (50 × 1.0 mm, 5 micron, Phenomenex), and the guard column was a KJO-4282 one (Phenomenex). The columns were conditioned prior to sample analysis with eluent B. For the ESI-MS analysis, ESI was performed in a negative mode, and the MS detector was operated in the SIM mode with optimized parameters (fragmentor voltage, 70 V; capillary voltage, 4 kV). Precursor ions with *m/z* of 413 and 499 were chosen, corresponding to PFOA and PFOS, respectively. The ions extracted at these mass units were used to determine the peak areas of PFOS/PFOA standards and analytical samples. External calibration standards (0.05–0.3 nmol/mL) were prepared by diluting the PFOS&PFOA stock solutions (1 mM in methanol) with D.I. water containing 1 mM $NaHCO_3$ and 1 mM NaCl. To deal with possible long-term bias within the measurement system, calibration standards were injected after every seven samples (not including calibration blanks) and a calibration curve was generated for every seven samples. Calibration blanks containing methanol and water (1:1, v/v) were run after every sample for monitoring the instrumental background. The concentrations of the analytes were quantified using 7-point matrix-matched calibration curves. The instrument detection limit (IDL) was defined as the concentration of PFOS and PFOA in the sample producing a peak with a signal-to-noise ratio of 3. The IDLs were determined to be 8 and 5 ng/mL

for PFOA and PFOS, respectively. Following each run sequence, the columns were completely flushed to ensure no crystallization on the stationary phase. The columns were capped and stored when not in use.

PFASs can adsorb to glassware and the jar test stirrer. Therefore, controls were performed in the same pattern as the jar test and at the same final pH, except that no coagulant was added. After coagulation and 30-min settling, samples were filtered and the concentration of PFOS/PFOA in the filtrate ($C_{control}$) was measured. The (control corrected) removal efficiency (E_r, %) was calculated by:

$$E_r = 100(C_{control} - C_w) / C_{control} \qquad (6.1)$$

Discussion throughout the remainder of the Chapter will relate to the removal efficiency of Eq 6.1, unless stated otherwise.

6.3 Results and discussion

6.3.1 PFOS/PFOA removal by coagulation: Effects of coagulant dosage and solution pH

As evident from Figure 6.2a, PFOS/PFOA removal was enhanced by adding more alum into the solution. Amorphous Al or Fe hydroxide flocs are fractal and highly porous aggregates made up of many primary particles. The surface area of the fine Al hydroxide flocs freshly formed at a hydrolysis ratio of 2.5 is 597 m^2/g at pH 6.5 (Rakotonarivo et al., 1988), close to activated carbon. The addition of Al hydroxide flocs with increasing alum dosage will increase the available surface area for adsorption/enmeshment of PFOS/PFOA.

The increasing removal, however, cannot solely be attributed to the increasing coagulant dosage. The solution pH is one factor that should be considered in maximizing coagulation performance and in describing PFAS behaviors at the solid–water interface (Higgins and Luthy, 2006; Tang et al., 2010; Wang and Shih, 2011; Xiao et al., 2012a; You et al., 2010). The solution pH dropped with the addition of alum (Figure 6.3) as Al(III) reacts with alkalinity producing intermediate Al hydrolyzed species and amorphous Al hydroxide, $Al(OH)_3$(am). The steps can be illustrated as

$$m\mathrm{Al}^{3+} + n\mathrm{H_2O} \rightarrow \mathrm{Al_m(OH)_n^{(3m-n)+}} + n\mathrm{H}^+ \rightarrow \mathrm{Al(OH)_3(am)}$$

When pH drops, the surface charge of flocs shifts in a positive direction (PZC of the freshly formed Al hydroxide flocs is 8.2 (Rakotonarivo et al., 1988)). In the region of mildly acidic to neutral pH, Al hydroxide flocs are positively charged, enabling the electrostatic attraction with the anionic PFOS/PFOA species. Therefore, the declining pH also contributed to the improved PFOS/PFOA removal (Figures 6.2 and 6.3).

The relative importance of the coagulant dosage and solution pH relates to two coagulation practices, enhanced coagulation (*increasing the coagulant dosage in excess of what is required for turbidity removal*) and optimized coagulation (*adjusting the solution pH before coagulation*) (Edzwald and Tobiason, 1999; Gregor et al., 1997; Singer and Bilyk, 2002). However, adjusting pH to the optimum value before coagulation is not always feasible especially for raw water with a high buffer capacity (Jekel, 1986). For this reason, enhanced coagulation is often applied to achieve a greater removal of water contaminants.

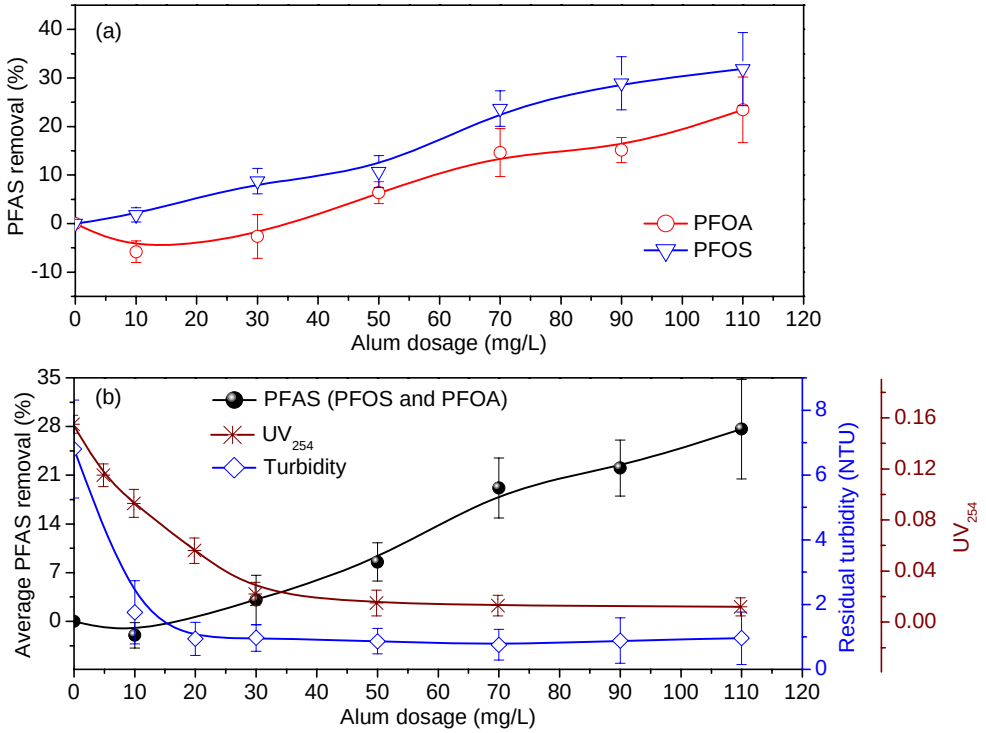

Figure 6.2 (a) PFOS/PFOA removal as a function of alum dosage at IpH 7.9 (the negative removals of PFOA at dosages of ≤ 30 mg/L were within the measurement reproducibility (11%)); (b) The effect of alum dosage on average removal efficiency of PFOS and PFOA, UV_{254}, and residual turbidity. Initial conditions: alkalinity = 1 mM HCO_3^-; turbidity = 10 NTU; DOC = 3 mg/L; [PFOS] = [PFOA] = 0.2 µM

It is typical for drinking-water treatment plants to determine the optimum coagulant dosage by measuring the residual turbidity of the settled water (Xiao et al., 2008b). As shown in Figure 6.2b, the residual turbidity sharply decreased with increasing alum dosage from 0 to 10 mg/L, and remained relatively stable (< 1 NTU) in a wide dosage range studied (20–110 mg/L). On the other hand, significant removals of PFOS and

PFOA were observed only after increasing the alum dosage to 50 mg/L. The distinctly different fates of turbidity particles and PFOS/PFOA indicate PFOS/PFOA was not co-removed with turbidity particles during coagulation, which is different from the mechanism proposed by a previous study (Deng et al., 2010). Coagulation of turbidity particles is mostly a matter of physical collisions and aggregation (Xiao et al., 2008b), whereas coagulation removal of PFOS/PFOA relies on adsorption to Al hydroxide flocs.

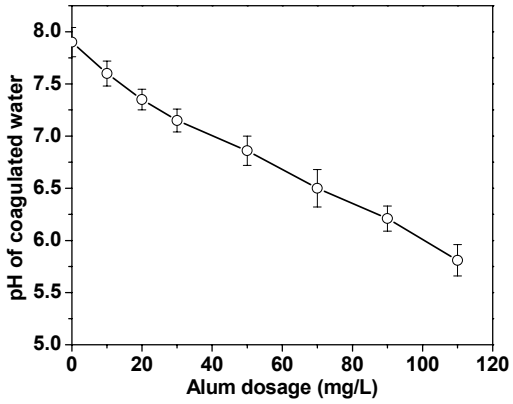

Figure 6.3 The pH of coagulated water as a function of alum dosage (initial conditions: alkalinity = 1 mM HCO_3^-; turbidity = 10 NTU; DOC = 3 mg/L; [PFOS] = [PFOA] = 0.2 μM).

6.3.2 Coagulation diagram

A coagulation diagram is a figure in which coagulant metal concentration–pH coordinates are used to outline the regions of different coagulation mechanisms. It has been used to select the appropriate coagulant product and coagulant dosage for a given application and to interpret coagulation results from both jar tests and plant studies (Amirtharajah and Mills, 1982; Kim et al., 2001; Liu and Chin, 2009; Xiao et al., 2008c).

The average removal efficiencies of PFOS and PFOA were plotted on a coagulation diagram of Al(III) with thermodynamic boundaries of Al^{3+}, $Al(OH)^{2+}$, $Al(OH)_2^+$, $Al(OH)_4^-$ and $Al(OH)_3(aq)$ indicated (see Figure 6.4), following the steps described elsewhere (Xiao et al., 2008c). $Al(OH)_3(am)$ is generally believed to be the predominant precipitate form in water treatment processes and thus is selected as the controlling solid phase in the coagulation diagram (Al species in equilibrium with $Al(OH)_3(am)$). As shown in Figure 6.4, the average removal efficiencies were mostly below 10% during conventional coagulation. This finding agrees well with a previous study in which PFOS was not removed by ferric chloride coagulation with a ferric chloride dosage of 3.0–5.0 mg/L (equivalent to 7.8 to 12.3 mg alum /L) (Eschauzier et al., 2012). Removals exceeding 25% occurred in the enhanced coagulation region characterized by higher alum dosages (e.g., >60 mg/L) and (thus) lower coagulated water pH (4.5–6.5). However, flocs formed in this moderate acidic pH region (below pH 6.5) were typically smaller and less well-defined than those formed at higher pH. These flocs usually exhibited poor settling characteristics but could be filtered. In general, the removal efficiencies were below 35% under the examined coagulation conditions (alum dosage = 3–110 mg/L; final pH = 4.5–8), indicating that alum coagulation is not an efficient process for removing PFOS/PFOA. A further increase in alum dosage above 110 mg/L can increase the available surface area for adsorption/enmeshment and thus may achieve a further higher removal rate. Too much inorganic coagulant would, however, consume the alkalinity, increase the volume of sludge to be dewatered, and expand the operating cost of water treatment.

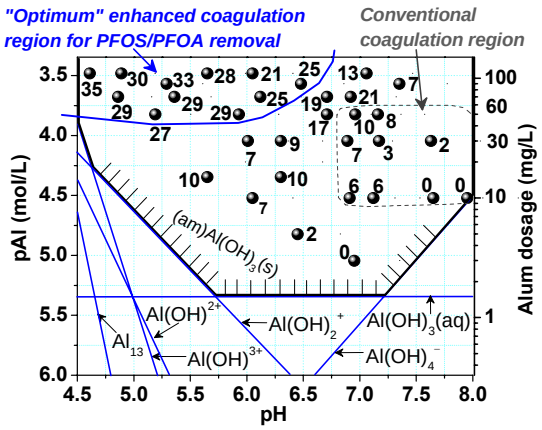

Figure 6.4 Average removals of PFOS and PFOA presented on an alum coagulation diagram (pAl = log [Al^{3+}]; Al_{13}: $Al_{13}O_4(OH)_{24}^{7+}$).

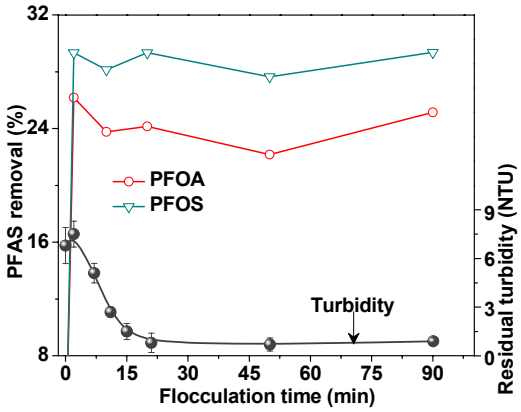

Figure 6.5 PFOS/PFOA removal as a function of flocculation time (IpH 7.9; 110 mg/L alum).

PFOS/PFOA removal by coagulation was also studied with ferric chloride (see Figure E-2, Appendix E). In general, ferric chloride as the coagulant achieved similar removal efficiencies as alum when they are compared on a molar basis. Although alum as $Al_2(SO_4)_3 \cdot 18H_2O$ has a gram molecular weight of approximately 666 and ferric chloride

as $FeCl_3 \cdot 6H_2O$ has an approximate weight of 271, alum forms two moles of Al^{3+} and ferric chloride forms only one mole of Fe^{3+} in solution. As a result, even the effectiveness of the two coagulants when compared on the basis of weight is similar if one considers that effectiveness is dependent on the metal ions in the solution.

6.3.3 Effect of flocculation time

When the concentration product ($[Al^{3+}][OH^-]^3$) is large enough for Al(III) to precipitate, Al hydroxide precipitate can be formed in a short time (1–7 sec) (Amirtharajah and Mills, 1982, Kim et al., 2001, Liu and Chin, 2009). The precipitate will bind together to form fine, filterable flocs which can be visible in the early stage of flocculation, and fine flocs will aggregate and eventually form large, settleable flocs (see Figure 6.1b). As evident in Figure 6.5, PFOS and PFOA were mostly removed during the initial 2-min flocculation; elongating flocculation time from 2 to 90 min could not improve the removal further, indicating that PFOS/PFOA was quickly adsorbed to fine flocs. On the other hand, for turbidity removal, a flocculation time from 2 to 15 min is essential for generating setteable flocs and lowering the residual turbidity (see Figure 6.5), indicating again a different removal mechanisms for turbidity particles as compared to PFOS/PFOA.

6.3.4 Effect of NOM

The interaction between PFOS/PFOA and dissolved natural organic substances have not yet been experimentally determined. It has been found that the DOC–water distribution coefficient (K_{DOC}) of 8:2 fluorotelomer alcohol is about a log unit higher than the organic

carbon-normalized sorption coefficient (K_{oc}) (Liu and Lee, 2005). If this relationship also holds for PFOS, its K_{DOC} can reach to $10^{3.57}$ (by using the K_{oc} of $10^{2.57}$ determined by Higgins and Luthy (2006)), corresponding to a NOM–water distribution coefficient (K_{NOM}) of $10^{3.29}$ (52.47% carbon composition in Suwannee River NOM). The estimated K_{NOM} value suggests a strong assocaition between PFOS and NOM. Thus, NOM in water may enhance PFOS removal because of the co-removal of PFOS with NOM by coagulation. As illustrated in Figure 6.2, the solution UV_{254} dropped by 70% when the alum dosage was larger than 20 mg/L, suggestive of a considerably high NOM removal rate by coagulation. However, the percentage removal of PFOS/PFOA is not higher than 10% at 20 mg alum/ L (Figures 6.1 and 6.2). As presented in Figure E-3 (Appendix E), removals of PFOS and PFOA were found to be nearly independent of the initial NOM concentration (from 0 to 13.3 mg NOM /L). Several possible factors can explain the difference between the expected and observed PFOS/PFOA removal efficiencies with the presence of NOM. First, the concentration of NOM in the current study is about two orders of magnitude above the concentration of PFOS/PFOA. Only a small portion of NOM should therefore be associated with PFOS/PFOA, and coagulation removal of NOM may have little impact on PFOS/PFOA. Second, NOM is able to form multidental chelate complexes with inorganic cations, including Al(III) and Fe(III), and thus influencing the speciation of metals and the performance of coagulation (Jekel, 1986; Masion et al., 2000; Saar and Weber, 1982; Srinivasan and Viraraghavan, 2004), Last, but not the least, the adsorbed/associated NOM on flocs may impede floc sorpiton of

PFOS/PFOA through charge neutralization of the positively charged of flocs and/or through steric effects.

6.3.5 Other possible mechanisms for removal of PFOS/PFOA by coagulation

Other coagulation mechanisms include complexation. For PFOS/PFOA, it may be possible that they complex and co-precipitate with Al(III). Coordination of PFOS/PFOA is straightforward: the sulfonate or carboxyl group is the only donor and gives monodentate complexes. However, a monodentate ligand is unlikely to affect the hydrolysis of Al(III) (Thomas et al., 1993). Furthermore, the functional groups of NOM can complex with Al species in the solution, which further reduces the possibility of the complexation between Al species and PFOS/PFOA.

Chapter 7: CONCLUSIONS AND RECOMMENDATIONS TO FUTURE WORK

Feng Xiao, Matt Simcik, John Gulliver, 2012. Perfluorooctane sulfonate (PFOS) contamination of fish in urban lakes: Lake prioritization for PFOS monitoring based on GIS-assisted exploratory data analysis (data analysis has been completed, and a manuscript has been written)

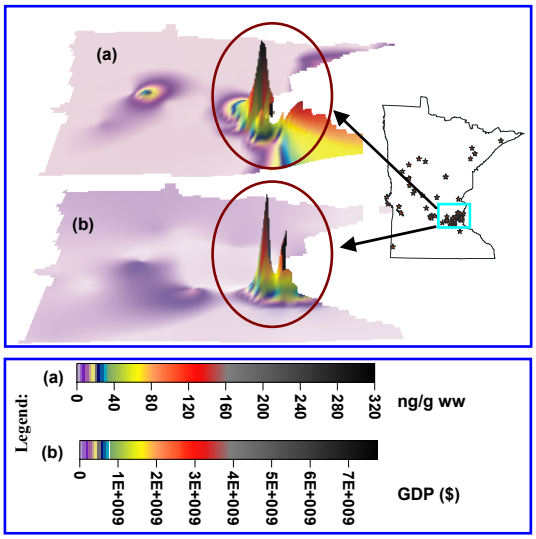

Graphical abstract: Surface plots (created by an ordinary Kriging method) of (a) median concentrations of PFOS ($C_{fish,PFOS}$) in fish captured from Minnesota lakes and (b) GDP of the nearest town/city to the lake surveyed. The data of $C_{fish,PFOS}$ are from (Delinsky et al., 2010, MPCA, 2009).

7.1 Conclusions

PFASs are anthropogenic environmental contaminants that are persistent, bioaccumulative and toxic. The objectives of this thesis were to determine the environmental occurrence and fate of PFASs in the Upper Mississippi River Basin and understand their removal from the aqueous phase by several processes.

Chapter 2 contributes to the limited knowledge of the levels and fate of these chemicals in urban runoff. The concentrations and spatial distributions of PFASs in urban stormwater runoff were investigated in order to determine possible sources of the contamination. Chapter 3 involves the application of an unsupervised, multivariate statistical method to PFAS concentrations in the influent from 37 WWTPs in a multi-city survey to delineate polluted areas and to distinguish between different types of pollution. In addition, because the fate and transport of PFASs in aquatic environments strongly depend on their interactions with solid surfaces, Chapter 4 investigates the adsorption PFASs on kaolinite clay were examined systematically and modeled regarding the effects of sodium on PFAS adsorption characteristics. Because Amberlite XAD resins have been employed to a great extent as the sorbent for removing or concentrating organic compounds from different matrices, the sorption of PFASs by XAD-7HP resins was discussed in Chapter 5. Chapter 6 describes the performance of coagulation in terms of PFAS removal by developing an operational coagulation diagram when the contaminants are associated with both turbidity and NOM. The experimental conditions cover both conventional coagulation and the enhanced coagulation. Using the coagulation diagram as a base, environmental chemists and the operators in water treatment plants can easily

evaluate and predict their removals during conventional coagulation. The major findings of this thesis are:

1. Chapter 2: PFASs were found in all runoff samples collected from industrial, commercial, heavy-traffic and residential areas, indicating that these compounds are widely distributed in the Minneapolis–St. Paul metropolitan area (MN, USA). Excluding runoff from an industrial area, the median stormwater runoff concentration in this area was estimated at 25.8 ng/L, which can be seen as a background runoff concentration in this metropolitan area. PFOS and PFOA are the most frequently detected PFASs in stormwater runoff. The frequencies of detection of PFASs in urban runoff were found to be PFOS (100%), PFOA (100%), PFNA (67%), PFDA (50%), PFHpA (44%), and PFUnDA (22%). The greater PFAS load from stormwater runoff than from atmospheric inputs implies that PFASs in the urban environment are solubilized in rain and transported. For vacant/remote areas, the background runoff concentration can be mainly attributed to rainfall.

2. Chapter 3: The application of the methodology (cluster analysis → compositional analysis → correlation analysis/scatter matrix) achieved a meaningful classification of the sources of PFASs in WWTPs; allowing the characterization of the data according to the geographical distribution of PFAS sources. The results revealed different PFAS patterns in WWTP influent conditionally named

"domestic cluster," "PFHxA cluster," "PFOS cluster" and "PFOA cluster." The technique was used to track down the locations of industrial sources of PFAS pollution in Minnesota, which can lead to an optimization of environmental/river monitoring nets. The results are consistent with known industrial pollution sources in the City of Pine Island, City of Brainerd and City of Cottage Grove. Generally, WWTPs receiving industrial wastewater from known or undiscovered industrial sources contain elevated levels of PFASs compared to WWTPs primarily receiving domestic wastewater. Fifty-nine percent of WWTPs receive considerably high levels of PFHxA or PFOA precursors, probably from industrial sources. Statistical analysis and compositional analysis suggests that certain PFASs at unusually high levels in WWTPs could have been derived directly from industrial sources or bio-transformed from their precursors within WWTPs. The results highlight industrial wastewater as an important source of PFASs that have been included in a wide range of industrial products. Along with previous reports of industrial influences (Becker et al., 2008; Clara et al., 2008; Hansen et al., 2002; Kunacheva et al., 2011; Lin et al., 2010; Lin et al., 2009; Möller et al., 2010; Müller et al., 2011b; Paul et al., 2011; Pistocchi and Loos, 2009; Rostkowski et al., 2006; Shivakoti et al., 2010; Sinclair and Kannan, 2006; So et al., 2007; So et al., 2004; Sun et al., 2011; Takazawa et al., 2009; Yoo et al., 2009), accumulated evidence points to ongoing emissions from industrial sources as a significant determinant of PFAS pollution in urban watersheds.

3. Chapter 4: The adsorption of PFAS on kaolinite clay can be substantially enhanced by the addition of cations. The results indicate that PFAS transport can be seriously retarded in high ionic strength conditions such as brackish groundwater, river estuaries, seawater, or snowmelt containing road salts. This supports the previous observation that PFOS was largely adsorbed to the sediment in estuaries (Pan and You, 2010). This study provides the first observation of the competitive adsorption of PFASs on a natural adsorbent, which contributes to the understanding of the behavior of ionizable surfactants at a solid–water interface. Furthermore, industry has been using a short-chain PFAS, perfluorobutane sulfonate (PFBS), which has four carbons, in place of PFOS (Betts, 2007). Very little is known about the fate and activity of short-chain PFASs in the environment. The results of this study imply that the adsorption of C_4 PFASs in freshwater systems is unlikely.

4. Chapter 5: The XAD-7HP resin shows a good potential ability for being used as a sorbent for concentrating or removing PFASs. The sorption processes were well described by either a linear isotherm or by the Freundlich model. Within the sorbate equilibrium concentration range of 0.2–7 μM, sorpiton was mainly close to linear for most target compounds. The isotherm-determined K_d values of PFASs for this resin can reach 10^6 L/kg. The column study shows that this resin can be used for treating large-volume samples and can be successfully regenerated without significant loss of performance. Sorption of PFASs on XAD-

7HP was strongly dependent on the length of the perfluorinated chain and the solution pH, indicating the importance of both hydrophobic and electrostatic effects. The strong sorption affinity of XAD-7HP for PFASs deserves further study to compare its performance with Oasis HLB and WAX resins that have been used to concentrate and/or cleanup in many PFAS studies.

5. Chapter 6: The removal of PFOS/PFOA by coagulation appears to be controlled by electrostatic effects. The dosage of coagulant (alum or ferric chloride) and solution pH are two dominant factors affecting the removal rate of PFOS/PFOA. Increasing coagulant dosage can increase the available surface area for adsorption/enmeshment, and the resulting decrease in pH (from the increase in coagulant dosage) can increase the number of protonated adsorption sites. In addition, it was demonstrated that 2-min flocculation time was sufficient to reach the maximum achievable PFOS/PFOA adsorption to freshly formed Al hydroxide flocs, and longer flocculation time only induced the growth of fine flocs to large, settleable flocs. The primary mechanism for the removal of PFOS/PFOA is due to fine floc adsorption. The different fates of PFOS/PFOA and turbidity particles during coagulation indicate that the chemicals were not co-removed with turbidity particles; they requires a different removal approach than what is required for reducing turbidity. Therefore, for PFOS/PFOA-contaminated water with low turbidity, such as groundwater, an enhanced coagulation process with a short flocculation time (e.g., 2 min) deserves to be investigated in the future as a

pretreatment to carbon filtration. Coagulation using ferric chloride achieved comparable removal efficiencies as alum coagulation when the two coagulants are compared on a molar basis. The results and discussion of possible mechanisms of removal presented in this thesis will add to the limited published studies aviable that examines the effects of current drinking-water treatment processes. The paper will provide information that could be used to improve current techniques to address the presence of emerging contaminants in drinking water. The PFOS/PFOA-removal coagulation diagram developed in this thesis can provide a hand-on tool for drinking-water companies to use. Using the coagulation diagram as a base, environmental chemists and the operators in water treatment plants can easily evaluate and predict their removals during coagulation.

7.2 Recommendations for future research

The following are three future PFAS research topics that would improve our understanding of PFASs.

7.2.1 PFAS physicochemical properties

PFASs show unique characteristics, and the chain length of long-chain PFASs can be 1 nm (see Chapter 4). Therefore, a major question regarding the transport and toxicity of long-chain PFASs is whether they could be considered as nanoparticles. In addition, the concentrations of two long-chain PFASs, PFOS and PFOA, in human blood are several tens ppb. The effects of cations, especially multivalent cations, on the formation of

(hemi-)micelles of PFASs are not clear, and their critical micelle concentrations in blood have not yet been experimentally determined.

7.2.2 Removal of shorter-chained PFASs (e.g., PFBA and PFBS)

Shorter-chained PFASs (< 7 perfluorocarbons) were not included in Chapter 6. Although shorter-chained PFASs are considered to be less bioaccumulative and less harmful than longer-chained PFASs (Conder et al., 2008; Hu et al., 2002; Upham et al., 1998), their toxicities and environmental effects may have not been fully understood. They have been detected in raw and treated tap water (Boiteux et al., 2012; Eschauzier et al., 2010; MPCA, 2009; Wilhelm et al., 2010), and were believed to dominate in the total PFAS levels in drinking water in the immediate future (Wilhelm et al., 2010). Shorter-chained PFASs are anticipated to have lower adsorptivity than longer-chained PFASs (Xiao et al., 2011) (see Chapter 4), and they are recalcitrant to be removed by coagulation, sand filtration, ozonation, and carbon filtration (Eschauzier et al., 2012). According to the modeling work (see Chapter 5), the XAD-7HP resin, however, may be able to remove these shorter-chained PFASs from water. Further studies on the removal of shorter-chained PFASs by enhanced treatment technologies are recommended in the future.

7.2.3 Geographical distribution of PFASs in Minnesota lakes and soils

a) Several lakes in the Minneapolis–St. Paul metropolitan area (Lake Calhoun, Lake Elmo, Lake Harriet, Lake Johanna, Little Johanna Lake and Lake of the Isles) have been PFOS-impaired (MPCA, 2009) and currently put on the list of impaired

waters by the MPCA because of the elevated concentrations of PFOS in fish (MPCA, 2012). The State of Minnesota (USA) advises one meal of fish per week if the concentration of PFOS in fish ($C_{fish,PFOS}$) is larger than 38 ng/g wet weight (ww) and one meal per month if the level exceeds 160 ng/g ww (Erickson, 2008). The implementation of the advice necessitates a statewide survey of PFOS in lake fish. However, a survey of this kind is often characterized by the relatively high costs of sampling, pretreatment and instrumental analysis, and by the large number of urban lakes. In support of TMDL, a new prioritization methodology is currently being developed to: (1) assess the sources of PFOS input to urban lakes that cause PFOS impairment; and (2) aid in the development of a cost- and time-efficient monitoring strategy with clearly-defined objectives for having a large-scale water quality monitoring activity. The methodology is a combination of exploratory data analysis (EDA) and geographic information system (GIS), which extends EDA to detect spatial properties of the data. The preliminary results show that PFOS is often present at concentrations of potential concern in the lakes near industrial/commercial centers and major highways where presumably source intensities are high. Urban lakes receive ongoing PFOS inputs from industrial and/or commercial activities and vehicular traffic, and urban runoff acts as an important pathway for PFOS entry into the lakes. Urban lakes in the Minneapolis–St. Paul metropolitan area tend to have higher $C_{fish,PFOS}$ than lakes outside. Thirty-four urban lakes have been prioritized by this methodology and recommended in future monitoring activities.

b) Transportation activities generate a wide range of contaminants, including particulate matter, heavy metals and persistent organic pollutants. There has been extensive research on particulates and heavy metals. However little is known about the highway runoff, highway dust and roadside soil contamination of PFASs. In Chapter 2, there is evidence that transportation activities contribute nonpoint source pollution of PFASs in Minnesota; however, a clear picture of PFASs in urban/rural highway runoff, highway dust and roadside soil is lacking in the literature. In addition, cars may act as pollutant carriers. The 3M Cottage Grove former PFOS facility is close to the Minnesota State Highway 61 (MN-61). MN-61 is the section of the National Highway 61 in Minnesota, and it is a scenic highway, following the North Shore of Lake Superior, the largest of the five traditionally demarcated Great Lakes of North America. It is possible that cars can carry PFOS-polluted soil particles and/or mud from the pollution source to remote areas.

c) The spatial distribution of PFASs on Minnesota soil is not well understood. Despite 3M's PFAS production phase-out, there is a substantial reservoir of PFAS-containing substances/products still in use in a wide range of industrial/commercial applications (see Chapters 2 and 3). PFASs may accumulate in human beings and animals (e.g. cows) through inhalation of PFAS-polluted fine soil particles, dermal contact and/or the intake of contaminated edible plants (Sepulvado et al., 2011; Stahl et al., 2009). Soil pollution of PFASs is of high concern for children who have a higher potential for exposure to PFASs

through the non-dietary ingestion route as a result of their hand-to-mouth behavior.

LIST OF REFERENCES

Adachi, Y. and Tanaka, Y. 1997. Settling velocity of an aluminium–kaolinite floc. Water Research 31 (3), 449–454.

Adak, A., Bandyopadhyay, M. and Pal, A. 2005. Removal of anionic surfactant from wastewater by alumina: a case study. Colloids and Surfaces A–Physicochemical and Engineering Aspects 254 (1–3), 165–171.

Ahrens, L., Shoeib, M., Harner, T., Lee, S.C., Guo, R. and Reiner, E.J. 2011a. Wastewater treatment plant and landfills as sources of polyfluoroalkyl compounds to the atmosphere. Environmental Science & Technology 45 (19), 8098–8105.

Ahrens, L., Yeung, L.W., Taniyasu, S., Lam, P.K. and Yamashita, N. 2011b. Partitioning of perfluorooctanoate (PFOA), perfluorooctane sulfonate (PFOS) and perfluorooctane sulfonamide (PFOSA) between water and sediment. Chemosphere 85 (5), 731–737.

Amirtharajah, A. and Mills, K.M. 1982. Rapid-mix design for mechanisms of alum coagulation. Journal American Water Works Association 74 (4), 210–216.

Armitage, J.M., Schenker, U., Scheringer, M., Martin, J.W., Macleod, M. and Cousins, I.T. 2009. Modeling the global fate and transport of perfluorooctane sulfonate (PFOS) and precursor compounds in relation to temporal trends in wildlife exposure. Environmental Science & Technology 43 (24), 9274–9280.

Arp, H.P.H., Niederer, C. and Goss, K.U. 2006. Predicting the partitioning behavior of various highly fluorinated compounds. Environmental Science & Technology 40 (23), 7298–7304.

Awad, E., Zhang, X.M., Bhavsar, S.P., Petro, S., Crozier, P.W., Reiner, E.J., Fletcher, R., Tittemier, S.A. and Braekevelt, E. 2011. Long-term environmental fate of perfluorinated compounds after accidental release at Toronto airport. Environmental Science & Technology 45 (19), 8081–8089.

Bao, L-J., Maruya, K.A., Snyder, S.A. and Zeng, E.Y. 2012. China's water pollution by persistent organic pollutants. Environmental Pollution 163, 100–108.

Barton, C.A., Botelho, M.A. and Kaiser, M.A. 2009. Solid vapor pressure and enthalpy of sublimation for ammonium perfluorooctanoate. Journal of Chemical and Engineering Data 54 (3), 752–755.

Barton, C.A., Kaiser, M.A. and Russell, M.H. 2007. Partitioning and removal of perfluorooctanoate during rain events: The importance of physical-chemical properties. Journal of Environmental Monitoring 38 (4), 991–996.

Baun, A., Eriksson, E., Ledin, A. and Mikkelsen, P.S. 2006. A methodology for ranking and hazard identification of xenobiotic organic compounds in urban stormwater. Science of the Total Environment 370 (1), 29–38.

Beach, S.A., Newsted, J.L., Coady, K. and Giesy, J.P. 2006 Reviews of Environmental Contamination and Toxicology, Vol 186. Ware, G.W. (ed), pp. 133–174.

Becker, A.M., Gerstmann, S. and Frank, H. 2008. Perfluorooctane surfactants in waste waters, the major source of river pollution. Chemosphere 72 (1), 115–121.

Bengtson, V.L. Acock, AC., Allen, K.R., Dilworth–Anderson, P. and Klein, D.M. 2005 Sourcebook of Family Theory & Research, Sage Publications, Inc., Thousand Oaks, CA.

Benskin, J.P., Yeung, L.W., Yamashita, N., Taniyasu, S., Lam, P.K. and Martin, J.W. 2010. Perfluorinated acid isomer profiling in water and quantitative assessment of manufacturing source. Environmental Science & Technology 44 (23), 9049–9054.

Berger, U., Glynn, A., Holmstrom, K.E., Berglund, M., Ankarberg, E.H. and Tornkvist, A. 2009. Fish consumption as a source of human exposure to perfluorinated alkyl substances in Sweden – Analysis of edible fish from Lake Vattern and the Baltic Sea. Chemosphere 76 (6), 799-804.

Betts, K.S. 2007. Perfluoroalkyl acids: What is the evidence telling us? Environmental Health Perspectives 115 (5), A250–A256.

Bhhatarai, B. and Gramatica, P. 2011. Prediction of aqueous solubility, vapor pressure and critical micelle concentration for aquatic partitioning of perfluorinated chemicals. Environmental Science & Technology 45 (19), 8120–8128.

Bischel, H.N., Macmanus-Spencer, L.A. and Luthy, R.G. 2010. Noncovalent interactions of long-chain perfluoroalkyl acids with serum albumin. Environmental Science & Technology 44 (13) 5263–5269.

Bjorklund, J.A., Thuresson, K. and De Wit, C.A. 2009. Perfluoroalkyl compounds (PFCs) in indoor dust: Concentrations, human exposure estimates, and sources. Environmental Science & Technology 43 (7), 2276–2281.

Boiteux, V., Dauchy, X., Rosin, C. and Munoz, J-F. 2012. National screening study on 10 perfluorinated compounds in raw and treated tap water in France. Archives of Environmental Contamination and Toxicology 63 (1), 1–12.

Boulanger, B., Vargo, J.D., Schnoor, J.L. and Hornbuckle, K.C. 2005. Evaluation of perfluorooctane surfactants in a wastewater treatment system and in a commercial surface protection product. Environmental Science & Technology 39 (15), 5524–5530.

Buck, R.C., Franklin, J., Berger, U., Conder, J.M., Cousins, I.T., de Voogt, P., Jensen, A.A., Kannan, K., Mabury, S.A. and van Leeuwen, S.P. 2011. Perfluoroalkyl and polyfluoroalkyl substances in the environment: Terminology, classification, and origins. Integrated Environmental Assessment and Management 7 (4), 513–541.

Burns, D.C., Ellis, D.A., Li, H., McMurdo, C.J. and Webster, E. 2008. Experimental pK_a determination for perfluorooctanoic acid (PFOA) and the potential impact of pK_a

concentration dependence on laboratory-measured partitioning phenomena and environmental modeling. Environmental Science & Technology 42 (24), 9283–9288.

Calafat, A.M., Kuklenyik, Z., Reidy, J.A., Caudill, S.P., Tully, J.S. and Needham, L.L. 2007. Serum concentrations of 11 polyfluoroalkyl compounds in the U.S. population: Data from the national health and nutrition examination survey (NHANES). Environmental Science & Technology 41 (7), 2237–2242.

Carnali, J.O. and Shah, P. 2008. Correlation of surfactant/polymer phase behavior with adsorption on target surfaces. The Journal of Physical Chemistry. B 112 (24), 7171–7182.

Chin, Y.P., Aiken, G. and O'Loughlin, E. 1994. Molecular weight, polydispersity, and spectroscopic properties of aquatic humic substances. Environmental Science & Technology 28 (11), 1853–1858.

Chocat, B., Ashley, R., Marsalek, J., Matos, M.R., Rauch, W., Schilling, W. and Urbonas, B. 2007. Toward the sustainable management of urban storm-water. Indoor and Built Environment 16 (3), 273–285.

Clara, M., Gans, O., Weiss, S., Sanz-Escribano, D., Scharf, S. and Scheffknecht, C. 2009. Perfluorinated alkylated substances in the aquatic environment: An Austrian case study. Water Research 43 (18), 4760–4768.

Clara, M., Scheffknecht, C., Scharf, S., Weiss, S. and Gans, O. 2008. Emissions of perfluorinated alkylated substances (PFAS) from point source—Identification of relevant branches. Water Science and Technology 58 (1), 59–66.

Comerton, A.M., Andyews, D.C. and Bagley, D.M. 2009. The influence of natural organic matter and cations on the rejection of endocrine disrupting and pharmaceutically active compounds by nanofiltration. Water Research 43 (3), 613–622.

Conder, J.M., Hoke, R.A., De Wolf, W., Russell, M.H. and Buck, R.C. 2008. Are PFCAs bioaccumulative? A critical review and comparison with regulatory criteria and persistent lipophilic compounds. Environmental Science & Technology 42 (4), 995–1003.

Cui, L., Zhou, Q.-F., Liao, C.-Y., Fu, L.-J. and Jiang, G.-B. 2009. Studies on the toxicological effects on PFOA and PFOS on rats using histological observation and chemical analysis. Archives of Environmental Contamination and Toxicology 56 (2), 338–349.

Davis, A.P., Shokouhian, M. and Ni, S.B. 2001. Loading estimates of lead, copper, cadmium, and zinc in urban runoff from specific sources. Chemosphere 44 (5), 997–1009.

Deletic, A., Maksimovic, C. and Ivetic, M. 1997. Modelling of storm wash-off of suspended solids from impervious surfaces. Journal of Hydraulic Research 35 (1), 99–118.

Delinsky, A.D., Strynar, M.J., McCann, P.J., Varns, J.L., McMillan, L., Nakayama, S.F. and Lindstrom, A.B. 2010. Geographical distribution of perfluorinated compounds in fish from Minnesota lakes and rivers. Environmental Science & Technology 44 (7), 2549–2554.

Deng, S.B., Yu, Q.A., Huang, J. and Yu, G. 2010. Removal of perfluorooctane sulfonate from wastewater by anion exchange resins: Effects of resin properties and solution chemistry. Water Research 44 (18), 5188–5195.

Dentel, K.S. 1988. Application of the precipitation-charge neutralization model of coagulation. Environmental Science & Technology 22 (7), 825–832.

D'eon, J.C. and Mabury, S.A. 2011. Is indirect exposure a significant contributor to the burden of perfluorinated acids observed in humans? Environmental Science & Technology 45 (19), 7974–7984.

Dinglasan, M.J.A., Ye, Y., Edwards, E.A. and Mabury, S.A. 2004. Fluorotelomer alcohol biodegradation yields poly- and perfluorinated acids. Environmental Science & Technology 38 (10), 2857–2864.

Dominguez, J.R., Gonzalez, T., Palo, P. and Cuerda-Correa, E.M. 2011. Removal of common pharmaceuticals present in surface waters by Amberlite XAD-7 acrylic-ester-resin: Influence of pH and presence of other drugs. Desalination 269 (1-3), 231–238.

Duda, Y., Govea-Rueda, R., Galicia, M., Beltran, H.I. and Zamudio-Rivera, L.S. 2005. Corrosion inhibitors: Design, performance, and computer simulations. The Journal of Physical Chemistry. B 109 (47), 22674–22684.

Edzwald, J.K. and Tobiason, J.E. 1999. Enhanced coagulation: US requirements and a broader view. Water Science and Technology 40 (9), 63–70.

Emmett, E.A., Shofer, F.S., Zhang, H., Freeman, D., Desai, C. and Shaw, L.M. 2006. Community exposure to perfluorooctanoate: Relationships between serum concentrations and exposure sources. Journal of Occupational and Environmental Medicine 48 (8), 759–770.

EPA 2012. Emerging contaminants – Perfluorooctane sulfonate (PFOS) and perfluorooctanoic acid (PFOA). http://www.epa.gov/fedfac/pdf/emerging_contaminants_pfos_pfoa.pdf

Erickson, M. 2008. Emerging contaminants and impaired waters/TMDLs. https://wiki.umn.edu/pub/Wilson/TMDL-SpecialProblem/PFCs_and_Impaired_Waters-TMDLs.pdf.

Ericson, I., Domingo, J.L., Nadal, M., Bigas, E., Llebaria, X., van Bavel, B. and Lindstrom, G. 2009. Levels of perfluorinated chemicals in municipal drinking water from Catalonia, Spain: Public health implications. Archives of Environmental Contamination and Toxicology 57 (4), 631–638.

Eriksson, E., Baun, A., Scholes, L., Ledin, A., Ahlman, S., Revitt, M., Noutsopoulos, C. and Mikkelsen, P.S. 2007. Selected stormwater priority pollutants—A European perspective. Science of the Total Environment 383 (1-3), 41–51.

Eschauzier, C., Beerendonk, E., Scholte-Veenendaal, P. and de Voogt, P. 2012. Impact of treatment processes on the removal of perfluoroalkyl acids from the drinking water production chain. Environmental Science & Technology 46 (3), 1708–1715.

Eschauzier, C., Haftka, J., Stuyfzand, P.J. and de Voogt, P. 2010. Perfluorinated compounds in infiltrated river Rhine water and infiltrated rainwater in coastal dunes. Environmental Science & Technology 44 (19), 7450–7455.

Fei, C., McLaughlin, J.K., Lipworth, L. and Olsen, J. 2009. Maternal levels of perfluorinated chemicals and subfecundity. Human Reproduction 1 (1), 1–6.

Freitas, P.A.M., Iha, K., Felinto, M. and Suarez-Iha, M.E.V. 2008. Adsorption of di-2-pyridyl ketone salicyloylhydrazone on Amberlite XAD-2 and XAD-7 resins: Characteristics and isotherms. Journal of Colloid and Interface Science 323 (1), 1–5.

Gewurtz, S.B., De Silva, A.O. Backus, S.M., McGoldrick, D.J., Keir, M.J., Small, J., Melymuk, L. and Muir, D.C.G. 2012. Perfluoroalkyl contaminants in Lake Ontario lake trout: Detailed examination of current status and long-term trends. Environmental Science & Technology 46 (11), 5842–5850.

Giesy, J.P. and Kannan, K. 2001. Global distribution of perfluorooctane sulfonate in wildlife. Environmental Science & Technology 35 (7), 1339–1342.

Giesy, J.P., Naile, J.E., Khim, J.S., Jones, P.D. and Newsted, J.L. 2010 Reviews of Environmental Contamination and Toxicology, Vol 202. Whitacre, D.M. (ed), pp. 1–52.

Goosey, E. and Harrad, S. 2011. Perfluoroalkyl compounds in dust from Asian, Australian, European, and North American homes and UK cars, classrooms, and offices. Environment International 37 (1), 86–92.

Goss, K.U. 2008. The pK_a values of PFOA and other highly fluorinated carboxylic acids. Environmental Science & Technology 42 (2), 456–458.

Goss, K.U. and Arp, H.P.H. 2009. Comment on "Experimental pK_a determination for perfluorooctanoic acid (PFOA) and the potential impact of pK_a concentration dependence on laboratory-measured partitioning phenomena and envrionmental modeling". Environmental Science & Technology 43 (13), 5150–5151.

Gregor, J.E., Nokes, C.J. and Fenton, E. 1997. Optimising natural organic matter removal from low turbidity waters by controlled pH adjustment of aluminum coagulation Water Research 32 (12), 2949–2958.

Guo, R., Sim, W.J., Lee, E.S., Lee, J.H. and Oh, J.E. 2010. Evaluation of the fate of perfluoroalkyl compounds in wastewater treatment plants. Water Research 44 (11), 3476–3486.

Ha, H.J. and Stenstrom, M.K. 2003. Identification of land use with water quality data in stormwater using a neural network. Water Research 37 (17), 4222–4230.

Haack, S.K., Fogarty, L.R. and Wright, C. 2003. *Escherichia coli* and enterococci at beaches in the Grand Traverse Bay, Lake Michigan: Sources, characteristics, and environmental pathways. Environmental Science & Technology 37 (15), 3275–3282.

Hansen, K.J., Johnson, H.O., Eldridge, J.S., Butenhoff, J.L. and Dick, L.A. 2002. Quantitative characterization of trace levels of PFOS and PFOA in the Tennessee River. Environmental Science & Technology 36 (8), 1681–1685.

Haug, L.S., Thomse, C. and Becher, G. 2009. Time trends and the influence of age and gender on serum concentrations of perfluorinated compounds in archived human samples. Environmental Science & Technology 43 (6), 2131–2136.

Haug, L.S., Thomsen, C., Brantsaeter, A.L., Kvalem, H.E., Haugen, M., Becher, G., Alexander, J., Meltzer, H.M. and Knutsen, H.K. 2010. Diet and particularly seafood are major sources of perfluorinated compounds in humans. Environment International 36 (7), 772-778.

Higgins, C.P. and Luthy, R.G. 2006. Sorption of perfluorinated surfactants on sediments. Environmental Science & Technology 40 (23), 7251–7256.

Higgins, C.P. and Luthy, R.G. 2007. Modeling sorption of anionic surfactants onto sediment materials: an a priori approach for perfluoroalkyl surfactants and linear alkylbenzene sulfonates. Environmental Science & Technology 41 (9), 3254–3261.

Hoffman, K., Webster, T.F., Bartell, S.M., Weisskopf, M.G., Fletcher, T. and Vieira, V.M. 2011a. Private drinking water wells as a source of exposure to perfluorooctanoic acid (PFOA) in communities surrounding a fluoropolymer production facility. Environmental Health Perspectives 119 (1), 92–97.

Hoffman, K., Webster, T.F., Bartell, S.M., Weisskopf, M.G., Fletcher, T. and Vieira, V.M. 2011b. Private drinking water wells as a source of exposure to perfluorooctanoic acid (PFOA) in communities surrounding a fluoropolymer production facility. Environmental Health Perspectives 119 (1), 92–97.

Hoffman, K., Webster, T.F., Weisskopf, M.G., Weinberg, J. and Vieira, V.M. 2010. Exposure to polyfluoroalkyl chemicals and attention deficit/hyperactivity disorder in U.S. children 12–15 years of age. Environmental Health Perspectives 118 (12), 1762–1767.

Houde, M., Martin, J.W., Letcher, R.J., Solomon, K.R. and Muir, D.C. 2006. Biological monitoring of polyfluoroalkyl substances: A review. Environmental Science & Technology 40 (11), 3463–3473.

Hu, W., Jones, P.D., Upham, B.L., Trosko, J.E., Lau, C. and Giesy, J.P. 2002. Inhibition of gap junctional intercellualr communication by perfluorinated compounds in rat liver and dolphin kidney epithelial cell lines *in Vitro* and Sprague–Dawley rats *in Vivo*. Toxicological Sciences 68 (2), 429–436.

Huset, C.A., Chiaia, A.C., Barofsky, D.F., Jonkers, N., Kohler, H.P., Ort, C., Giger, D.W. and Field, J.A. 2008. Occurrence and mass flows of fluorochemicals in the Glatt Valley watershed, Switzerland. Environmental Science & Technology 42 (17), 6369–6377.

Ikonomou, M.G., Fernandez, M.P., Knapp, W. and Sather, P. 2002. PCBs in dungeness crab reflect distinct source fingerprints among harbor/industrial sites in British Columbia. Environmental Science & Technology 36 (12), 2545–2551.

IHSS – International Humic Substances Society http://www.humicsubstances.org/ (Accessed April 2012).

Inoue, Y., Hashizume, N., Yakata, N., Murakami, H., Suzuki, Y., Kikushima, E. and Otsuka, M. 2012. Unique physicochemical properties of perfluorinated compounds and their bioconcentration in common carp *Cyprinus carpio* L. Archives of Environmental Contamination and Toxicology. 62 (4) 672–680.

Jahnke, A. and Berger, U. 2009. Trace analysis of per- and polyfluorinated alkyl substances in various matrices—How do current methods perform? Journal of Chromatography A 1216 (3), 410–421.

Jekel, M.R., 1986. Interactions of humic acids and aluminum salts in the flocculation process. Water Research 20 (12) 1535–1542.

Jeon, J., Kannan, K., Lim, B.J., An, K.G. and Kim, S.D. 2011. Effects of salinity and organic matter on the partitioning of perfluoroalkyl acid (PFAs) to clay particles. Journal of Environmental Monitoring 13 (6), 1803–1810.

Jeon, J., Kannan, K., Lim, H.K., Moon, H.B. and Kim, S.D. 2010. Bioconcentration of perfluorinated compounds in blackrock fish, *Sebastes schlegeli*, at different salinity levels. Environmental Toxicology and Chemistry 29 (11), 2529–2535.

Jin, Y.H., Liu, W., Sato, I., Nakayama, S.F., Sasaki, K., Saito, N. and Tsuda, S. 2009. PFOS and PFOA in environmental and tap water in China. Chemosphere 77 (5), 605–611.

Johnson, R.A. and Wichern, D.W. 1998. Applied multivariate statistical analysis, Prentice Hall ;Prentice-Hall International, Upper Saddle River, N.J. London.

Johnson, R.L., Anschutz, A.J., Smolen, J.M., Simcik, M.F. and Penn, R.L. 2007. The adsorption of perfluorooctane sulfonate onto sand, clay, and iron oxide surfaces. Journal of Chemical and Engineering Data 52 (4), 1165–1170.

Kaiser, M.A., Cobranchi, D.P., Kao, C.P.C., Krusic, P.J., Marchione, A.A. and Buck, R.C. 2004. Physicochemical properties of 8:2 fluorinated Telomer B alcohol. Journal of Chemical and Engineering Data 49 (4), 912–916.

Kannan, K. 2011. Perfluoroalkyl and polyfluoroalkyl substances: Current and future perspectives. Environmental Chemistry 8 (4), 333–338.

Kärrman, A., Mueller, J.F., Van Bavel, B., Harden, F., Toms, L.M.L. and Lindstrom, G. 2006. Levels of 12 perfluorinated chemicals in pooled Australian serum, collected

2002–2003, in relation to age, gender, and region. Environmental Science & Technology 40 (12), 3742–3748.

Kato, K., Wong, L.Y., Jia, L.T., Kuklenyik, Z. and Calafat, A.M. 2011. Trends in exposure to polyfluoroalkyl chemicals in the U.S. population: 1999–2008. Environmental Science & Technology 45 (19), 8037–8045.

Kavouras, I.G., Koutrakis, P., Tsapakis, M., Lagoudaki, E., Stephanou, E.G., Von Baer, D. and Oyola, P. 2001. Source apportionment of urban particulate aliphatic and polynuclear aromatic hydrocarbons (PAHs) using multivariate methods. Environmental Science & Technology 35 (11), 2288–2294.

Kelly, B.C., Ikonomou, M.G., Blair, J.D., Surridge, B., Hoover, D., Grace, R. and Gobas, F.A.P.C. 2009. Perfluoroalkyl contaminants in an Arctic marine food web: Trophic magnification and wildlife exposure. Environmental Science & Technology 43 (11), 4037–4043.

Kelly, J. and Solem, L. 2008. Identification of a major source of perfluorooctane sulfonate (PFOS) at a wastewater treatment plant in Brainerd, Minnesota. Epidemiology 19 (6), S303–S304.

Kim, J.Y. and Sansalone, J.J. 2008. Event-based size distributions of particulate matter transported during urban rainfall-runoff events. Water Research 42 (10-11), 2756–2768.

Kim, S.H., Moon, B.H. and Lee, H.I. 2001. Effects of pH and dosage on pollutant removal and floc structure during coagulation. Microchemical Journal 68 (2–3), 197–203.

Kim, S.K. and Kannan, K. 2007. Perfluorinated acids in air, rain, snow, surface runoff, and lakes: Relative importance of pathways to contamination of urban lakes. Environmental Science & Technology 41 (24), 8328–8334.

Korshin, G.V., Li, C.W. and Benjamin, M.M. 1997. Monitoring the properties of natural organic matter through UV spectroscopy: A consistent theory. Water Research 31 (7), 1787–1795.

Kretzschmar, R., Hesterberg, D. and Sticher, H. 1997. Effects of adsorbed humic acid on surface charge and flocculation of kaolinite. Soil Science Society of America Journal 61 (1), 101–108.

Kunacheva, C., Tanaka, S., Fujii, S., Boontanon, S.K., Musirat, C., Wongwattana, T. and Shivakoti, B.R. 2011. Mass flows of perfluorinated compounds (PFCs) in central wastewater treatment plants of industrial zones in Thailand. Chemosphere 83 (6), 737–744.

Kyriakopoulos, G.L., Doulia, D. and Anagnostopoulos, E. 2005. Adsorption of pesticides on porous polymeric adsorbents. Chemical Engineering Science 60 (4), 1177–1186.

Lamesa, C. and Sesta, B. 1987. Micelles in perfluorinated surfactant solutions. Journal of Physical Chemistry 91 (6), 1450–1454.

Lee, S. and Elimelech, M. 2007. Salt cleaning of organic-fouled reverse osmosis membranes. Water Research 41 (5), 1134–1142.

Letterman, R.D. and Vanderbrook, S.G. 1983. Effect of solution chemistry on coagulation with hydrolyzed Al(III): Significance of sulfate ion and pH. Water Research 17 (2), 195–204.

Li, H.X., Ellis, D. and Mackay, D. 2007. Measurement of low air-water partition coefficients of organic acids by evaporation from a water surface. Journal of Chemical and Engineering Data 52 (5), 1580–1584.

Liao, C.Z. and Nicklaus, M.C. 2009. Comparison of nine programs predicting pK_a Values of pharmaceutical substances. Journal of Chemical Information and Modeling 49 (12), 2801–2812.

Lin, A.Y., Panchangam, S.C. and Ciou, P.S. 2010. High levels of perfluorochemicals in Taiwan's wastewater treatment plants and downstream rivers pose great risk to local aquatic ecosystems. Chemosphere 80 (10), 1167–1174.

Lin, A.Y., Panchangam, S.C. and Lo, C.C. 2009. The impact of semiconductor, electronics and optoelectronic industries on downstream perfluorinated chemical contamination in Taiwanese rivers. Environmental Pollution 157 (4), 1365–1372.

Lindstrom, A.B., Strynar, M.J. and Libelo, E.L. 2011. Polyfluorinated compounds: Past, present, and future. Environmental Science & Technology 45 (19), 7954–7961.

Liu, J.X. and Lee, L.S. 2005. Solubility and sorption by soils of 8:2 fluorotelomer alcohol in water and cosolvent systems. Environmental Science & Technology 39 (19), 7535–7540.

Liu, T.K. and Chin, C.J.M. 2009. Improved coagulation performance using preformed polymeric iron chloride (PICl). Colloids and Surfaces A—Physicochemical and Engineering Aspects 339 (1–3), 192–198.

Loi, E.I.H., Yeung L.W.Y., Taniyasu, S., Lam, P.K.S., Kannan, K. and Yamashita, N. 2011. Trophic magnification of poly- and perfluorianted compounds in a subtropical food web. Environmental Science & Technology 45 (13), 5506–5513.

Loganathan, B.G., Sajwan, K.S., Sinclair, E., Kumar, K.S. and Kannan, K. 2007. Perfluoroalkyl sulfonates and perfluorocarboxylates in two wastewater treatment facilities in Kentucky and Georgia. Water Research 41 (20), 4611–4620.

Lohmann, R., Green, N.J.L. and Jones, K.C. 1999. Detailed studies of the factors controlling atmospheric PCDD/F concentrations. Environmental Science & Technology 33 (24), 4440–4447.

Mak, Y.L., Taniyasu, S., Yeung, L.W., Lu, G., Jin, L., Yang, Y., Lam, P.K., Kannan, K. and Yamashita, N. 2009. Perfluorinated compounds in tap water from China and several other countries. Environmental Science & Technology 43 (13), 4824–4829.

Martin, J.W., Kannan, K., Berger, U., de Voogt, P., Field, J., Franklin, J., Giesy, J.P., Harner, T., Muir, D.C., Scott, B., Kaiser, M., Järnberg, U., Jones, K.C., Mabury,

S.A., Schröder, H., Simcik, M., Sottani, C., van Bavel, B., Kärrman, A., Lindström, G. and van Leeuwen, S. 2004a. Analytical challenges hamper perfluoroalkyl research. Environmental Science & Technology 38 (13), 248A–255A.

Martin, J.W., Whittle, M., Muir, D.C.G. and Mabury, S.A. 2004b. Perfluoroalkyl contaminants in food web from Lake Ontario. Environmental Science & Technology 38 (20), 5379–5385.

Martin, J.W., Ellis, D.A., Mabury, S.A., Hurley, M.D. and Wallington, T.J. 2006. Atmospheric chemistry of perfluoroalkanesulfonamides: Kinetic and product studies of the OH radical ad Cl atom initiated oxidation of *N*-ehyl perfluorobutanesulfonamide. Environmental Science & Technology 40 (3), 864–872.

Masion, A., Vilgé-Ritter, A., Rose, J., Stone, W.E.E., Teppen, B.J., Rybacki, D. and Bottero, J-Y. 2000. Coagulation–flocculation of natural organic matter with Al salts: Speciation and structure of the aggregates. Environmental Science & Technology 34 (15), 3242–3246.

McMurdo, C.J., Ellis, D.A., Webster, E., Butler, J., Christensen, R.D. and Reid, L.K. 2008. Aerosol enrichment of the surfactant PFO and mediation of the water – Air transport of gaseous PFOA. Environmental Science & Technology 42 (11), 3969–3974.

Meyer, T., De Silva, A.O., Spencer, C. and Wania, F. 2011. Fate of perfluorinated carboxylates and sulfonates during snowmelt within an urban watershed. Environmental Science & Technology 45 (19), 8113–8119.

Moody, C.A., Hebert, G.N., Strauss, S.H. and Field, J.A. 2003. Occurrence and persistence of perfluorooctanesulfonate and other perfluorinated surfactants in groundwater at a fire-training area at Wurtsmith Air Force Base, Michigan, USA. Journal of Environmental Monitoring 5, 341–345.

Möller, A., Ahrens, L., Surm, R., Westerveld, J., van der Wielen, F., Ebinghaus, R. and de Voogt, P. 2010. Distribution and sources of polyfluoroalkyl substances (PFAS) in the River Rhine watershed. Environmental Pollution 158 (10), 3243–3250.

MPCA 2009. PFCs in Minnesota's ambient environment: 2008 progress report, Minnesota Pollution Control Agency, St. Paul, MN.

MPCA. Fact Sheet for Draft NPDES and SDS Permit to 3M Cottage Grove Wastewater Treatment Facility: http://www.pca.state.mn.us/news/data/bdc.cfm?noticeID=286619&blobID=29585&docTypeID=4). (Accessed April 2012).

MPCA 2012. Impaired Waters List http://www.pca.state.mn.us/index.php/water/water-types-and-programs/minnesotas-impaired-waters-and-tmdls/impaired-waters-list.html. (Accessed April 2012).

MPRB 2008. Water Resources Report. Minneapolis Park & Recreation Board, Minneapolis, MN.

Müller, C.E., De Silva, A.O., Small, J., Williamson, M., Wang, X., Morris, A., Katz, S., Gamberg, M. and Muir, D.C.G., 2011a. Biomagnification of perfluorinated compounds in a remote terrestrial food chain: Lichen–caribou–wolf. Environmental Science & Technology 45 (20), 8665–8673.

Müller, C.E., Spiess, N., Gerecke, A.C., Scheringer, M. and Hungerbuhler, K. 2011b. Quantifying diffuse and point Inputs of perfluoroalkyl acids in a nonindustrial river catchment. Environmental Science & Technology 45 (23), 9901–9909.

Murakami, M., Imamura, E., Shinohara, H., Kiri, K., Muramatsu, Y., Harada, A. and Takada, H. 2008. Occurrence and sources of perfluorinated surfactants in rivers in Japan. Environmental Science & Technology 42 (17), 6566–6572.

Murakami, M., Shinohara, H. and Takada, H. 2009. Evaluation of wastewater and street runoff as sources of perfluorinated surfactants (PFSs). Chemosphere 74 (4), 487–493.

Murakami, M. and Takada, H. 2008. Perfluorinated surfactants (PFSs) in size-fractionated street dust in Tokyo. Chemosphere 73 (8), 1172–1177.

Nakata, H., Kannan, K., Nasu, T., Cho, H.S., Sinclair, E. and Takemurai, A. 2006. Perfluorinated contaminants in sediments and aquatic organisms collected from shallow water and tidal flat areas of the Ariake Sea, Japan: Environmental fate of perfluorooctane sulfonate in aquatic ecosystems. Environmental Science & Technology 40 (16), 4916–4921.

Nakayama, S.F., Strynar, M.J., Reiner, J.L., Delinsky, A.D. and Lindstrom, A.B. 2010. Determination of perfluorinated compounds in the Upper Mississippi River Basin. Environmental Science & Technology 44 (11), 4103–4109.

Nguyen, V.T., Reinhard, M. and Karina, G.Y.H. 2011. Occurrence and source characterization of perfluorochemicals in an urban watershed. Chemosphere 82 (9), 1277–1285.

Ni, N. and Yalkowsky, S.H. 2003. Prediction of Setschenow constants. International Journal of Pharmaceutics 254 (2), 167–172.

OECD 2002 Cooperation on Existing Chemicals: Hazard assessment of perfluorooctane sulfonate and its salts, Paris.

Pagano, M. and Gauvreau, K. 2000. Principles of biostatistics, Duxbury, Pacific Grove.

Pan, G. and You, C. 2010. Sediment-water distribution of perfluorooctane sulfonate (PFOS) in Yangtze River Estuary. Environmental Pollution 158 (5), 1363–1367.

Parida, S.K., Dash, S., Patel, S. and Mishra, B.K. 2006. Adsorption of organic molecules on silica surface. Advances in Colloid and Interface Science 121 (1–3), 77–110.

Paul, A.G., Johns, K.C. and Sweentman, A.J. 2009. A first global production, emission, and environmental inventory for perfluorooctane sulfonate. Environmental Science & Technology 43 (2), 386–392.

Paul, A.G., Scheringer, M., Hungerbuhler, K., Loos, R., Jones, K.C. and Sweetman, A.J. 2011. Estimating the aquatic emissions and fate of perfluorooctane sulfonate (PFOS) into the river Rhine. Journal of Environmental Monitoring 14 (2), 524–530.

Pavan, P.C., Crepaldi, E.L., Gomes, G.D. and Valim, J.B. 1999. Adsorption of sodium dodecylsulfate on a hydrotalcite-like compound. Effect of temperature, pH and ionic strength. Colloids and Surfaces A–Physicochemical and Engineering Aspects 154 (3), 399–410.

Pistocchi, A. and Loos, R. 2009. A map of European emissions and concentrations of PFOS and PFOA. Environmental Science & Technology 43 (24), 9237–9244.

Post, G.B., Cohn, P.D., and Cooper, K.R. 2012. Perfluorooctanoic acid (PFOA), an emerging drinking water contaminant: A critical review of recent literature. Environmnetal Research 116, 93–117.

Post, G.B., Louis, J.B., Cooper, K.R., Boros–Russo, B.J. and Lippincott, R.L. 2009. Occurrence and potential significance of perfluorooctanoic acid (PFOA) detected in New Jersey public drinking water systems. Environmental Science & Technology 43 (12), 4547–4554.

Prevedouros, K., Cousins, I.T., Buck, R.C. and Korzeniowski, S.H. 2006. Sources, fate and transport of perfluorocarboxylates. Environmental Science & Technology 40 (1), 32–44.

Rakotonarivo, E., Bottero, J.Y., Thomas, F., Poirier, J.E. and Cases, J.M. 1988. Electrochemical modelling of freshly precipitated aluminum hydroxide – Electrolyte interface. Colloids and Surfaces 33 (3–4), 191–207.

Rao, P.S.C., Hornsby, A.G., Kilcrease, D.P. and Nkedikizza, P. 1985. Sorption and transport of hydrophobic organic-chemicals in aqueous and mixed-solvent systems – Model development and preliminary evaluation. Journal of environmental quality 14 (3), 376–383.

Rayne, S. and Forest, K. 2009. Congener-specific organic carbon-normalized soil and sediment-water partitioning coefficients for the C(1) through C(8) perfluoroalkyl carboxylic and sulfonic acids. Journal of Environmental Science and Health Part A–Toxic/Hazardous Substances & Environmental Engineering 44 (13), 1374–1387.

Rhoads, K.R., Janssen, E.M.L., Luthy, R.G. and Criddle, C.S. 2008. Aerobic biotransformation and fate of N-ethyl perfluorooctane sulfonamidoethanol (N-EtFOSE) in activated sludge. Environmental Science & Technology 42 (8), 2873–2878.

Rosen, M.J. 2004 Surfactants and interfacial phenomena, Wiley, Hoboken.

Rostkowski, P., Yamashita, N., So, I.M.K., Taniyasu, S., Lam, P.K.S., Falandysz, J., Lee, K.T., Kim, S.K., Khim, J.S., Im, S.H., Newsted, J.L., Jones, P.D., Kannan, K. and Giesy, J.P. 2006. Perfluorinated compounds in streams of the Shihwa industrial zone and Lake Shihwa, South Korea. Environmental Toxicology and Chemistry 25 (9), 2374–2380.

Saar R.A. and Weber, J.H. 1982. Fulvic acid: Modifier of metal-ion chemistry. Environmental Science & Technology 16 (19), 510A–517A.

Schröder, H.F. and Meesters, R.J.W. 2005. Stability of fluorinated surfactants in advanced oxidation processes – A follow up of degradation products using flow injection-mass spectrometry, liquid chromatography-mass spectrometry and liquid chromatography-multiple stage mass spectrometry. Journal of Chromatography A 1082 (1), 110–119.

Schultz, M.M., Barofsky, D.F. and Field, J.A. 2006a. Quantitative determination of fluorinated alkyl substances by large-volume-injection liquid chromatography tandem mass spectrometry – Characterization of municipal wastewaters. Environmental Science & Technology 40 (1), 289–295.

Schultz, M.M., Higgins, C.P., Huset, C.A., Luthy, R.G., Barofsky, D.F. and Field, J.A. 2006b. Fluorochemical mass flows in a municipal wastewater treatment facility. Environmental Science & Technology 40 (23), 7350–7357.

Schwarzenbach, R.P., Gschwend, P.M. and Imboden, D.M. 1993 Environmental organic chemistry, Wiley, New York, NY ; Chichester.

Scott, B.F., Moody, C.A., Spencer, C., Small, J.M., Muir, D.C.G. and Mabury, S.A. 2006. Analysis for perfluorocarboxylic acids/anions in surface waters and precipitation using GC-MS and analysis of PFOA from large-volume samples. Environmental Science & Technology 40 (20), 6405–6410.

Senevirathna, S., Tanaka, S., Fujii, S., Kunacheva, C., Harada, H., Ariyadasa, B. and Shivakoti, B.R. 2010a. Adsorption of perfluorooctane sulfonate (*n*-PFOS) onto non ion-exchange polymers and granular activated carbon: Batch and column test. Desalination 260 (1–3), 29–33.

Senevirathna, S., Tanaka, S., Fujii, S., Kunacheva, C., Harada, H., Shivakoti, B.R. and Okamoto, R. 2010b. A comparative study of adsorption of perfluorooctane sulfonate (PFOS) onto granular activated carbon, ion-exchange polymers and non-ion-exchange polymers. Chemosphere 80 (6), 647–651.

Sepulvado, J.G., Blaine, A.C., Hundal, L.S. and Higgins, C.P. 2011. Occurrence and fate of perfluorochemicals in soil following the land application of municipal biosolids. Environmental Science & Technology 45 (19), 8106–8112.

Shivakoti, B.R., Tanaka, S., Fujii, S., Kunacheva, C., Boontanon, S.K., Musirat, C., Seneviratne, S.T.M.L.D. and Tanaka, H. 2010. Occurrences and behavior of perfluorinated compounds (PFCs) in several wastewater treatment plants (WWTPs) in Japan and Thailand. Journal of Environmental Monitoring 12 (6), 1255–1264.

Simcik, M.F. and Dorweiler, K.J. 2005. Ratio of perfluorochemical concentrations as a tracer of atmospheric deposition to surface waters. Environmental Science & Technology 39 (22), 8678–8683.

Sinclair, E. and Kannan, K. 2006. Mass loading and fate of perfluoroalkyl surfactants in wastewater treatment plants. Environmental Science & Technology 40 (5), 1408–1414.

Singer, P.C. and Bilyk, K. 2002. Enhanced coagulation using a magnetic ion exchange resin. Water Research 36 (16), 4009–4022.

Skutlarek, D., Exner, M. and Farber, H. 2006. Perfluorinated surfactants in surface and drinking waters. Environmental science and pollution research international 13 (5), 299–307.

Smithwick, M., Mabury, S.A., Solomon, K.R., Sonne, C., Martin, J.W., Born, E.W., Dietz, R., Derocher, A.E., Letcher, R.J., Evans, T.J., Gabrielsen, G.W., Nagy, J., Stiring, I., Taylor, M.K. and Muir, D.C.G. 2005. Circumpolar study of perfluoroalkyl contaminants in polar bears (*Ursus maritimus*). Environmental Science & Technology 39 (15) 5517–5523.

Snoeyink, V.L. and Jenkins, D. 1980 Water chemistry, Wiley, New York.

So, M.K., Miyake, Y., Yeung, W.Y., Ho, Y.M., Taniyasu, S., Rostkowski, P., Yamashita, N., Zhou, B.S., Shi, X.J., Wang, J.X., Giesy, J.P., Yu, H. and Lam, P.K. 2007. Perfluorinated compounds in the Pearl River and Yangtze River of China. Chemosphere 68 (11), 2085–2095.

So, M.K., Taniyasu, S., Yamashita, N., Giesy, J.P., Zheng, J., Fang, Z., Im, S.H. and Lam, P.K.S. 2004. Perfluorinated compounds in coastal waters of Hong Kong, South China, and Korea. Environmental Science & Technology 38 (15), 4056–4063.

Srinivasan, R.T. and Viraraghavan, T. 2004. Influence of natural organic matter (NOM) on the speciation of aluminum during water treatment. Water, Air, and Soil Pollution 152, 35–54.

Stahl, T., Heyn, J., Thiele, H., Huther, J., Failing, K., Georgii, S. and Brunn, H. 2009. Carryover of perfluorooctanoic acid (PFOA) and perfluorooctane sulfonate (PFOS) from soil to plants. Archives of Environmental Contamination and Toxicology 57 (2), 289–298.

Steenland, K., Tinker, S., Shankar, A. and Ducatman, A. 2010. Association of perfluorooctanoic acid (PFOA) and perfluorooctane sulfonate (PFOS) with uric acid among adults with elevated community exposure to PFOA. Environmental Health Perspectives 118 (2), 229–233.

Stock, N.L., Muir, D.C.G. and Mabury, S. 2010. Perfluoroalkyl Compounds. In *Persistent Organic Pollutants*; Harrad, S., (ed), pp. 25–70, Wiley: Chichester, UK.

Stumm, W. and O'Melia, C.R. 1968. Stoichiometry of coagulation. Journal of American Water Works Association 60 (5), 514–539.

Suja, F., Pramanik, B.K. and Zain, S.M. 2009. Contamination, bioaccumulation and toxic effects of perfluorinated chemicals (PFCs) in the water environment: A review paper. Water Science and Technology 60 (6), 1533–1544.

Sun, H.W., Li, F.S., Zhang, T., Zhang, X.Z., He, N., Song, Q., Zhao, L.J., Sun, L.N. and Sun, T.H. 2011. Perfluorinated compounds in surface waters and WWTPs in Shenyang, China: Mass flows and source analysis. Water Research 45 (15), 4483–4490.

Takagi, S., Adachi, F., Miyano, K., Koizumi, Y., Tanaka, H., Mimura, M., Watanabe, I., Tanabe, S. and Kannan, K. 2008. Perfluorooctanesulfonate and perfluorooctanoate in raw and treated tap water from Osaka, Japan. Chemosphere 72 (10), 1409–1412.

Takagi, S., Adachi, F., Miyano, K., Koizumi, Y., Tanaka, H., Watanabe, I., Tanabe, S. and Kannan, K. 2011. Fate of perfluorooctanesulfonate and perfluorooctanoate in drinking water treatment processes. Water Research 45 (13), 3925–3932.

Tanaka, S., Fujii, S., Kunacheva, C., Senevirathna, S., Kimura, K. and Saito, N. 2012. PFAA distribution in source water and their effective treatment technologies. Reproductive Toxicology 33 (4), 588–589.

Takazawa, Y., Nishino, T., Sasaki, Y., Yamashita, H., Suzuki, N., Tanabe, K. and Shibata, Y. 2009. Occurrence and distribution of perfluorooctane sulfonate and perfluorooctanoic acid in the rivers of Tokyo. Water Air and Soil Pollution 202 (1–4), 57–67.

Tang, C.Y., Fu, Q.S., Gao, D.W., Criddle, C.S. and Leckie, J.O. 2010. Effect of solution chemistry on the adsorption of perfluorooctane sulfonate onto mineral surfaces. Water Research 44 (8), 2654–2662.

Thomas, F., Masion, A., Bottero, J.Y., Rouiller, J., Montigny, F. and Genevrier, F. 1993. Aluminum(III) speciation with hydroxy carboxylic acids. Aluminum-27 NMR study. Environmental Science & Technology 27 (12), 2511–2516.

Tittlemier, S.A., Pepper, K., Seymour, C., Moisey, J., Bronson, R., Cao, X.L. and Dabeka, R.W. 2007. Dietary exposure of Canadians to perfluorinated carboxylates and perfluorooctane sulfonate via consumption of meat, fish, fast foods, and food items prepared in their packaging. Journal of Agricultural and Food Chemistry 55 (8), 3203–3210.

Upham, B.L., Deocampo, N.D., Wurl, B. and Trosko, J.E. 1998. Inhibition of gap junctional intercelllular communication by perfluorinated fatty acids is dependent on chain length of the fluorinated tail. International Journal of Cancer 78 (4), 491–495.

Vergili, I., Kaya, Y., Gonder, Z.B. and Barlas, H. 2010. Column studies for the adsorption of cationic surfactant onto an organic polymer resin and a granular activated carbon. Water Environment Research 82 (3), 209–215.

Vestergren, R. and Cousins, I.T. 2009. Tracking the pathways of human exposure to perfluorocarboxylates. Environmental Science & Technology 43 (15), 5565–5575.

Villagrasa, M., de Alda, M.L. and Barcelo, D. 2006. Environmental analysis of fluorinated alkyl substances by liquid chromatography-(tandem) mass spectrometry: A review. Analytical and Bioanalytical Chemistry 386 (4), 953–972.

Wang, F. and Shih, K.M. 2011. Adsorption of perfluorooctanesulfonate (PFOS) and perfluorooctanoate (PFOA) on alumina: Influence of solution pH and cations. Water Research 45 (9), 2925–2930.

Wang, J.B., Han, B.X., Dai, M., Yan, H.K., Li, Z.X. and Thomas, R.K. 1999. Effects of chain length and structure of cationic surfactants on the adsorption onto Na-Kaolinite. Journal of Colloid and Interface Science 213 (2), 596–601.

Wania, F., Mackay, D., 2003. The evolution of mass balance models of persistent organic pollutant fate in the environment. Environmental Pollution 100 (1–3), 223–240.

Wania, F., Shen, L., Lei, Y.D., Teixeira, C. and Muir, D.C.G. 2003. Development and calibration of a resin-based passive sampling system for monitoring persistent organic pollutants in the atmosphere. Environmental Science & Technology 37 (7), 1352–1359.

Washino, N., Saijo, Y., Sasaki, S., Kato, S., Ban, S., Konishi, K., Ito, R., Nakata, A., Iwasaki, Y., Saito, K., Nakazawa, H. and Kishi, R. 2009. Correlations between prenatal exposure to perfluorinated chemicals and reduced fetal growth. Environmental Health Perspectives 117 (4), 660–667.

Water Environment Federation 2006. Clarifier design, McGraw-Hill, New York ; London.

Weinberg, I., Dreyer, A. and Ebinghaus, R. 2011. Waste water treatment plants as sources of polyfluorinated compounds, polybrominated diphenyl ethers and musk fragrances to ambient air. Environmental Pollution 159 (1), 125–132.

Weiss, P.T., Gulliver, J.S. and Erickson, A.J. 2007. Cost and pollutant removal of storm-water treatment practices. Journal of Water Resources Planning and Management—ASCE 133 (3), 218–229.

Wilhelm, M., Bergmann, S. and Dieter, H.H. 2010. Occurrence of perfluorinated compounds (PFCs) in drinking water of North Rhine-Westphalia, Germany and new approach to assess drinking water contamination by shorter-chained C4–C7 PFCs. International Journal of Hygiene and Environmental Health 213 (3), 224–232.

Wongphatarakul, V., Friedlander, S.K. and Pinto, J.P. 1998. A comparative study of PM2.5 ambient aerosol chemical databases. Environmental Science & Technology 32 (24), 3926–3934.

Wu, S.C. and Gschwend, P.M. 1986. Sorption kinetics of hydrophobic organic compounds to natural sediments and soils. Environmental Science & Technology 20 (7), 717–725.

Xiao, F., Zhang, X. and Lee, C. 2008a. Is electrophoretic mobility determination meaningful for aluminum(III) coagulation of kaolinite suspension? Journal of Colloid and Interface Science 327 (2), 348–353.

Xiao, F., Ma, J., Yi, P. and Huang, J.C.H. 2008b. Effects of low temperature on coagulation of kaolinite suspensions. Water Research 42 (12), 2983–2992.

Xiao, F., Zhang, B. and Lee, C. 2008c. Effects of low temperature on aluminum(III) hydrolysis: Theoretical and experimental studies. Journal of Environmental Sciences 20, 907–914.

Xiao, F., Zhang, X., Zhai, H., Yang, M. and Lo, I.M.C. 2010. Effects of enhanced coagulation on polar halogenated disinfectioin byproducts in drinking water. Separation and Purification Technology 76 (1), 26–32.

Xiao, F., Simcik, M.F. and Gulliver, J.S. 2011a. Perfluoroalkyl acids in urban stormwater runoff: Influence of land use. Water Research, DOI: 10.1016/j.watres.2011.11.029.

Xiao, F., Zhang, X., Penn, L., Gulliver, J.S. and Simcik, M.F. 2011b. Effects of monovalent cations on the competitive adsorption of perfluoroalkyl acids by kaolinite: Experimental studies and modeling. Environmental Science & Technology 45 (23), 10028–10035.

Xiao, F., Davidsavor, K.J., Park, S., Nakayama, M. and Phillips, B.R. 2012a. Batch and column study: Sorption of perfluorinated surfactants from water and cosolvent systems by Amberlite XAD resins. Journal of Colloid and Interface Science 368 (1), 505–511.

Xiao, F., Halbach, T.R., Simcik, M.F. and Gulliver, J.S. 2012b. Input characterization of perfluoroalkyl substances in wastewater treatment plants: Source discrimination by exploratory data analysis. Water Research 46 (9), 3101–3109.

Yeung, L.W.Y., Loi, E.I.H., Wong, V.Y.Y., Guruge, K.S., Yamanaka, N., Tanimura, N., Hasegawa, J., Yamashita, N., Miyazaki, S. and Lam, P.K.S. 2009. Biochemical responses and accumulation properties of long-chain perfluorinated compounds (PFOS/PFDA/PFOA) in juvenile chickens (*Gallus gallus*) Archives of Environmental Contamination and Toxicology 57 (2), 377–386.

Yeung, L.W.Y., So, M.K., Jiang, G., Taniyasu, S., Yamashita, N., Song, M., Wu, Y., Li, J., Giesy, J.P., Guruge, K.S. and Lam, P.K. 2006. Perfluorooctanesulfonate and related fluorochemicals in human blood samples from China. Environmental Science & Technology 40 (3), 715–720.

Yoo, H., Yamashita, N., Taniyasu, S., Lee, K.T., Jones, P.D., Newsted, J.L., Khim, J.S. and Giesy, J.P. 2009. Perfluoroalkyl acids in marine organisms from Lake Shihwa, Korea. Archives of Environmental Contamination and Toxicology 57 (3), 552–560.

You, C., Jia, C.X. and Pan, G. 2010. Effect of salinity and sediment characteristics on the sorption and desorption of perfluorooctane sulfonate at sediment–water interface. Environmental Pollution 158 (5), 1343–1347.

Young, C.J., Furdui, V.I., Franklin, J., Koerner, R.M., Muir, D.C.G. and Mabury, S.A. 2007. Perfluorinated acids in arctic snow: New evidence for atmospheric formation. Environmental Science & Technology 41 (10), 3455–3461.

Yu, J., Hu, J.Y., Tanaka, S. and Fujii, S. 2009a. Perfluorooctane sulfonate (PFOS) and perfluorooctanoic acid (PFOA) in sewage treatment plants. Water Research 43 (9), 2399–2408.

Yu, Q., Zhang, R., Deng, S., Huang, J. and Yu, G. 2009b. Sorption of perfluorooctane sulfonate and perfluorooctanoate on activated carbons and resin: Kinetic and isotherm study. Water Research 43 (4), 1150–1158.

Zhou, Q., Deng, S.B., Zhang, Q.Y., Fan, Q., Huang, J. and Yu, G. 2010. Sorption of perfluorooctane sulfonate and perfluorooctanoate on activated sludge. Chemosphere 81 (4), 453–458.

Zushi, Y. and Masunaga, S. 2009. First-flush loads of perfluorinated compounds in stormwater runoff from Hayabuchi River basin, Japan served by separated sewerage system. Chemosphere 76 (6), 833–840.

Zushi, Y., Takeda, T. and Masunaga, S. 2008. Existence of nonpoint source of perfluorinated compounds and their loads in the Tsurumi River basin, Japan. Chemosphere 71 (8), 1566–1573.

Appendix A: Supplementary data for Chapter 2

Table A-1. A list of PFASs involved in this study.

Chemicals	CAS Number	Molecular Formula	MW	Chemical Structure
Perfluoroheptanoic acid (PFHpA)	*375-85-9*	$C_7F_{13}HO_2$	*363*	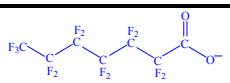
Perfluorooctanoic acid (PFOA)	*335-67-1*	$C_8F_{15}HO_2$	*413*	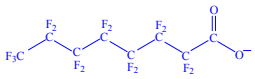
Perfluorononanoic acid (PFNA)	*375-95-1*	$C_9F_{17}HO_2$	*463*	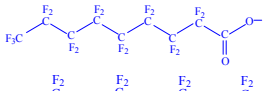
Perfluorooctane sulfonate (PFOS)	*2795-39-3*	$C_8F_{17}O_3S$	*499*	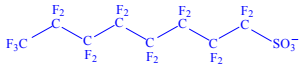
Perfluorodecanoic acid (PFDA)	*335-76-2*	$C_{10}F_{19}HO_2$	*513*	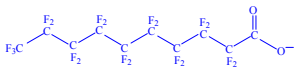
Perfluoroundecanoic acid (PFUnDA)	*2058-94-8*	$C_{11}F_{21}HO_2$	*563*	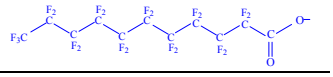

Table A-2 Impervious areas in Twin Cities (Minneapolis and St. Paul, MN) metropolitan area.

	Area (acres)		Area (km^2)
County	total	Impervious	
Anoka	285078	22256	
Hennepin	388100	61546	
Ramsay	108739	27518	
Carver	240450	9085	
Dakota	374980	31189	
Washington	270980	16410	
Total		168004	**679.888**

Table A-3. Calculation of runoff coefficient *k* for the Capitol Regions Watershed District, which is in St. Paul and a few surrounding cities of Minnesota (U.S.).

Capitol Region WD Subwatersheds					
	SAP	Kitt	Phalen	Trout Brook	Como7
% Roof	16.8	19.6	19.6	13.9	16.9
Connected	*11.8*	*13.7*	*13.7*	*9.7*	*11.8*
Disconnected	*5.0*	*5.9*	*5.9*	*4.2*	*5.1*
% Road	33.6	23.5	29	27.4	15
Connected	*21.2*	*14.8*	*18.3*	*17.3*	*9.5*
Disconnected	*12.4*	*8.7*	*10.7*	*10.1*	*5.6*
Area (m2)	13,754,306	7,523,208	5,793,626	20,342,823	1,206,892
% Total Conn Imp:	32.9	28.5	32.0	27.0	21.3
%Total Disconn. Imp:	17.5	14.6	16.6	14.3	10.6
		Area-averaged Totals			
Connected Impervious:		**29.4** *in percent of total watershed area*			
Disconn. Impervious:		**15.4** *in percent of total watershed area*			

A runoff coefficient *k* of 0.9 is pretty common for urban areas. However, only connected impervious areas contribute runoff to surface waters; runoff from disconnected impervious areas will flow to rain gardens. For the table shown above, the connected impervious is 29.4% of the total, and the disconnected impervious is 15.4% of the total. Thus, the connected impervious is 29.4/(29.4+15.4) = 0.67 of the total impervious area. Therefore, the value of *k* used in Eq 2.1 is $0.67 \times 0.9 =$ **0.6**.

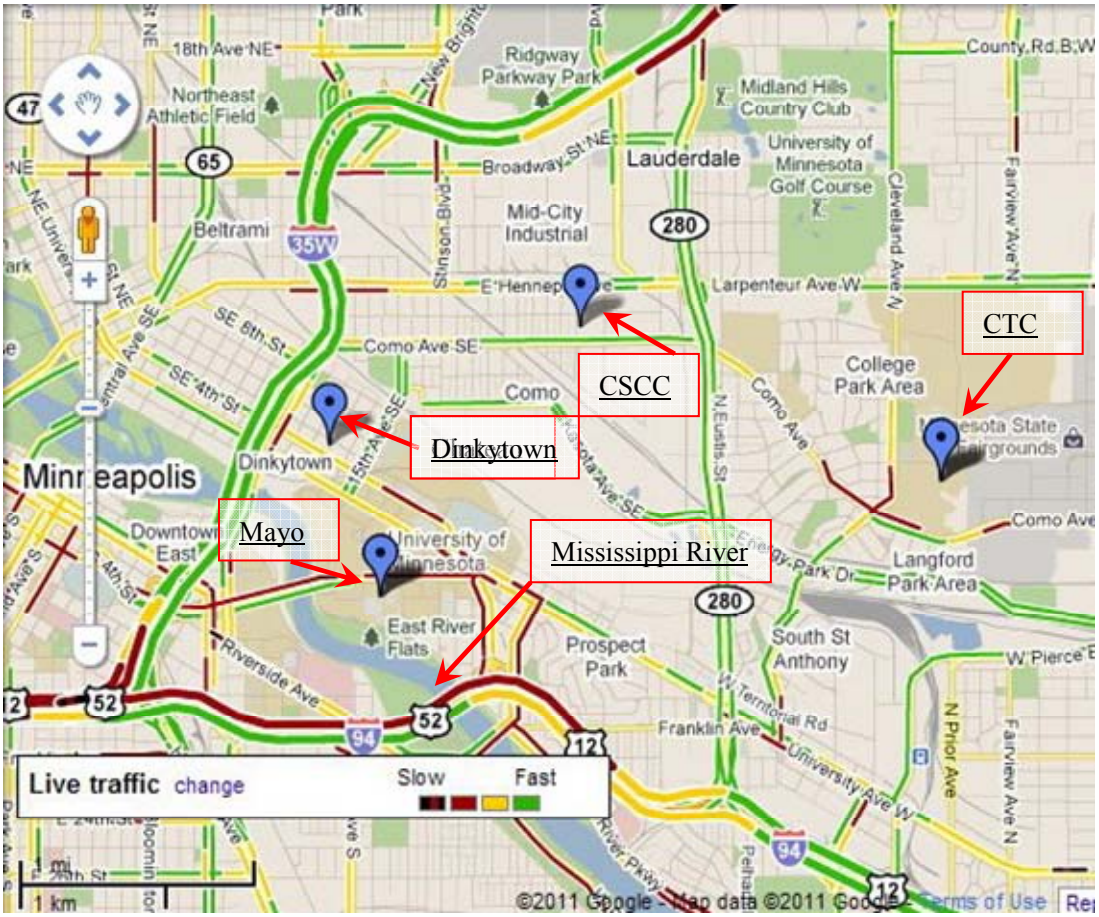

Figure A-1 Samples were collected at three residential sites (CSCC, CTC and Mayo) and one commercial site (Dinkytown) in Minneapolis, MN.

Figure A-2 Samples were collected at five locations near an industrial site suspected to be a source of PFASs in runoff.

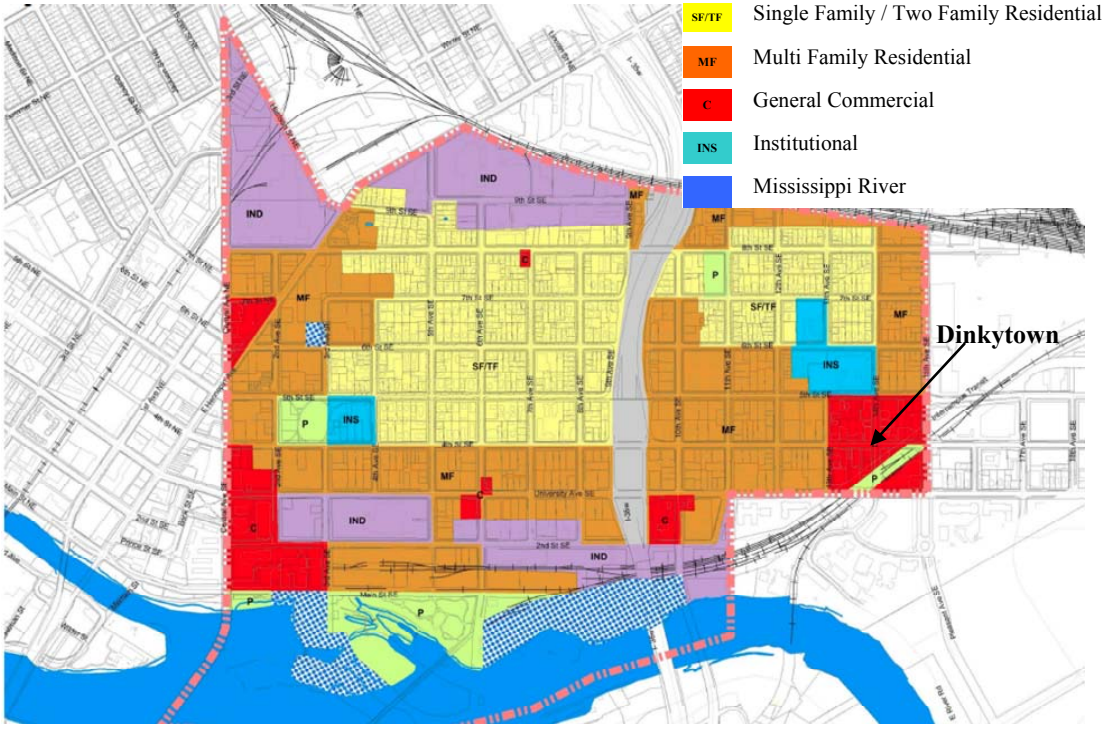

Figure A-3 Land use information around Dinkytown.

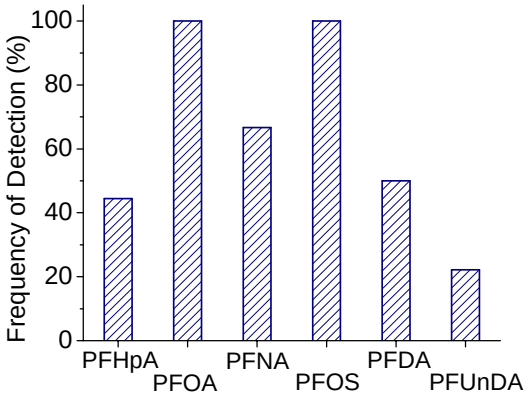

Figure A-4 Frequency of detection of PFASs in urban stormwater runoff.

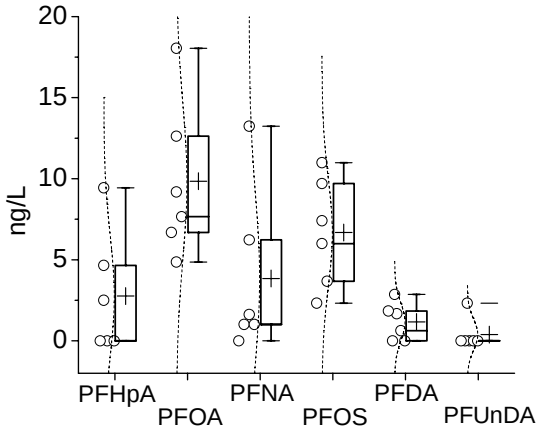

Figure A-5 PFAS concentrations in rainfall water from six events at Twin Cities (Minneapolis and St. Paul, MN) metropolitan area (Aug 20 2010, Sep 15 2010, Sep 26 2010, Nov 10 2010, Mar 22 2011, and April 26 2011). Each time, ~3 liters of rainfall water were (solid-phase) extracted, concentrated, and analyzed). The recovery rates ranged from 73% to 127%. The detailed background and pretreatment steps are not presented here.

Comparing PFAS concentrations in urban areas: One-way ANOVA and Tamhane's T2 post-hoc test

1.

ANOVA

PFHpA Concentrations

	Sum of Squares	df	Mean Square	F	Sig.
Between Groups	50.282	3	16.761	3.601	.041
Within Groups	65.156	14	4.654		
Total	115.437	17			

Post Hoc Tests

Multiple Comparisons

PFHpA Concentrations

Tamhane

Residential Areas	Residential Areas	Mean Difference (I-J)	Std. Error	Sig.
Dinkytown	CTC	3.87500	1.10333	.067
	CSCC	4.29167	1.02163	.050
	Mayo	2.05000	1.46190	.720
CTC	Dinkytown	-3.87500	1.10333	.067
	CSCC	.41667	.41667	.963
	Mayo	-1.82500	1.12562	.632
CSCC	Dinkytown	-4.29167	1.02163	.050
	CTC	-.41667	.41667	.963
	Mayo	-2.24167	1.04566	.413
Mayo	Dinkytown	-2.05000	1.46190	.720
	CTC	1.82500	1.12562	.632
	CSCC	2.24167	1.04566	.413

Multiple Comparisons

PFHpA Concentrations

Tamhane

Residential Areas	Residential Areas	99.67% Confidence Interval	
		Lower Bound	Upper Bound
Dinkytown	CTC	-3.1681	10.9181
	CSCC	-3.6900	12.2733
	Mayo	-5.2366	9.3366
CTC	Dinkytown	-10.9181	3.1681
	CSCC	-17.3305	18.1638
	Mayo	-9.0478	5.3978
CSCC	Dinkytown	-12.2733	3.6900
	CTC	-18.1638	17.3305
	Mayo	-10.4110	5.9276
Mayo	Dinkytown	-9.3366	5.2366
	CTC	-5.3978	9.0478
	CSCC	-5.9276	10.4110

2.

ANOVA

PFOA Concentrations

	Sum of Squares	df	Mean Square	F	Sig.
Between Groups	860.197	3	286.732	15.317	.000

Within Groups	262.083	14	18.720
Total	1122.280	17	

Post Hoc Tests

Multiple Comparisons

PFOA Concentrations

Tamhane

(I) ResidentialAreas	(J) ResidentialAreas	Mean Difference (I-J)	Std. Error	Sig.
Dinkytown	CTC	15.98333	2.55831	.008
	CSCC	10.71667	3.64820	.160
	Mayo	15.10000	2.70836	.007
CTC	Dinkytown	-15.98333	2.55831	.008
	CSCC	-5.26667	2.64659	.697
	Mayo	-.88333	1.01503	.961
CSCC	Dinkytown	-10.71667	3.64820	.160
	CTC	5.26667	2.64659	.697
	Mayo	4.38333	2.79190	.792
Mayo	Dinkytown	-15.10000	2.70836	.007
	CTC	.88333	1.01503	.961
	CSCC	-4.38333	2.79190	.792

Multiple Comparisons

PFOA Concentrations

Tamhane

(I) ResidentialAreas	(J) ResidentialAreas	99.67% Confidence Interval	
		Lower Bound	Upper Bound
Dinkytown	CTC	-3.3273	35.2940
	CSCC	-15.2220	36.6554
	Mayo	-2.1359	32.3359
CTC	Dinkytown	-35.2940	3.3273
	CSCC	-106.8491	96.3157
	Mayo	-7.5346	5.7679
CSCC	Dinkytown	-36.6554	15.2220
	CTC	-96.3157	106.8491
	Mayo	-57.7618	66.5284
Mayo	Dinkytown	-32.3359	2.1359
	CTC	-5.7679	7.5346
	CSCC	-66.5284	57.7618

3.

ANOVA

PFNA Concentrations

	Sum of Squares	df	Mean Square	F	Sig.
Between Groups	46.068	3	15.356	1.419	.279
Within Groups	151.528	14	10.823		
Total	197.596	17			

Post Hoc Tests

Multiple Comparisons

PFNA Concentrations

Tamhane

ResidentialAreas	ResidentialAreas	Mean Difference (I-J)	Std. Error	Sig.
Dinkytown	CTC	1.60000	1.88403	.966
	CSCC	4.13333	2.28804	.521
	Mayo	3.15000	2.14571	.692
CTC	Dinkytown	-1.60000	1.88403	.966
	CSCC	2.53333	1.49481	.747
	Mayo	1.55000	1.26625	.840
CSCC	Dinkytown	-4.13333	2.28804	.521
	CTC	-2.53333	1.49481	.747
	Mayo	-.98333	1.81354	.997
Mayo	Dinkytown	-3.15000	2.14571	.692
	CTC	-1.55000	1.26625	.840
	CSCC	.98333	1.81354	.997

Multiple Comparisons

PFNA Concentrations

Tamhane

ResidentialAreas	ResidentialAreas	99.67% Confidence Interval	
		Lower Bound	Upper Bound
Dinkytown	CTC	-11.3533	14.5533
	CSCC	-9.9002	18.1669
	Mayo	-8.3695	14.6695
CTC	Dinkytown	-14.5533	11.3533
	CSCC	-30.6412	35.7079
	Mayo	-6.3463	9.4463
CSCC	Dinkytown	-18.1669	9.9002
	CTC	-35.7079	30.6412
	Mayo	-15.8812	13.9145
Mayo	Dinkytown	-14.6695	8.3695
	CTC	-9.4463	6.3463

Multiple Comparisons
PFNA Concentrations

ResidentialAreas	ResidentialAreas	Tamhane 99.67% Confidence Interval	
		Lower Bound	Upper Bound
Dinkytown	CTC	-11.3533	14.5533
	CSCC	-9.9002	18.1669
	Mayo	-8.3695	14.6695
CTC	Dinkytown	-14.5533	11.3533
	CSCC	-30.6412	35.7079
	Mayo	-6.3463	9.4463
CSCC	Dinkytown	-18.1669	9.9002
	CTC	-35.7079	30.6412
	Mayo	-15.8812	13.9145
Mayo	Dinkytown	-14.6695	8.3695
	CTC	-9.4463	6.3463
	CSCC	-13.9145	15.8812

4.

ANOVA
PFOS Concentrations

	Sum of Squares	df	Mean Square	F	Sig.
Between Groups	1707.114	3	569.038	9.258	.001
Within Groups	860.458	14	61.461		
Total	2567.572	17			

Post Hoc Tests

Multiple Comparisons
PFOS Concentrations
Tamhane

ResidentialAreas	ResidentialAreas	Mean Difference (I-J)	Std. Error	Sig.
Dinkytown	CTC	22.31667	5.01046	.019
	CSCC	20.34667	6.31519	.110
	Mayo	19.83333	4.87040	.030
CTC	Dinkytown	-22.31667	5.01046	.019
	CSCC	-1.97000	4.98054	1.000
	Mayo	-2.48333	2.94023	.968
CSCC	Dinkytown	-20.34667	6.31519	.110
	CTC	1.97000	4.98054	1.000
	Mayo	-.51333	4.83961	1.000
Mayo	Dinkytown	-19.83333	4.87040	.030
	CTC	2.48333	2.94023	.968

Multiple Comparisons

PFOS Concentrations

Tamhane

ResidentialAreas	ResidentialAreas	Mean Difference (I-J)	Std. Error	Sig.
Dinkytown	CTC	22.31667	5.01046	.019
	CSCC	20.34667	6.31519	.110
	Mayo	19.83333	4.87040	.030
CTC	Dinkytown	-22.31667	5.01046	.019
	CSCC	-1.97000	4.98054	1.000
	Mayo	-2.48333	2.94023	.968
CSCC	Dinkytown	-20.34667	6.31519	.110
	CTC	1.97000	4.98054	1.000
	Mayo	-.51333	4.83961	1.000
Mayo	Dinkytown	-19.83333	4.87040	.030
	CTC	2.48333	2.94023	.968
	CSCC	.51333	4.83961	1.000

Multiple Comparisons

PFOS Concentrations

Tamhane

Residential Areas	Residential Areas	99.67% Confidence Interval	
		Lower Bound	Upper Bound
Dinkytown	CTC	-8.3691	53.0024
	CSCC	-23.2001	63.8934
	Mayo	-10.0105	49.6771
CTC	Dinkytown	-53.0024	8.3691
	CSCC	-83.1119	79.1719
	Mayo	-25.8502	20.8835
CSCC	Dinkytown	-63.8934	23.2001
	CTC	-79.1719	83.1119
	Mayo	-90.4784	89.4517
Mayo	Dinkytown	-49.6771	10.0105
	CTC	-20.8835	25.8502
	CSCC	-89.4517	90.4784

5.

ANOVA

PFDA Concentrations

	Sum of Squares	df	Mean Square	F	Sig.
Between Groups	53.659	3	17.886	2.228	.130
Within Groups	112.368	14	8.026		
Total	166.027	17			

Post Hoc Tests

Multiple Comparisons

PFDA Concentrations

Tamhane

Residential Areas	Residential Areas	Mean Difference (I-J)	Std. Error	Sig.
Dinkytown	CTC	4.76667	1.49859	.138
	CSCC	2.55667	1.98365	.811
	Mayo	3.06667	1.84602	.569
CTC	Dinkytown	-4.76667	1.49859	.138
	CSCC	-2.21000	1.29965	.793
	Mayo	-1.70000	1.07796	.686
CSCC	Dinkytown	-2.55667	1.98365	.811
	CTC	2.21000	1.29965	.793
	Mayo	.51000	1.68852	1.000
Mayo	Dinkytown	-3.06667	1.84602	.569
	CTC	1.70000	1.07796	.686
	CSCC	-.51000	1.68852	1.000

Multiple Comparisons

PFDA Concentrations

Tamhane

Residential Areas	Residential Areas	99.67% Confidence Interval	
		Lower Bound	Upper Bound
Dinkytown	CTC	-6.9412	16.4746
	CSCC	-10.1110	15.2244
	Mayo	-6.5255	12.6589
CTC	Dinkytown	-16.4746	6.9412
	CSCC	-57.5664	53.1464
	Mayo	-10.1217	6.7217
CSCC	Dinkytown	-15.2244	10.1110
	CTC	-53.1464	57.5664
	Mayo	-13.2577	14.2777
Mayo	Dinkytown	-12.6589	6.5255
	CTC	-6.7217	10.1217
	CSCC	-14.2777	13.2577

Comparing the median concentrations of PFASs in urban runoff: Mann–Whitney–Wilcoxon Test

Mann-Whitney Test

Ranks

	PFASs	N	Mean Rank	Sum of Ranks
Concentration	PFHpA	18	10.14	182.50
	PFOA	18	26.86	483.50
	Total	36		

Test Statistics[b]

	Concentration
Mann-Whitney U	11.500
Wilcoxon W	182.500
Z	-4.799
Asymp. Sig. (2-tailed)	.000
Exact Sig. [2*(1-tailed Sig.)]	.000[a]

a. Not corrected for ties.

b. Grouping Variable: PFASs

Mann-Whitney Test

Ranks

	VAR00005	N	Mean Rank	Sum of Ranks
Concentration	PFHpA	18	16.64	299.50
	PFNA	18	20.36	366.50
	Total	36		

Test Statistics[b]

	VAR00004
Mann-Whitney U	128.500
Wilcoxon W	299.500
Z	-1.100
Asymp. Sig. (2-tailed)	.271
Exact Sig. [2*(1-tailed Sig.)]	.293[a]

a. Not corrected for ties.

b. Grouping Variable: VAR00005

Mann-Whitney Test

Ranks

	VAR00007	N	Mean Rank	Sum of Ranks
Concentration	PFHpA	18	11.17	201.00
	PFOS	18	25.83	465.00
	Total	36		

Test Statistics[b]	
	PFHpA vs PFOS
Mann-Whitney U	30.000
Wilcoxon W	201.000
Z	-4.209
Asymp. Sig. (2-tailed)	.000
Exact Sig. [2*(1-tailed Sig.)]	.000[a]

a. Not corrected for ties.
b. Grouping Variable: VAR00007

Mann-Whitney Test

Ranks				
	VAR00010	N	Mean Rank	Sum of Ranks
Concentration	PFHpA	18	18.42	331.50
	PFDA	18	18.58	334.50
	Total	36		

Test Statistics[b]	
	VAR00009
Mann-Whitney U	160.500
Wilcoxon W	331.500
Z	-.051
Asymp. Sig. (2-tailed)	.960
Exact Sig. [2*(1-tailed Sig.)]	.963[a]

a. Not corrected for ties.
b. Grouping Variable: VAR00010

Mann-Whitney Test

Ranks				
	VAR00012	N	Mean Rank	Sum of Ranks
Concentration	PFHpA	18	21.78	392.00
	PFUnDA	18	15.22	274.00
	Total	36		

Test Statistics[b]	
	VAR00011
Mann-Whitney U	103.000
Wilcoxon W	274.000
Z	-2.171
Asymp. Sig. (2-tailed)	.030

Exact Sig. [2*(1-tailed Sig.)]	.064[a]

a. Not corrected for ties.
b. Grouping Variable: VAR00012

Mann-Whitney Test

Ranks

	VAR00014	N	Mean Rank	Sum of Ranks
Concentration	PFOA	18	25.58	460.50
	PFNA	18	11.42	205.50
	Total	36		

Test Statistics[b]

	VAR00013
Mann-Whitney U	34.500
Wilcoxon W	205.500
Z	-4.044
Asymp. Sig. (2-tailed)	.000
Exact Sig. [2*(1-tailed Sig.)]	.000[a]

a. Not corrected for ties.
b. Grouping Variable: VAR00014

Mann-Whitney Test

Ranks

	VAR00016	N	Mean Rank	Sum of Ranks
Concentration	PFOA	18	18.36	330.50
	PFOS	18	18.64	335.50
	Total	36		

Test Statistics[b]

	VAR00015
Mann-Whitney U	159.500
Wilcoxon W	330.500
Z	-.079
Asymp. Sig. (2-tailed)	.937
Exact Sig. [2*(1-tailed Sig.)]	.938[a]

a. Not corrected for ties.
b. Grouping Variable: VAR00016

Mann-Whitney Test

Ranks

	VAR00018	N	Mean Rank	Sum of Ranks
Concentration	PFOA	18	26.50	477.00
	PFDA	18	10.50	189.00
	Total	36		

Test Statistics[b]

	VAR00017
Mann-Whitney U	18.000
Wilcoxon W	189.000
Z	-4.592
Asymp. Sig. (2-tailed)	.000
Exact Sig. [2*(1-tailed Sig.)]	.000[a]

a. Not corrected for ties.

b. Grouping Variable: VAR00018

Mann-Whitney Test

Ranks

	VAR00020	N	Mean Rank	Sum of Ranks
Concentration	PFOA	18	27.50	495.00
	PFUnDA	18	9.50	171.00
	Total	36		

Test Statistics[b]

	VAR00019
Mann-Whitney U	.000
Wilcoxon W	171.000
Z	-5.282
Asymp. Sig. (2-tailed)	.000
Exact Sig. [2*(1-tailed Sig.)]	.000[a]

a. Not corrected for ties.

b. Grouping Variable: VAR00020

Mann-Whitney Test

Ranks

	VAR00022	N	Mean Rank	Sum of Ranks
Concentration	PFNA	18	12.19	219.50
	PFOS	18	24.81	446.50
	Total	36		

Test Statistics[b]	
	VAR00021
Mann-Whitney U	48.500
Wilcoxon W	219.500
Z	-3.600
Asymp. Sig. (2-tailed)	.000
Exact Sig. [2*(1-tailed Sig.)]	.000[a]

a. Not corrected for ties.
b. Grouping Variable: VAR00022

Mann-Whitney Test

Ranks				
	VAR00024	N	Mean Rank	Sum of Ranks
Concentration	PFNA	18	20.25	364.50
	PFDA	18	16.75	301.50
	Total	36		

Test Statistics[b]	
	VAR00023
Mann-Whitney U	130.500
Wilcoxon W	301.500
Z	-1.035
Asymp. Sig. (2-tailed)	.301
Exact Sig. [2*(1-tailed Sig.)]	.323[a]

a. Not corrected for ties.
b. Grouping Variable: VAR00024

Mann-Whitney Test

Ranks				
	VAR00026	N	Mean Rank	Sum of Ranks
Concentration	PFNA	18	23.61	425.00
	PFUnDA	18	13.39	241.00
	Total	36		

Test Statistics[b]	
	VAR00025
Mann-Whitney U	70.000
Wilcoxon W	241.000
Z	-3.197
Asymp. Sig. (2-tailed)	.001
Exact Sig. [2*(1-tailed Sig.)]	.003[a]

a. Not corrected for ties.
b. Grouping Variable: VAR00026

Mann-Whitney Test

Ranks

	VAR00028	N	Mean Rank	Sum of Ranks
Concentration	PFOS	18	25.56	460.00
	PFDA	18	11.44	206.00
	Total	36		

Test Statistics[b]

	VAR00027
Mann-Whitney U	35.000
Wilcoxon W	206.000
Z	-4.049
Asymp. Sig. (2-tailed)	.000
Exact Sig. [2*(1-tailed Sig.)]	.000[a]

a. Not corrected for ties.
b. Grouping Variable: VAR00028

Mann-Whitney Test

Ranks

	VAR00030	N	Mean Rank	Sum of Ranks
Concentration	PFOS	18	27.14	488.50
	PFUnDA	18	9.86	177.50
	Total	36		

Test Statistics[b]

	VAR00029
Mann-Whitney U	6.500
Wilcoxon W	177.500
Z	-5.071
Asymp. Sig. (2-tailed)	.000
Exact Sig. [2*(1-tailed Sig.)]	.000[a]

a. Not corrected for ties.
b. Grouping Variable: VAR00030

Mann-Whitney Test

Ranks

	VAR00032	N	Mean Rank	Sum of Ranks
Concentration	PFDA	18	21.89	394.00
	PFUnDA	18	15.11	272.00
	Total	36		

Test Statistics[b]

	VAR00031
Mann-Whitney U	101.000
Wilcoxon W	272.000
Z	-2.244
Asymp. Sig. (2-tailed)	.025
Exact Sig. [2*(1-tailed Sig.)]	.055[a]

a. Not corrected for ties.

b. Grouping Variable: VAR00032

Comparing the frequencies of detection of PFASs in urban runoff: Chi-square test

PFNA versus PFOA

VAR00001 * VAR00002 Crosstabulation

			VAR00002		
			1.00	2.00	Total
VAR00001	PFNA	Count	33	67	100
		Expected Count	16.5	83.5	100.0
	PFOA	Count	0	100	100
		Expected Count	16.5	83.5	100.0
Total		Count	33	167	200
		Expected Count	33.0	167.0	200.0

Chi-Square Tests

	Value	df	Asymp. Sig. (2-sided)	Exact Sig. (2-sided)	Exact Sig. (1-sided)
Pearson Chi-Square	39.521[a]	1	.000		
Continuity Correction[b]	37.162	1	.000		
Likelihood Ratio	52.312	1	.000		
Fisher's Exact Test				.000	.000
N of Valid Cases	200				

a. 0 cells (.0%) have expected count less than 5. The minimum expected count is 16.50.

b. Computed only for a 2x2 table

PFOA versus PFOS

VAR00001 * VAR00002 Crosstabulation

			VAR00002	
			2.00	Total
VAR00001	PFOA	Count	100	100
		Expected Count	100.0	100.0
	PFOS	Count	100	100
		Expected Count	100.0	100.0
Total		Count	200	200
		Expected Count	200.0	200.0

Chi-Square Tests

	Value
Pearson Chi-Square	.[a]
N of Valid Cases	200

a. No statistics are computed because VAR00002 is a constant.

PFDA versus PFOA

VAR00001 * VAR00002 Crosstabulation

			VAR00002		
			1.00	2.00	Total
VAR00001	PFDA	Count	50	50	100
		Expected Count	25.0	75.0	100.0
	PFOA	Count	0	100	100
		Expected Count	25.0	75.0	100.0
Total		Count	50	150	200
		Expected Count	50.0	150.0	200.0

PFNA versus PFOS

VAR00001 * VAR00002 Crosstabulation

			VAR00002		
			1.00	2.00	Total
VAR00001	PFNA	Count	33	67	100
		Expected Count	16.5	83.5	100.0
	PFOS	Count	0	100	100
		Expected Count	16.5	83.5	100.0
Total		Count	33	167	200
		Expected Count	33.0	167.0	200.0

Chi-Square Tests

	Value	df	Asymp. Sig. (2-sided)	Exact Sig. (2-sided)	Exact Sig. (1-sided)
Pearson Chi-Square	39.521[a]	1	.000		
Continuity Correction[b]	37.162	1	.000		
Likelihood Ratio	52.312	1	.000		
Fisher's Exact Test				.000	.000
N of Valid Cases	200				

a. 0 cells (.0%) have expected count less than 5. The minimum expected count is 16.50.
b. Computed only for a 2x2 table

PFDA versus PFNA

VAR00001 * VAR00002 Crosstabulation

			VAR00002		
			1.00	2.00	Total
VAR00001	PFDA	Count	50	50	100
		Expected Count	41.5	58.5	100.0
	PFNA	Count	33	67	100
		Expected Count	41.5	58.5	100.0
Total		Count	83	117	200
		Expected Count	83.0	117.0	200.0

Chi-Square Tests

	Value	df	Asymp. Sig. (2-sided)	Exact Sig. (2-sided)	Exact Sig. (1-sided)
Pearson Chi-Square	5.952[a]	1	.015		
Continuity Correction[b]	5.272	1	.022		
Likelihood Ratio	5.986	1	.014		
Fisher's Exact Test				.021	.011
N of Valid Cases	200				

a. 0 cells (.0%) have expected count less than 5. The minimum expected count is 41.50.
b. Computed only for a 2x2 table

PFDA versus PFOS

VAR00001 * VAR00002 Crosstabulation

			VAR00002		
			1.00	2.00	Total
VAR00001	PFDA	Count	50	50	100
		Expected Count	25.0	75.0	100.0
	PFOS	Count	0	100	100
		Expected Count	25.0	75.0	100.0
Total		Count	50	150	200
		Expected Count	50.0	150.0	200.0

Chi-Square Tests

	Value	df	Asymp. Sig. (2-sided)	Exact Sig. (2-sided)	Exact Sig. (1-sided)
Pearson Chi-Square	66.667[a]	1	.000		
Continuity Correction[b]	64.027	1	.000		
Likelihood Ratio	86.305	1	.000		
Fisher's Exact Test				.000	.000
N of Valid Cases	200				

a. 0 cells (.0%) have expected count less than 5. The minimum expected count is 25.00.
b. Computed only for a 2x2 table

PFOS versus PFUnDA

VAR00001 * VAR00002 Crosstabulation

			VAR00002		
			1.00	2.00	Total
VAR00001	PFOS	Count	0	100	100
		Expected Count	39.0	61.0	100.0
	PFUnDA	Count	78	22	100
		Expected Count	39.0	61.0	100.0
Total		Count	78	122	200
		Expected Count	78.0	122.0	200.0

Chi-Square Tests

	Value	df	Asymp. Sig. (2-sided)	Exact Sig. (2-sided)	Exact Sig. (1-sided)
Pearson Chi-Square	127.869[a]	1	.000		
Continuity Correction[b]	124.611	1	.000		
Likelihood Ratio	162.118	1	.000		
Fisher's Exact Test				.000	.000
N of Valid Cases	200				

a. 0 cells (.0%) have expected count less than 5. The minimum expected count is 39.00.
b. Computed only for a 2x2 table

PFNA versus PFUnDA

VAR00001 * VAR00002 Crosstabulation

			VAR00002		
			1.00	2.00	Total
VAR00001	PFNA	Count	33	67	100
		Expected Count	55.5	44.5	100.0
	PFUnD	Count	78	22	100
	A	Expected Count	55.5	44.5	100.0
Total		Count	111	89	200
		Expected Count	111.0	89.0	200.0

Chi-Square Tests

	Value	df	Asymp. Sig. (2-sided)	Exact Sig. (2-sided)	Exact Sig. (1-sided)
Pearson Chi-Square	40.996[a]	1	.000		
Continuity Correction[b]	39.194	1	.000		
Likelihood Ratio	42.617	1	.000		
Fisher's Exact Test				.000	.000
N of Valid Cases	200				

a. 0 cells (.0%) have expected count less than 5. The minimum expected count is 44.50.
b. Computed only for a 2x2 table

PFOA versus PFUnDA

VAR00001 * VAR00002 Crosstabulation

			VAR00002		
			1.00	2.00	Total
VAR00001	PFOA	Count	0	100	100
		Expected Count	39.0	61.0	100.0
	PFUnD	Count	78	22	100
	A	Expected Count	39.0	61.0	100.0
Total		Count	78	122	200
		Expected Count	78.0	122.0	200.0

Chi-Square Tests

	Value	df	Asymp. Sig. (2-sided)	Exact Sig. (2-sided)	Exact Sig. (1-sided)
Pearson Chi-Square	127.869[a]	1	.000		
Continuity Correction[b]	124.611	1	.000		
Likelihood Ratio	162.118	1	.000		
Fisher's Exact Test				.000	.000
N of Valid Cases	200				

a. 0 cells (.0%) have expected count less than 5. The minimum expected count is 39.00.
b. Computed only for a 2x2 table

PFHpA versus PFOA

VAR00001 * VAR00002 Crosstabulation

			VAR00002		
			1.00	2.00	Total
VAR00001	PFHpA	Count	56	44	100
		Expected Count	28.0	72.0	100.0
	PFOA	Count	0	100	100
		Expected Count	28.0	72.0	100.0
Total		Count	56	144	200
		Expected Count	56.0	144.0	200.0

Chi-Square Tests

	Value	df	Asymp. Sig. (2-sided)	Exact Sig. (2-sided)	Exact Sig. (1-sided)
Pearson Chi-Square	77.778[a]	1	.000		
Continuity Correction[b]	75.025	1	.000		
Likelihood Ratio	99.995	1	.000		
Fisher's Exact Test				.000	.000
N of Valid Cases	200				

a. 0 cells (.0%) have expected count less than 5. The minimum expected count is 28.00.
b. Computed only for a 2x2 table

PFHpA versus PFNA

VAR00001 * VAR00002 Crosstabulation

			VAR00002		
			1.00	2.00	Total
VAR00001	PFHpA	Count	56	44	100
		Expected Count	44.5	55.5	100.0
	PFNA	Count	33	67	100
		Expected Count	44.5	55.5	100.0
Total		Count	89	111	200
		Expected Count	89.0	111.0	200.0

Chi-Square Tests

	Value	df	Asymp. Sig. (2-sided)	Exact Sig. (2-sided)	Exact Sig. (1-sided)
Pearson Chi-Square	10.710[a]	1	.001		
Continuity Correction[b]	9.799	1	.002		
Likelihood Ratio	10.812	1	.001		
Fisher's Exact Test				.002	.001
N of Valid Cases	200				

a. 0 cells (.0%) have expected count less than 5. The minimum expected count is 44.50.

Chi-Square Tests

	Value	df	Asymp. Sig. (2-sided)	Exact Sig. (2-sided)	Exact Sig. (1-sided)
Pearson Chi-Square	10.710[a]	1	.001		
Continuity Correction[b]	9.799	1	.002		
Likelihood Ratio	10.812	1	.001		
Fisher's Exact Test				.002	.001
N of Valid Cases	200				

a. 0 cells (.0%) have expected count less than 5. The minimum expected count is 44.50.
b. Computed only for a 2x2 table

PFHpA versus PFOS

VAR00001 * VAR00002 Crosstabulation

			VAR00002		
			1.00	2.00	Total
VAR00001	PFHpA	Count	56	44	100
		Expected Count	28.0	72.0	100.0
	PFOS	Count	0	100	100
		Expected Count	28.0	72.0	100.0
Total		Count	56	144	200
		Expected Count	56.0	144.0	200.0

Chi-Square Tests

	Value	df	Asymp. Sig. (2-sided)	Exact Sig. (2-sided)	Exact Sig. (1-sided)
Pearson Chi-Square	77.778[a]	1	.000		
Continuity Correction[b]	75.025	1	.000		
Likelihood Ratio	99.995	1	.000		
Fisher's Exact Test				.000	.000
N of Valid Cases	200				

a. 0 cells (.0%) have expected count less than 5. The minimum expected count is 28.00.
b. Computed only for a 2x2 table

PFDA versus PFHpA

VAR00001 * VAR00002 Crosstabulation

			VAR00002		
			1.00	2.00	Total
VAR00001	PFDA	Count	50	50	100
		Expected Count	53.0	47.0	100.0
	PFHpA	Count	56	44	100
		Expected Count	53.0	47.0	100.0
Total		Count	106	94	200

VAR00001 * VAR00002 Crosstabulation					
			VAR00002		
			1.00	2.00	Total
VAR00001	PFDA	Count	50	50	100
		Expected Count	53.0	47.0	100.0
	PFHpA	Count	56	44	100
		Expected Count	53.0	47.0	100.0
		Count	106	94	200
		Expected Count	106.0	94.0	200.0

Chi-Square Tests					
	Value	df	Asymp. Sig. (2-sided)	Exact Sig. (2-sided)	Exact Sig. (1-sided)
Pearson Chi-Square	.723[a]	1	.395		
Continuity Correction[b]	.502	1	.479		
Likelihood Ratio	.723	1	.395		
Fisher's Exact Test				.479	.239
N of Valid Cases	200				

a. 0 cells (.0%) have expected count less than 5. The minimum expected count is 47.00.
b. Computed only for a 2x2 table

PFDA versus PFOS

VAR00001 * VAR00002 Crosstabulation					
			VAR00002		
			1.00	2.00	Total
VAR00001	PFHpA	Count	56	44	100
		Expected Count	67.0	33.0	100.0
	PFUnDA	Count	0	22	22
		Expected Count	14.7	7.3	22.0
Total		Count	134	66	200
		Expected Count	134.0	66.0	200.0

Chi-Square Tests			
	Value	df	Asymp. Sig. (2-sided)
Pearson Chi-Square	88.557[a]	2	.000
Likelihood Ratio	116.485	2	.000
N of Valid Cases	200		

a. 0 cells (.0%) have expected count less than 5. The minimum expected count is 7.26.

Comparing PFAS concentrations in rainfall and urban runoff

Mann-Whitney Test

Ranks

	RainVsRunoff, PFOS	N	Mean Rank	Sum of Ranks
RainVsDinkytown	1.00	6	3.50	21.00
	2.00	6	9.50	57.00
	Total	12		

Test Statistics[b]

	RainVsDinkytown
Mann-Whitney U	.000
Wilcoxon W	21.000
Z	-2.882
Asymp. Sig. (2-tailed)	.004
Exact Sig. [2*(1-tailed Sig.)]	.002[a]

a. Not corrected for ties.
b. Grouping Variable: RainVsRunoffPFOS

Mann-Whitney Test

Ranks

	RainVsRunoff, PFOS	N	Mean Rank	Sum of Ranks
RainVsCTC	1.00	6	5.17	31.00
	2.00	3	4.67	14.00
	Total	9		

Test Statistics[b]

	RainVsCTC
Mann-Whitney U	8.000
Wilcoxon W	14.000
Z	-.258
Asymp. Sig. (2-tailed)	.796
Exact Sig. [2*(1-tailed Sig.)]	.905[a]

a. Not corrected for ties.

Test Statistics[b]	
	RainVsCTC
Mann-Whitney U	8.000
Wilcoxon W	14.000
Z	-.258
Asymp. Sig. (2-tailed)	.796
Exact Sig. [2*(1-tailed Sig.)]	.905[a]
a. Not corrected for ties.	
b. Grouping Variable: RainVsRunoffPFOS	

Mann-Whitney Test

Ranks				
	RainVsRunoff, PFOS	N	Mean Rank	Sum of Ranks
RainVsCSCC	1.00	6	4.83	29.00
	2.00	3	5.33	16.00
	Total	9		

Test Statistics[b]	
	RainVsCSCC
Mann-Whitney U	8.000
Wilcoxon W	29.000
Z	-.258
Asymp. Sig. (2-tailed)	.796
Exact Sig. [2*(1-tailed Sig.)]	.905[a]
a. Not corrected for ties.	
b. Grouping Variable: RainVsRunoffPFOS	

Mann-Whitney Test

Ranks				
	RainVsRunoff, PFOS	N	Mean Rank	Sum of Ranks
RainVsMayo	1.00	6	6.00	36.00
	2.00	6	7.00	42.00
	Total	12		

Test Statistics[b]	
	RainVsMayo
Mann-Whitney U	15.000
Wilcoxon W	36.000
Z	-.480

Asymp. Sig. (2-tailed)	.631
Exact Sig. [2*(1-tailed Sig.)]	.699[a]
a. Not corrected for ties.	
b. Grouping Variable: RainVsRunoffPFOS	

Mann-Whitney Test

Ranks

	RainVsRunoff, PFOS	N	Mean Rank	Sum of Ranks
RainVsIndustrial	1.00	6	3.83	23.00
	2.00	5	8.60	43.00
	Total	11		

Test Statistics[b]

	RainVsIndustrial
Mann-Whitney U	2.000
Wilcoxon W	23.000
Z	-2.373
Asymp. Sig. (2-tailed)	.018
Exact Sig. [2*(1-tailed Sig.)]	.017[a]
a. Not corrected for ties.	
b. Grouping Variable: RainVsRunoffPFOS	

Normality of data: Shapiro–Wilk Test

PFHpA

Case Processing Summary

	Cases					
	Valid		Missing		Total	
	N	Percent	N	Percent	N	Percent
PFHpA	18	100.0%	0	.0%	18	100.0%

Tests of Normality

	Kolmogorov-Smirnov[a]			Shapiro-Wilk		
	Statistic	df	Sig.	Statistic	df	Sig.
PFHpA	.306	18	.000	.791	18	.001
a. Lilliefors Significance Correction						

PFOA

Case Processing Summary

	Cases					
	Valid		Missing		Total	
	N	Percent	N	Percent	N	Percent
PFOA	18	100.0%	0	.0%	18	100.0%

Tests of Normality

	Kolmogorov-Smirnov[a]			Shapiro-Wilk		
	Statistic	df	Sig.	Statistic	df	Sig.
PFOA	.213	18	.030	.871	18	.018

a. Lilliefors Significance Correction

PFNA

Case Processing Summary

	Cases					
	Valid		Missing		Total	
	N	Percent	N	Percent	N	Percent
PFNA	18	100.0%	0	.0%	18	100.0%

Tests of Normality

	Kolmogorov-Smirnov[a]			Shapiro-Wilk		
	Statistic	df	Sig.	Statistic	df	Sig.
PFNA	.202	18	.051	.888	18	.035

a. Lilliefors Significance Correction

PFOS

Case Processing Summary

	Cases					
	Valid		Missing		Total	
	N	Percent	N	Percent	N	Percent
PFOS	18	100.0%	0	.0%	18	100.0%

Tests of Normality

	Kolmogorov-Smirnov[a]			Shapiro-Wilk		
	Statistic	df	Sig.	Statistic	df	Sig.
PFOS	.189	18	.090	.886	18	.033

a. Lilliefors Significance Correction

PFDA

Case Processing Summary

	Cases					
	Valid		Missing		Total	
	N	Percent	N	Percent	N	Percent
PFDA	18	100.0%	0	.0%	18	100.0%

Tests of Normality

	Kolmogorov-Smirnov[a]			Shapiro-Wilk		
	Statistic	df	Sig.	Statistic	df	Sig.
PFDA	.290	18	.000	.805	18	.002

a. Lilliefors Significance Correction

PFUnDA

Case Processing Summary

	Cases					
	Valid		Missing		Total	
	N	Percent	N	Percent	N	Percent
PFUnDA	18	100.0%	0	.0%	18	100.0%

Tests of Normality

	Kolmogorov-Smirnov[a]			Shapiro-Wilk		
	Statistic	df	Sig.	Statistic	df	Sig.
PFUnDA	.472	18	.000	.560	18	.000

a. Lilliefors Significance Correction

Appendix B: Supplementary data for Chapter 3

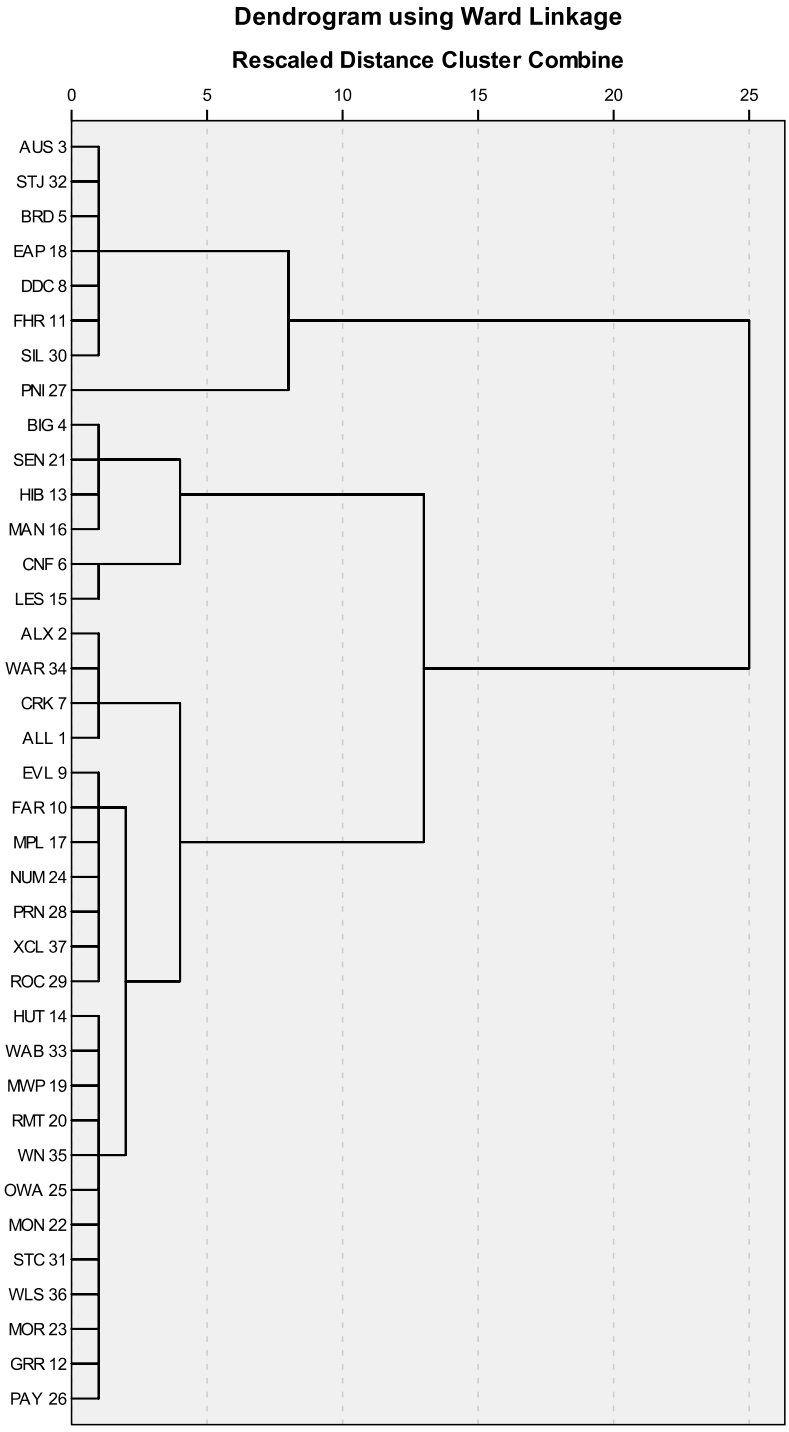

Figure B-1 Cluster analysis dendrogram

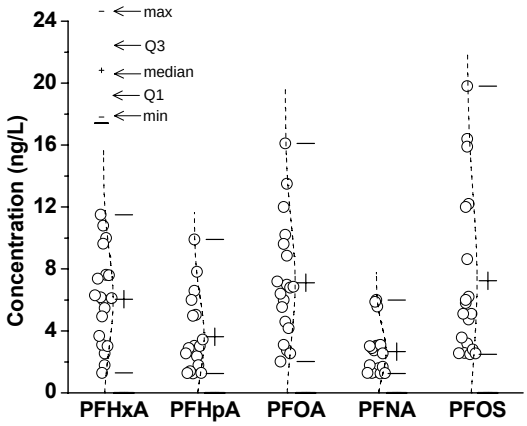

Figure B-2 Box and whisker plots of influent PFAS concentrations in Subclusters 1 and 2 WWTPs (n = 19).

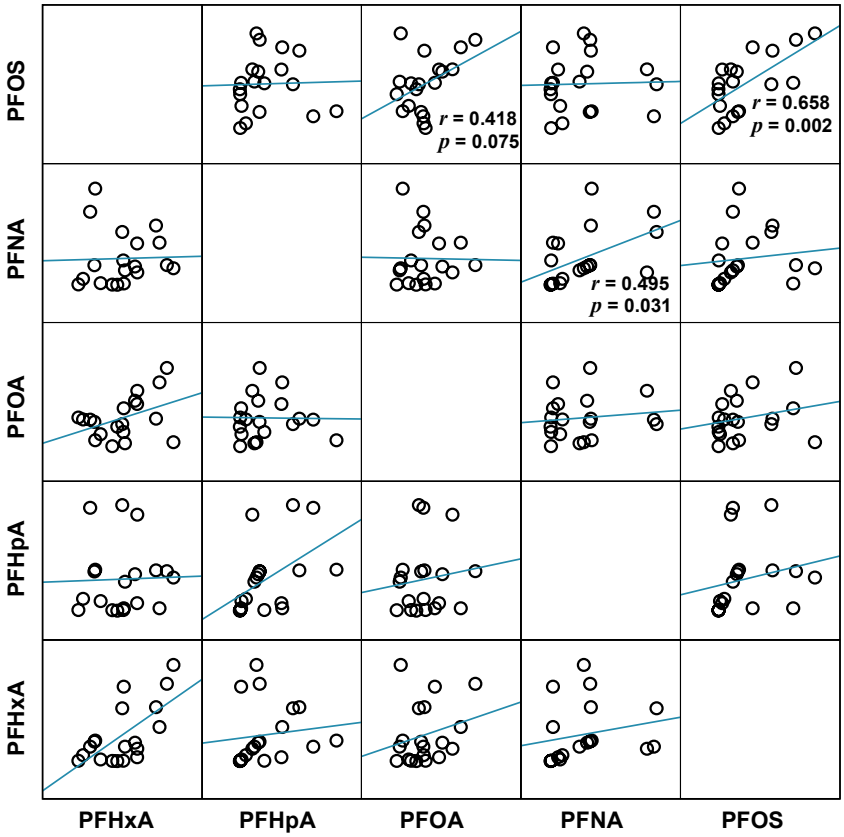

Figure B-3 2-D scatter matrix of influent PFAS concentration in Subclusters 1 and 2 WWTPs (n = 19).

Table B-1. Input parameters of STP model (Trent University). Parameters of the primary clarifier, aeration tank, and final settling tank are the typical design or operating values recommended by the Ontario Ministry of Environment (Clark and Mackay, 1995) and the default data of the model.

Degradation half-life (h)	144.03 (calculated from Table 2 of the work by Wang et al., 2005)		
Vapor pressure (Pa)	3 (Kaiser et al., 2004)		
Log K_{ow} (octanol/water partition coefficient)	5.58 (Carmosini and Lee, 2008)		
	Primary clarifier	**Aeration tank**	**Final settling tank**
Area (m^2)	266.7	800	727.3
Depth (m)	3.8	10	3.8
Biomass fraction of VSS	0.005	0.0025	0.00055
Sludge VSS concentration (g/m^3)	50000		5500
Aeration rate (m^3/h)		8960	

Table B-2. Three major clusters (I–III) and corresponding WWTPs.

I		II (PFOS)		III (PFOA)	
Domestic sources		Plausible non-domestic sources			
1	2	3 (PFHxA)	4	5	6	7
EVL	GRR	ALL	AUS	PNI	BIG	CNF
FAR	HUT	ALX	BRD		HIB	LES
NUM	MPL	CRK	DDC		MAN	
PRN	MWP	WAR	FHR		SEN	
ROC	RMT		EAP			
XCL	MON		SIL			
	MOR		STJ			
	OWA					
	PAY					
	STC					
	WAB					
	WIN					
	WLS					

Table B-3. Output of ANOVA and post-hoc tests.

Multiple Comparisons

Concentrations

Tamhane

(I) PFASs		(J) PFASs	Mean Difference (I-J)	Std. Error	Sig.	95% Confidence Interval	
						Lower Bound	Upper Bound
dimension2	PFHxA	dimension3 PFHpA	2.43158	.89828	.100	-.2539	5.1170
		PFOA	-1.06842	1.12321	.986	-4.4291	2.2923
		PFNA	3.37868*	.78442	.002	.9887	5.7687
		PFOS	-1.19395	1.42035	.995	-5.5040	3.1161
	PFHpA	dimension3 PFHxA	-2.43158	.89828	.100	-5.1170	.2539
		PFOA	-3.50000*	1.04831	.022	-6.6607	-.3393
		PFNA	.94711	.67281	.844	-1.0825	2.9767
		PFOS	-3.62553	1.36190	.125	-7.8009	.5499
	PFOA	dimension3 PFHxA	1.06842	1.12321	.986	-2.2923	4.4291
		PFHpA	3.50000*	1.04831	.022	.3393	6.6607
		PFNA	4.44711*	.95256	.001	1.5109	7.3833
		PFOS	-.12553	1.51969	1.000	-4.6883	4.4373
	PFNA	dimension3 PFHxA	-3.37868*	.78442	.002	-5.7687	-.9887
		PFHpA	-.94711	.67281	.844	-2.9767	1.0825
		PFOA	-4.44711*	.95256	.001	-7.3833	-1.5109
		PFOS	-4.57263*	1.28964	.019	-8.6021	-.5431
	PFOS	d PFHxA	1.19395	1.42035	.995	-3.1161	5.5040

	PFHpA	3.62553	1.36190	.125	-.5499	7.8009
	PFOA	.12553	1.51969	1.000	-4.4373	4.6883
	PFNA	4.57263*	1.28964	.019	.5431	8.6021

*. The mean difference is significant at the 0.01 level.

Appendix C: Supplementary data for Chapter 4

Table C-0. The linear solid–water distribution coefficients (K_d, L/kg) and corresponding standard deviation (SD).

	Mean ($\overline{x_1}$) $n = 3$ Single-compound System	**SD_1**	**Mean ($\overline{x_2}$) $n = 3$ Multi-compound System**	**SD_2**	**SD_p**	**SE (diff)**	**$\overline{x_1} - \overline{x_2}$**	**95% confidence intervals for the difference between means**
PFNA	5.5	0.71	2.0	0.44	0.60	0.48	3.5	*(2.2, 4.8)* [a]
PFOS	14.6	1.06	7.5	0.53	0.84	0.68	7.1	*(5.2, 9.0)* [a]
PFDA	19.8	1.50	11.2	0.80	1.20	0.98	8.6	*(5.9, 11.3)* [a]
PFUnDA	49.5	4.60	52.3	4.24	4.42	3.61	2.8	*(−7.2, 12.8)* [b]

[a] the difference the differences in K_d values between the single-compound system and the multi-compound system are significant at the alpha level of 0.05.
[b] because the 95% confidence interval contain 0, the difference the difference in K_d values of PFUnDA between the two systems are not significant at the alpha level of 0.05.

95% confidence interval for difference between two means

$\overline{x_1} - \overline{x_2}$ ± (Confidence Coefficient × SE(diff)),

where SE(diff) is the standard error of the difference of the means and was calculated from pooled SD (SD_p). SD_p was calculated by

$$SD_p = \sqrt{\frac{(n_1 - 1)SD_1^2 + (n_2 - 1)SD_2^2}{n_1 + n_2 - 2}}$$

Table C-1. Chemical Information of Perfluoroalkyl Acids (PFASs)

Chemicals	Molecular Formula	MW (g/mol)	Provider	Grade	Chemical Structure
Tridecafluoroheptanoic acid (PFHpA)	$C_7F_{13}HO_2$	364	Aldrich	99%	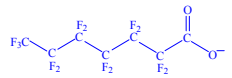
Perfluorooctanoic acid (PFOA)	$C_8F_{15}HO_2$	414	Sigma–Aldrich	~95%	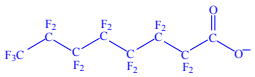
Potassium salt of heptadecafluorooctane (PFOS)	$C_8F_{17}KO_3S$	538	Sigma–Aldrich	≥98%	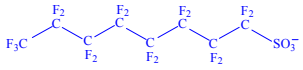
Perfluorononanoic acid (PFNA)	$C_9F_{17}HO_2$	464	Aldrich	97%	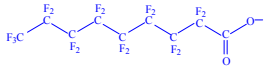
Perfluorodecanoic acid (PFDA)	$C_{10}F_{19}HO_2$	514	Aldrich	98%	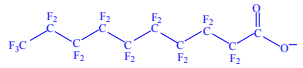
Perfluoroundecanoic acid (PFUnDA)	$C_{11}F_{21}HO_2$	564	Aldrich	95%	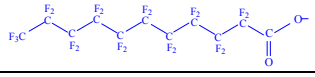

Table C-2. Free energy changes (kJ/mol) during PFAS adsorption on kaolinite in NaCl (1 mM) at pH 7.5. $\Delta G_{adsorption} = RT \ln K_d$; $\Delta G_{hydrophobic} = m \times \Delta G_{CF2}$; $\Delta G_{electrostatic,adsorbate–adsorbent} = -F\Psi_d \approx -F\zeta$; $\Delta G_{elect,adsorbate\text{-}adsorbate} = \Delta G_{adsorption} - (\Delta G_{hydrophobic} + \Delta G_{electrostatic,adsorbate–adsorbate})$

	$\Delta G_{adsorption}$	$\Delta G_{hydrophob}$	ΔG_{elect}	$\Delta G_{elect,adsorbate\text{-}adsorbent}$	$\Delta G_{elect,adsorbate\text{-}adsorbate}$
PFOA	–1.9	–18.1	16.1	4.4	11.7
PFNA	–4.1	–20.6	16.6	4.7	11.9
PFDA	–6.7	–23.2	16.5	5.0	11.6
PFUnDA	–9.7	–25.8	16.1	5.2	11.0

Table C-3. LFER between log K_d (L/kg) and log C_w^{sat} (mol/L) for different compound classes

Compound class	$\log K_d = -a \log C_w^{sat} + b$	
	a	R^2
Perfluororinated carboxylates (this study)	0.35	0.99
Phenyl ureas[15]	0.56	0.94
Chlorinated hydrocarbons[15]	0.70	0.99
Aromatic hydrocarbons[15]	0.93	0.94

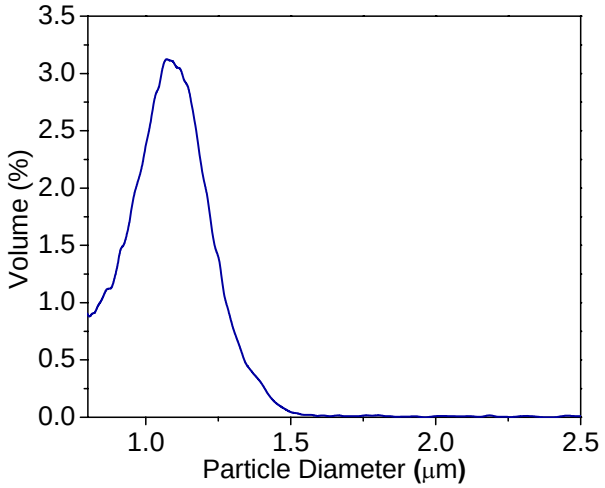

Figure C-1 Particle size distribution of kaolinite suspension.

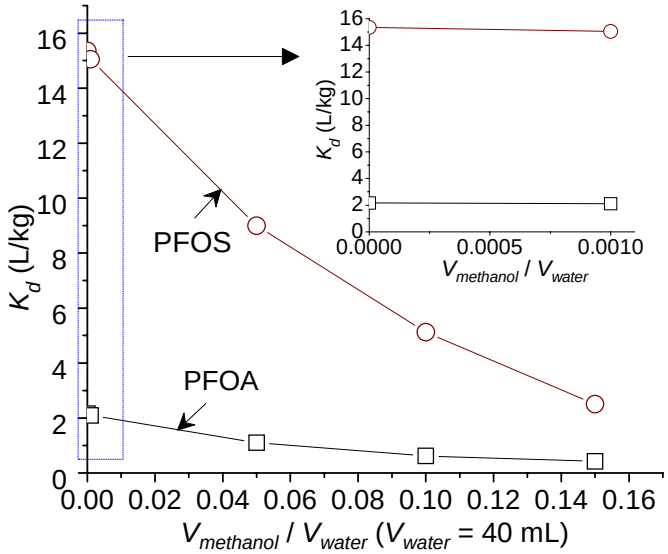

Figure C-2 Effects of cosolvent (methanol) on the adsorption of PFOS and PFOA by kaolinite (test water components and the experimental protocol is the same as the text; Initial dosed concentrations of PFOS and PFOA were both 1×10^{-6} mol/L).

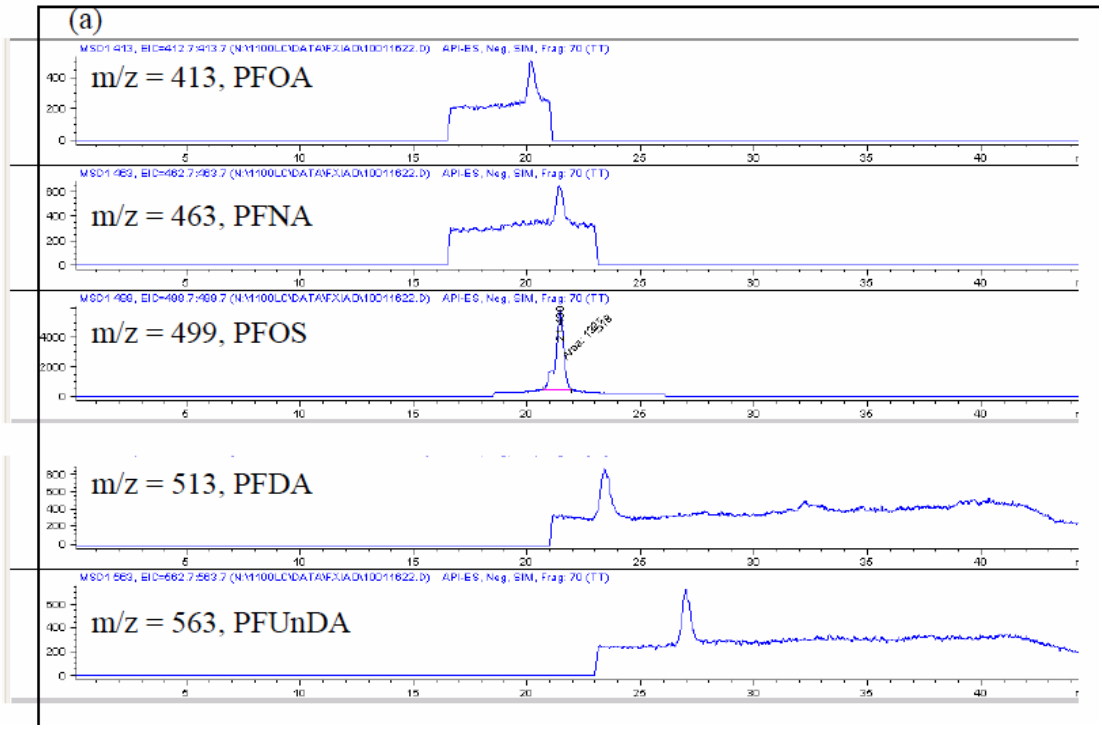

Figure C-3a HPLC–(SIM-)MS chromatograms of PFAS standard solutions (7.5×10^{-8} mol/L).

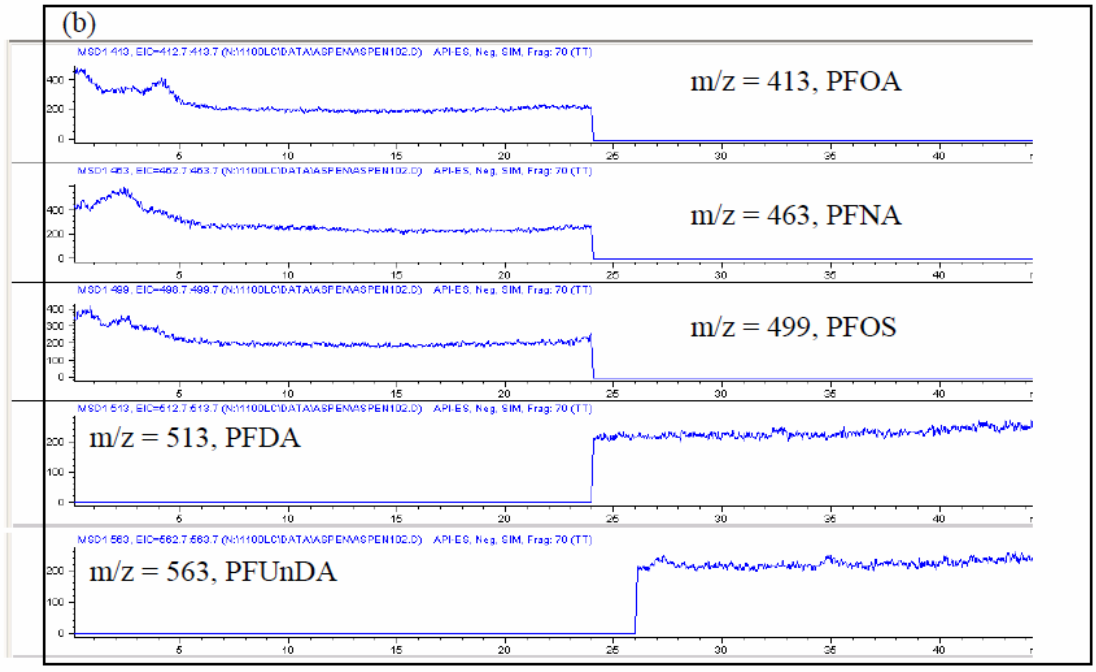

Figure C-3b HPLC–(SIM-)MS chromatograms of blank.

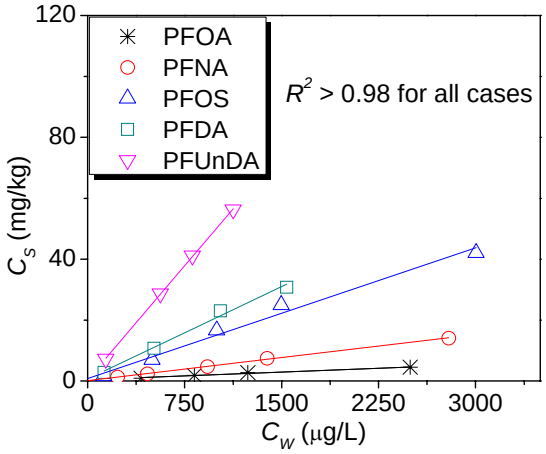

Figure C-4 Adsorption isotherms for PFASs in a single-compound system (pH 7.5; 1×10^{-3} mol/L NaCl).

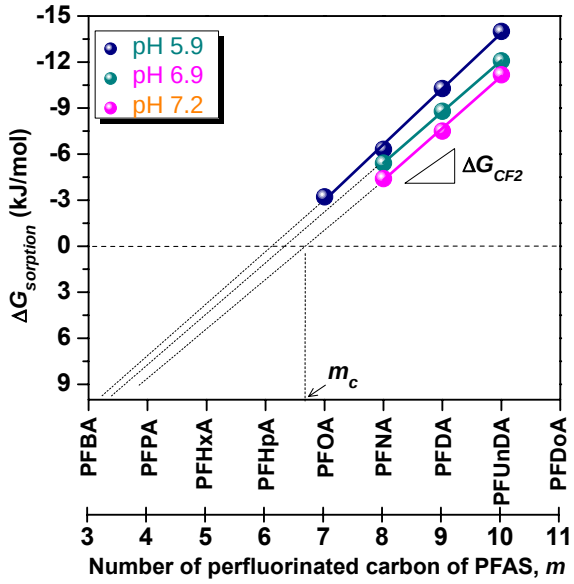

Figure C-5 The adsorption free energy ($\Delta G_{sorption}$) as a function of *m* during PFAS sorption to sediment in 0.5 mmol/L $CaCl_2$ (reanalyzed data from the work of Higgins and Luthy, 2006). $\Delta G_{sorption} = -3.63\ m + 22.41$ (pH = 5.9); $\Delta G_{sorption} = -3.33\ m + 21.22$ (pH = 6.9); $\Delta G_{sorption} = -3.39\ m + 22.80$ (pH = 7.2). R^2>0.97 for the linearity of all the fitted lines. m_c is *m* corresponding to spontaneous adsorption ($\Delta G_{sorption} = 0$). PFHxA: perfluorohexanoic acid; PFPA: perfluoropentanoic acid; PFBA: perfluorobutanoic acid; PFDoA: perfluorodecanoic acid.

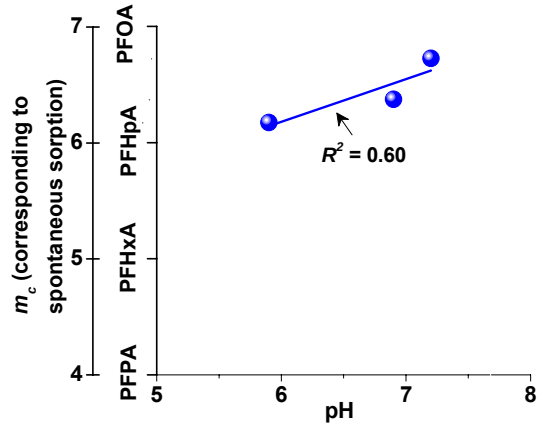

Figure C-6 The number of perfluorinated carbon of PFAS corresponding to $\Delta G_{sorption} = 0$ during PFAS sorption to sediment in 0.5 mmol/L $CaCl_2$ (reanalyzed data from the work of Higgins and Luthy[9]). $m_c = 0.36$ pH + 3.97.

Linear Free Energy Relationship. The distribution coefficient K_d reflects how a compound will "escape" from water. The linear free energy relationship has been used to describe the relationship between K_d and solubility C_w^{sat}, as given by the following equation:

$$\log K_d = -a \log C_w^{sat} + b$$

where a is a coefficient for a class of compounds. Figure C-7 shows the relationship between logK_d and logC_w^{sat} for perfluorinated carboxylates. The logC_w^{sat} values were estimated using SPARC software. The data fit the above equation well, resulting in an a value of 0.35. In comparison with hydrophobic compounds such as chlorinated and aromatic hydrocarbons, the amphiphilic PFASs had much smaller a values (Table C-3). In other words, the difference in K_d values between two PFASs was much smaller than that between two hydrophobic compounds that have a solubility difference similar to that of the two PFASs.

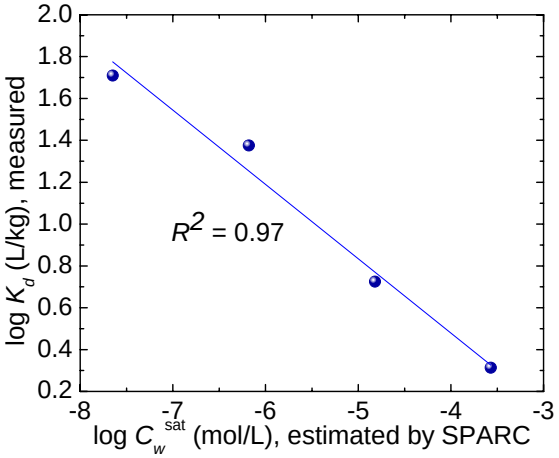

Figure C-7 Relationship of log K_d and log C_w^{sat} for PFASs (log K_d = –0.35 × log C_w^{sat} – 0.94).

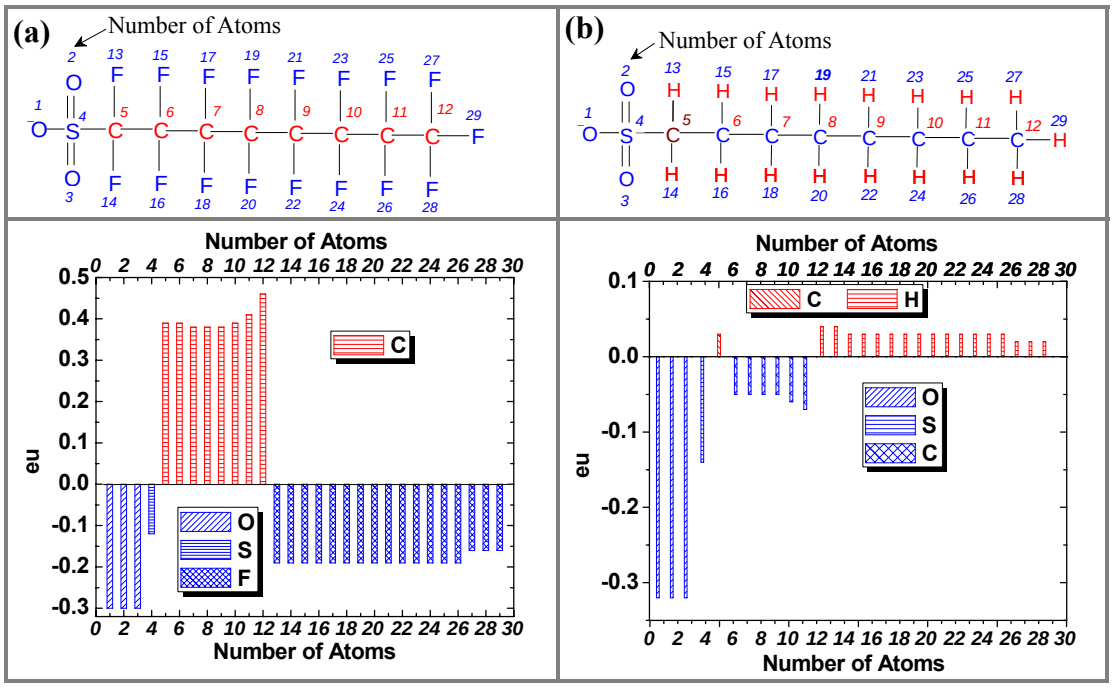

Figure C-8 Partial charge distributions in (a) a PFOS molecule and (b) an octanesulfonate molecule ("eu" stands for electron unit).

Partial atomic charges are the charges with absolute values, which are less than elementary charges. Partial atomic charges are created as a result of the asymmetric distribution of electrons in chemical bonds. Though they are very intuitive, but partial charges are difficult to calculate. A common approach for calculating partial atomic charges is the Mulliken population analysis. However, this method has a low accuracy. At the end of 1970s, an empirical method was developed by Miller and Savchik to calculate the partial atomic charges and has been widely used. This empirical method can be processed by computer software, like the MarvinSketch software, which allows one to have a quick estimation of partial atomic charges. The partial atomic charges of PFOS and octanesulfonate shown in Figure 4.1 in the text and Figure C-9 were calculated by the software.

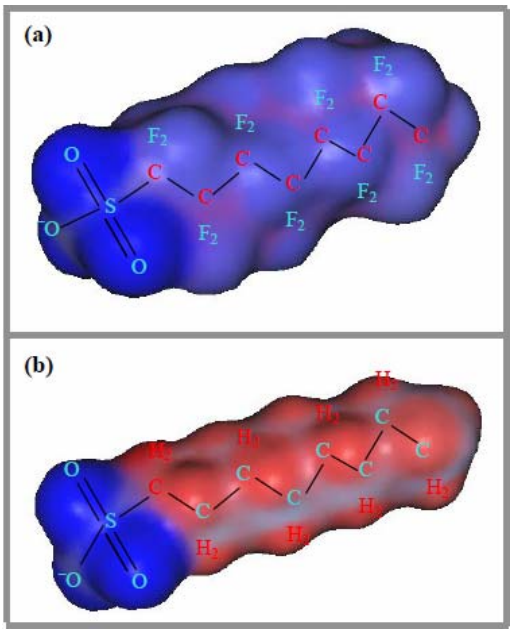

Figure C-9 Electrostatic potential maps of (a) a PFOS molecule and (b) an octanesulfonate molecule (blue: partial negative charge; red: partial positive charge).

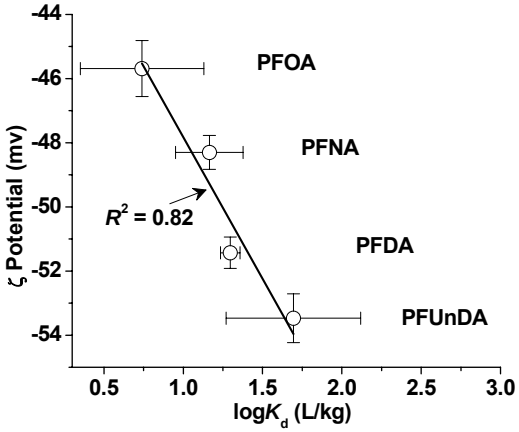

Figure C-10 The association between PFAS adsorption potential and the change of kaolinite surface charge with the addition of PFASs.

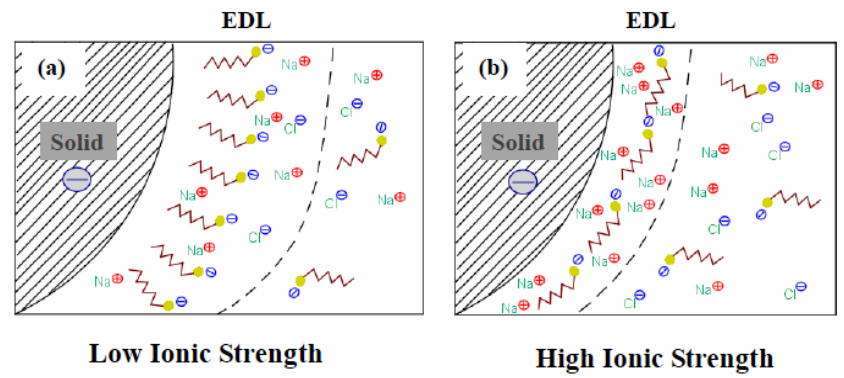

Figure C-11 Possible alignment of PFOA molecules around kaolinite surface.

Lengths of PFOA and PFOS:

Bond length (pm): C— F 134
C—C (sp3 hybridization): 154
C—O: 143
C—S: 181
S═O : 143
Bond angle: ~109^o = 1.902 radians

PFOA

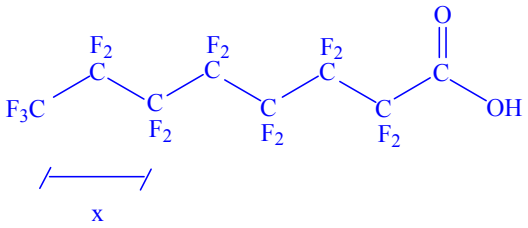

x = 2 × sin(109^o/2) × 154 = 250.7
So the total length of a PFOA molecule is 250.7 × 3.5 + 134 × cos(109^o/2) + 143 × cos(109^o/2) = 1036.6 pm = 1.0 nm

PFOS

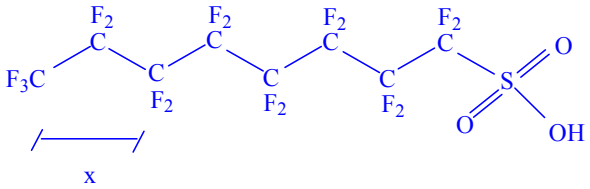

The total length of a PFOS molecule is 250.7 × 3.5 + 134 × cos(109°/2) + 181 × cos (109°/2) + 143 = 1203.4 pm = 1.2 nm

Determination of solid–water distribution coefficient (K_d). After 48 h of shaking, the tube was centrifuged immediately with an Eppendorf centrifuge at 4000 rpm (or 3250 × *g*) for 15 min. The supernatant was then filtered through a 0.2-μm polycarbonate membrane (Millipore). The filtration lasted less than 40 sec. No measurable PFAS adsorption onto the filters was observed by running PFAS-spiked HPLC grade water through the filter. The concentration of PFAS (C_w, ng/mL or μg/L) in the filtrate (V, mL) was quantified using a Hewlett-Packard 1090 HPLC interfaced to an electrospray ionization-MS (ESI-MS) with a selected ion-monitoring (SIM) mode. The remaining kaolinite in the tube was extracted with methanol in a sonication bath. The mixture was then centrifuged and the supernatant was collected. The pellet was resuspended in methanol, centrifuged again, and the supernatant was combined with the first one. The combined extract was then concentrated to a final volume of ~0.4 mL (V_m, mL) for quantification (C_e). A single-point solid–water distribution coefficient was calculated as $K_d = (C_e \times V_m)/(10^{-3} \times C_w \times m_s)$ (where m_s is the kaolinite mass in mg). The mass balance was checked by comparing the value of $C_w \times V + C_w \times K_d \times m_s$ with the initially spiked mass of PFAS. The test was repeated if the difference was larger than 7% of the initially spiked mass.

Parameters for operating the HPLC/ESI-MS system. The flow rate of the mobile phase was 0.20 mL/min. The mobile phase consisted of eluent A (2.0 mM NH_4Ac in a mixture of water and methanol (7:3, v/v)) and eluent B (2.0 mM NH_4Ac in methanol). The A/B ratio changed linearly in the first 13 min from 100/0 to 43.9/57.1, which was held for 5 min then changed linearly over the next 15 min to 0/100, which was held for 3 min then changed linearly over the next 1 min to 100/0, which was held for 8 min. Although the latest eluting peak (PFUnDA) was observed at approximately 27 min, sufficient run time (45 min) was used to condition the column for subsequent injections. The column temperature was maintained at 38 °C. The analytical column was conditioned prior to sample analysis with eluent B. For ESI-MS analysis, the MS detector was operated in the SIM mode with optimized parameters (fragmentor voltage, 70 V; capillary voltage, 4 kV). Precursor ions with *m/z* 363, 413, 463, 499, 513, and 563 were chosen, corresponding to PFHpA, PFOA, PFNA, PFOS, PFDA, and PFUnDA, respectively. The ions extracted at these mass units were used to determine the peak areas of PFAS standards and analytical samples. PFAS calibration standards were prepared by diluting the PFAS stock solutions with water containing $NaHCO_3$ (1.0 mM) and NaCl

(varied concentrations to match the matrices of the analytes), and these were used as (external) calibration standards. To deal with possible long-term bias within the measurement system, calibration standards (0.05–3 nmol/mL) were injected after every seven samples (not including calibration blanks) and a calibration curve was generated for every seven samples. Calibration blanks containing methanol and water (1:1, v/v) were run after every sample for monitoring the instrumental background. The concentrations of the analytes were quantified using 7-point matrix-matched calibration curves.

Instrumental detection/quantification limits. The instrumental detection limits (based on a signal-to-noise ratio of 3:1) were as follows: PFHpA 20 ng/mL, PFOA 8 ng/mL, PFNA 8 ng/mL, PFOS 5 ng/mL, PFDA 5 ng/mL, and PFUnDA 5 ng/mL. The instrumental quantification limits (based on a signal-to-noise ratio of 10:1) were as follows: PFHpA 50 ng/mL, PFOA 20 ng/mL, PFNA 20 ng/mL, PFOS 12 ng/mL, PFDA 15 ng/mL, and PFUnDA 12 ng/mL. Following each run sequence, the analytical column was completely flushed to ensure no crystallization on the stationary phase. The analytical column was capped and stored when not in use. Typical HPLC/ESI-MS chromatograms for the calibration standard and blank are shown in Figure C-3. Recoveries were as follows: PFHxA – 105%, PFHpA – 99.7%, PFOA – 102%, PFOS – 108%, PFNA – 108%, PFDA – 119%, and PFUnA – 103%.

Quality assurance and quality control. The use of Teflon was avoided during the experiment because of possible contamination from additives in this perfluorinated polymer. The extraction efficiency or recovery of PFASs on kaolinite by methanol was examined by spiking blank kaolinite (20 mg) with a low (100 ng) (n = 7) and high (1000 ng) (n = 7) level of PFASs. The recoveries were as follows (mean±SD): PFHpA, 95.2±9.2%; PFOA, 103.3±5.8%; PFNA, 97.5±8.7%; PFOS, 106.1±7.4%; PFDA, 99.7±8.3%; PFUnDA, 102±10.6%. Depending on the compounds, the extraction recovery of analytes ranged from 95% to 106%, which indicated that methanol could extract the adsorbed PFASs on kaolinite. Therefore, the concentrations of PFASs were not corrected by recoveries.

Two types of blanks were measured for the adsorption experiments: blank tubes without PFAS but with kaolinite were used to check the possible contamination of kaolinite and the polystyrene tube by PFASs; blank polystyrene tubes with PFAS but without kaolinite were used to check the possible PFAS loss due to adsorption on the tube walls (no significant adsorption to tubes was found, which is consistent with the observation by Tang et al. (2010)). Furthermore, because these PFASs are resistant to the transformation processes, no concern is needed about the loss of PFAS due to hydrolysis, photolysis, and biodegradation during the batch adsorption tests

Appendix D: Supplementary data for Chapter 5

Table D-1. Properties of Amerlite XAD resins

Resin	Chemical Nature	Surface Area (m^2/g)	Pore Diameter (nm)	West Mesh Size	Porosity
XAD-2	Hydrophobic Polyaromatic	300	9	20–60	0.41 mL pore/mL bead
XAD-7	Non ionic aliphatic acrylic polymer	≥380	45–50	20–60	≥0.50 mL pore/mL bead

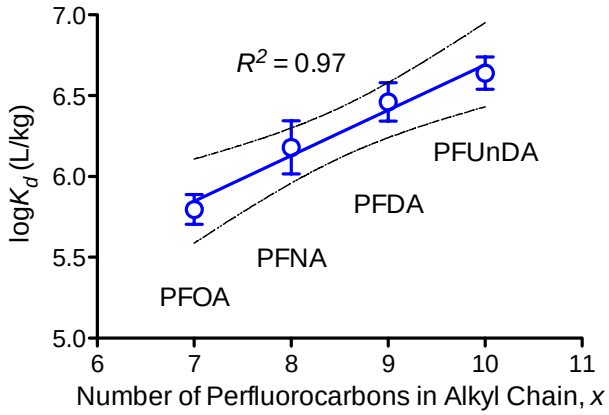

Figure D-1 logK_d versus the number of perfluorocarbons in PFASs (sorbent: XAD-7HP).

Parameters for operating the HPLC/ESI-MS system

The flow rate of the mobile phase was 0.20 mL/min. The mobile phase consisted of eluent A (2.0 mM NH_4Ac in a mixture of water and methanol (7:3, v/v)) and eluent B (2.0 mM NH_4Ac in methanol). The A/B ratio changed linearly in the first 13 min from 100/0 to 43.9/57.1, which was held for 5 min then changed linearly over the next 15 min to 0/100, which was held for 3 min then changed linearly over the next 1 min to 100/0, which was held for 8 min. Although the latest eluting peak (PFDA) was observed at approximately 25 min, sufficient run time (45 min) was used to condition the column for subsequent injections. The column temperature was maintained at 38 °C. The analytical column was conditioned prior to sample analysis with eluent B. For ESI-MS analysis, the MS detector was operated in the SIM mode with optimized parameters (fragmentor voltage, 70 V; capillary voltage, 4 kV). ESI was performed in a negative mode. Precursor ions with *m/z* 363, 413, 463, 499, and 513 were chosen, corresponding to PFHpA, PFOA, PFNA, PFOS, and PFDA respectively. The ions extracted at these mass units were used to determine the peak areas of PFAS standards and analytical samples. PFAS calibration standards were prepared by diluting the PFAS stock solutions with water containing $NaHCO_3$ (1.0 mM) and NaCl (varied concentrations to match the matrices of the analytes), and these were used as (external) calibration standards. To deal with possible long-term bias within the measurement system, calibration standards (0.05–3 nmol/mL) were injected after every seven samples (not including calibration blanks) and a calibration curve was generated for every seven samples. Calibration blanks containing methanol and water (1:1, v/v) were run after every sample for monitoring the instrumental background. The concentrations of the analytes were quantified using 7-point matrix-matched calibration curves. The instrumental quantification limits (based on a signal-to-noise ratio of 10:1) were as follows: PFOA 20 ng/mL, PFNA 20 ng/mL, PFOS 15 ng/mL, and PFDA 15 ng/mL. Following each run sequence, the analytical column was completely flushed to ensure no crystallization on the stationary phase. The analytical column was capped and stored when not in use.

t test results of the slope of the least squares regression line of the recoveries on the number of times XAD-7 regenerated (corresponding to Fig. 7a, Mississippi River water).

Best-fit values	PFOA	PFOS
Slope	-0.3750 ± 1.397	0.5548 ± 1.729
Y-intercept when X=0.0	96.45 ± 7.054	94.93 ± 8.732
X-intercept when Y=0.0	257.2	-171.1
1/slope	-2.667	1.803
95% Confidence Intervals		
Slope	-3.793 to 3.043	-3.677 to 4.786
Goodness of Fit		
R square	0.01187	0.01686
Sy.x	9.053	11.21

Is slope significantly non-zero?		
F	0.07207	0.1029
DFn, DFd	1.000, 6.000	1.000, 6.000
P value	**0.7973**	**0.7592**
Deviation from zero?	**Not Significant**	**Not Significant**
Data		
Number of X values	8	8
Maximum number of Y replicates	1	1
Total number of values	8	8
Number of missing values	0	0

t test results of the slope of the least squares regression line of the recoveries on the number of times XAD-7 regenerated (corresponding to Fig. 7b, tap water).

Best-fit values	PFOS
Slope	0.5833 ± 0.9769
Y-intercept when X=0.0	90.58 ± 5.497
X-intercept when Y=0.0	-155.3
1/slope	1.714
95% Confidence Intervals	
Slope	-1.727 to 2.894
Goodness of Fit	
R square	0.04847
Sy.x	7.567
Is slope significantly non-zero?	
F	0.3566
DFn, DFd	1.000, 7.000
P value	**0.5692**
Deviation from zero?	**Not Significant**
Data	
Number of X values	9
Maximum number of Y replicates	1
Total number of values	9
Number of missing values	0

Appendix E: Supplementary data for Chapter 6

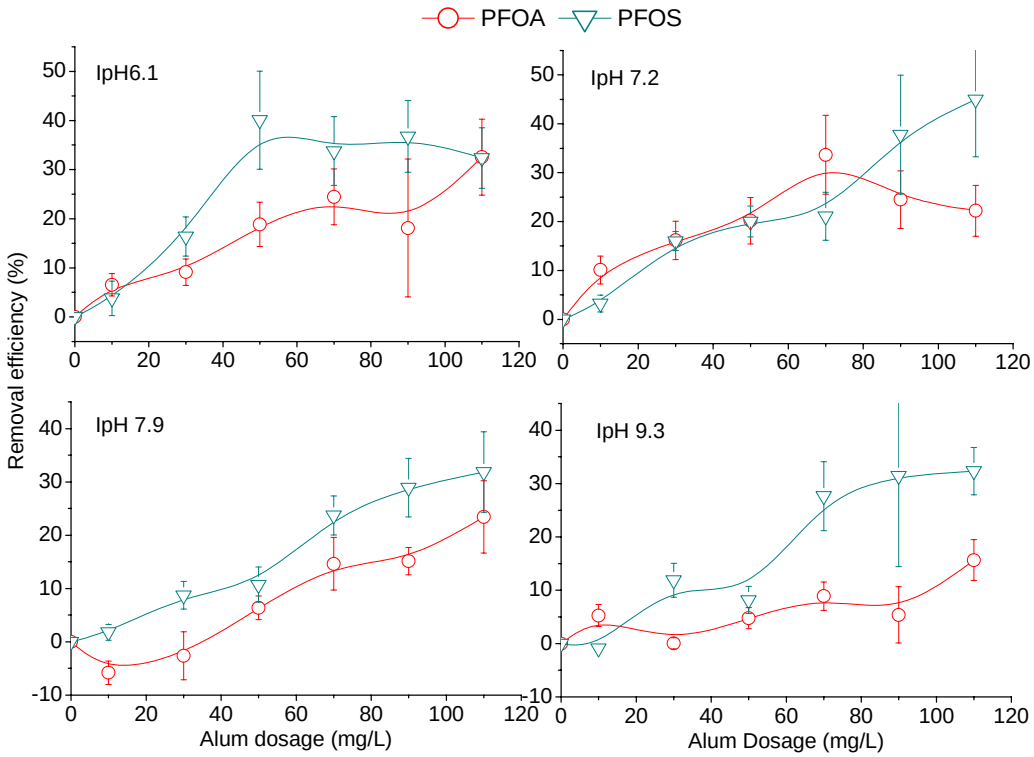

Figure E-1 PFOS/PFOA removal as a function of alum dosage at different initial pHs (IpHs)

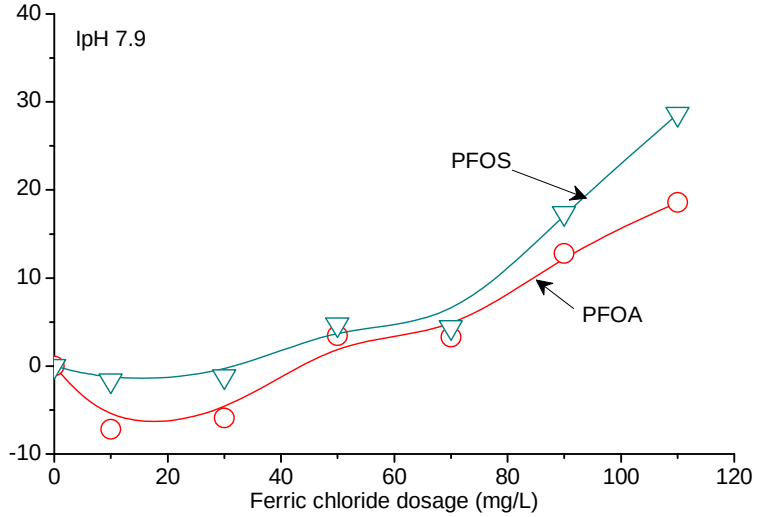

Figure E-2 PFOS/PFOA removal as a function of ferric chloride dosage at IpH 7.9.

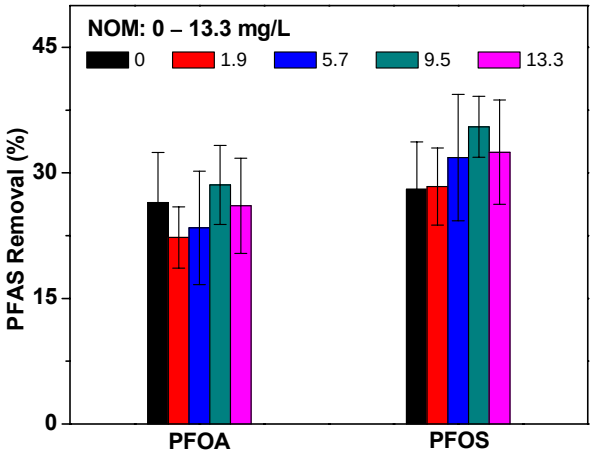

Figure E-3 PFOS/PFOA removal during coagulation at different NOM levels (0–13.3 mg/L corresponding to 0–7 mg/L DOC) (IpH = 7.9; alum dosage = 110 mg/L).